



# AXIAL FORCE AND BENDING INTERACTION OF STAINLESS STEEL MEMBER

Author: Denny Syamsuddin

Supervisor: Ing. Michal Jandera, Ph.D

University: Czech Technical University in Prague



Czech Technical University in Prague  
Date: 20.12.2014

## DECLARATION ON WORD OF HONOUR

I hereby declare that the submitted project was written by myself and I have stated all information resources used in conformity with the Methodical guide for ethical development of university final thesis

Prague, 20 December 2013

.....

Denny Syamsuddin

## ACKNOWLEDGEMENTS

I would like to express my gratitude to my supervisor Ing. Michal Jandera, Ph.D for giving me the opportunity to work on this interesting topic and for his interminable support and guidance. I would also like to thank him for his patient in assistance, encouragement and motivation during the completion of this thesis.

I extensively would like to thank Prof. Ing. František Wald, CSc as coordinator of our SUSCOS\_M Master program for organizing interesting programs, classes and excursions in the Czech Republic. Many thanks to Věra Klátová for her assistance and help with the visa and immigration administration, and for helping the students with any concerns or problems they had, this made the stay in the Czech Republic enjoyable and worry free.

My thanks and appreciations also go to my colleagues in SUSCOS\_M program for supportive encouragement and wonderful moments together throughout this program.

My deepest and heartfelt appreciation goes to my beloved wife, Ika Febriani, my beautiful daughters, Alyssa Zahra Chairani Putri and Almira Khanza Aisyah Putri, although you have not been literary beside me when I am finishing this manuscript, I would like you to know that you are my inspiration and motivation in every steps I took, as I dedicate this manuscript to all of you. Thank you for your endless support, enduring love, and constant motivation and encouragement. I love you all.

Special thanks to my parents and my big extensive family in Indonesia for their social and financial support and never ending motivation and encouragement.

Thank you to all friends in Indonesian Student Association in Czech Republic, Indonesian people and society in Prague, and Indonesian embassy in Prague (The Indonesian Ambassador, Emeria WA Siregar, and her staffs and their family) for warmest welcome and supporting throughout my staying in Prague.

Finally I would like to acknowledge the Erasmus Mundus scholarship, as without this funding, I would not have been able to participate in this program and meet amazing people.

*Dedicated to my beloved wife, Ika Febriani, my daughters, Alyssa and Almira,  
my parents and all my family members*

## ABSTRACT

Stainless steel have been introduced and increasingly utilized in architectural and structural application due to their good corrosion resistance, ease of maintenance, aesthetic appearance, and its mechanical properties which differs from carbon steel. However, the stainless steel design standards have been developed largely in-line and refer to carbon steel design guidelines, even though they were both different on its mechanical behavior. Current stainless steel interaction of axial force and bending moment formula were derived from modified Eurocode EN1993 Part 1-1 (Carbon steel standard code), considering the non-linearity behavior of stainless steel and then this interaction approached establish in Eurocode EN1993 Part 1-4 : General rules - Supplementary rules for stainless steels. Hence, the main objective of this thesis is to compare the analysis result with existing design formulas and some design formula proposed by researchers taken from experimental and parametric study in order to have possible development of general interaction formula for stainless steel.

In this thesis provides a summary of stainless steel material behavior, its non-linearity behavior of stress and strain relationship and wide variety of stainless steel materials mechanical properties. The study of relevant interaction of axial force and bending moment formula proposed by existing standard code (EN 1993 Part 1-1, ENV 1993-1-1) and proposed formula by researchers in their publishing journal (Talja, Lopes, and Greiner) as comparison for current standard code for stainless steel (EN 1993-1-4), and also the probability of Aluminium standard code interaction axial force and bending moment formula to be applied (EN 1999-1-1) are followed.

Full length three dimension models of various section members were modeled in the finite element program Abaqus to simulate the compressive test (both concentric and eccentric compressive test). The simulations were intended to compare the member resistance result of finite element model and experimental compressive test as published in some research reports. Finally, it was concluded that no significant differences found between them.

A parametric and numerical study of the behavior of beam-columns in several stainless steel grades (austenitics, ferritic and duplex grades) were also presented considering different section type (hollow and open section) and various of slenderness. Based on individual comparison, distribution test data and t-test method, this study indicates that the modified Aluminium 2 approach more likely to have the same result as finite element result. Therefore it was suggested to modify and make some improvements on modified Aluminium 2 approach for development of general interaction formula for stainless steel.

Keywords : Axial force and bending interaction, Stainless steel, Interaction formula, Aluminium, Parametric study, Eurocode.

## TABLE OF CONTENT

1.	Introduction .....	1
2.	Materials .....	1
2.1.	Stainless steel .....	1
2.2.	Stress and strain behavior .....	2
3.	Structural Member Cross section.....	6
3.1.	Class Classification.....	6
3.2.	Effective width in class 4 cross-section .....	7
3.3.	Cross section subject to compression .....	8
3.4.	Cross section subject to bending moment.....	10
3.5.	Interaction of axial compression and bending moment (Eurocode EN1993-1-4) .....	11
3.6.	Interaction of axial compression and bending moment (Eurocode EN1993-1-1) .....	12
3.7.	Interaction of axial compression and bending moment (Lopes, Real, & Silva – 2009).....	12
3.8.	Interaction of axial compression and bending moment (R. Greiner & M Kettler – 2008).....	13
3.9.	Interaction of axial compression and bending moment (ENV 1993-1-1 and Talja - Salmi – 1995) .	14
3.10.	Interaction of axial compression and bending moment (EN 1999-1-1).....	15
4.	Stainless steel materials grade of published test report .....	18
5.	Conventions of member axis.....	22
6.	I-Section validation study and experimental investigation.....	23
6.1.	Concentric compression experimental buckling test – major axis.....	23
6.2.	Concentric compression test result and numerical investigation.....	25
6.3.	Eccentric compression test .....	29
6.4.	Eccentric compression test result and numerical investigation.....	29
7.	Rectangular Hollow Section (RHS) validation study and experimental investigation.....	31
7.1.	Concentric compression experimental buckling test – major axis.....	32
7.2.	Concentric compression test result and numerical investigation.....	35

7.3.	Eccentric compression test .....	41
7.4.	Eccentric compression test result and numerical investigation.....	44
8.	Summary of comparison FE results and experimental test .....	49
9.	Parametric study .....	55
9.1.	SHS 60 X 60 X 5 ( $\psi = 1$ ) Comparison result .....	58
9.2.	RHS 150 X 100 X 3 ( $\psi = 1$ ) Comparison result .....	66
9.3.	I 160 X 80 ( $\psi = 1$ ) Comparison result .....	74
9.4.	SHS 60 X 60 X 5 ( $\psi = 0$ and $\psi = -1$ ) Comparison result.....	82
9.5.	Ratio of $k_y/k_{y,FEM}$ comparison distribution data (Overall group data result) .....	87
9.6.	Analysis variance test of the simulation result .....	106
10.	Result and conclusion.....	110
11.	References.....	112
APPENDIX 1 : EN 1993-1-1 METHOD 1 : Interaction factor $k_{ij}$ .....		114
APPENDIX 2 : EN 1993-1-1 METHOD 2 : Interaction factor $k_{ij}$ .....		117

## 1. Introduction

Stainless steel have been introduced and increasingly utilized in architectural and structural application due to their good corrosion resistance, ease of maintenance, aesthetic appearance, and its mechanical properties which differs from carbon steel.

Unlike carbon steel which has an elastic response, with a clearly defined yield point, followed by a yield plateau and a moderate degree of strain hardening, stainless steel has predominantly non-linear stress–strain behavior with significant strain hardening. The stainless steel design standards have been developed largely in-line and refer to carbon steel design guidelines, even though they were both different on its mechanical behavior. The study on buckling behavior of stainless steel and the interaction axial force and bending moment relation will then be advantageous to develop the application rules on stainless steel.

Combined axial force and bending moment formula of stainless steel were derived from modified Eurocode EN1993 Part 1-1, which is for Carbon steel, considering the non-linearity behavior of stainless steel and then this interaction approached establish in Eurocode EN1993 Part 1-4 : General rules - Supplementary rules for stainless steels.

Though the formula has been accepted and published in the Eurocode EN1993 Part 1-4, The interaction axial force and bending moment formula were not well established as written in two notes that the National Annexes may give other interaction formula as alternatives to the equations, so that the main objective of this thesis is to compare the analysis result with existing design formulas and some design formula proposed by researchers taken from experimental and parametric study in order to have possible development of general interaction formula for stainless steel.

A parametric and numerical study of the behavior of beam-columns in several stainless steel grades (austenitics, austenitic-ferritic and ferritics grades) is presented considering different section type (hollow and open section) and various of slenderness.

## 2. Materials

### 2.1. Stainless steel

Stainless steels are alloy steels with at least 10,5 % of chromium and maximum 1,2 % of carbon. There are various types of stainless steel and categorized into five basic groups of stainless steel, classified according to their metallurgical structure (according to EN 10088-1,2005):

1. Ferritic
2. Austenitic
3. Martensitic
4. Austenitic-ferritic (Duplex) and



### 5. Precipitation-hardening

The austenitic stainless steels and the duplex stainless steels are generally the more useful groups for structural applications.

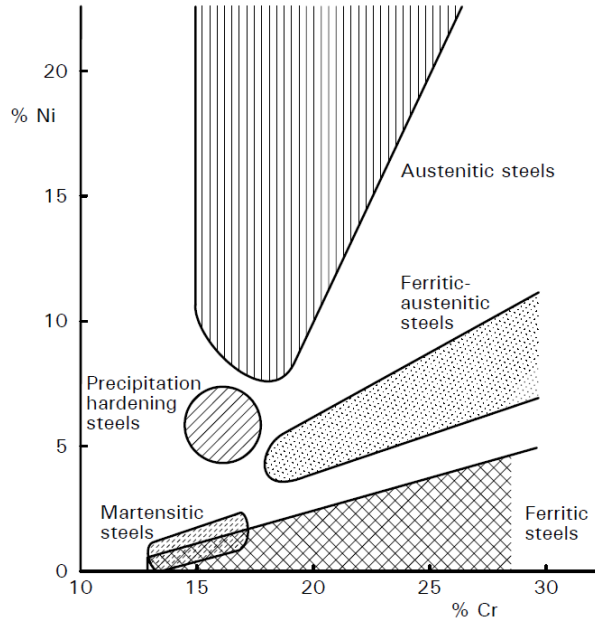


Figure 2-1 : Classification of stainless steels according to nickel and chromium content

Grade and designation system adopted in Stainless steel is European steel number and steel name. For example Stainless steel grade 304L has a steel number 1.4307, where:

<b>1</b>	<b>43</b>	<b>07</b>
Denotes steel	Denotes one group of stainless steels	Individual grade identification

The steel name system provides some understanding of the steel composition. The name of the steel number 1.4307 is X2CrNi18-9, where :

<b>X</b>	<b>2</b>	<b>CrNi</b>	<b>18-9</b>
Denotes high alloy steel (> 5% of one alloying element)	100 x % of carbon	Chemical symbols of main alloying elements	% of main alloying elements

### 2.2. Stress and strain behavior

The mechanical properties are difference between carbon and stainless steel on its stress-strain relationship. Stainless steel has a continuous, but non-linear relationship between stress and strain, whereas carbon steel has a clearly defined yield point

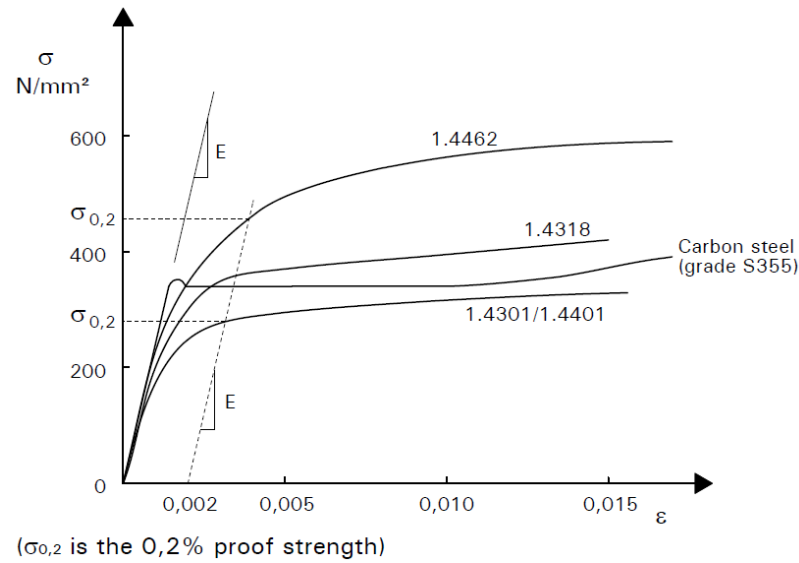


Figure 2-2 : Typical stress-strain curves for stainless steel and carbon

The non-linearity behavior of stress and strain relationship follow the Ramberg-Osgood formula :

$$\varepsilon = \frac{\sigma}{E} + 0.002 \left( \frac{\sigma}{\sigma_{0,2}} \right)^n \quad (2.1)$$

The equation shows that there are three independent parameters required to define a particular stress-strain curve, i.e :

$E$  is Young's modulus of stainless steel material (200 000 N/mm<sup>2</sup>)

$\sigma_{0,2}$  is the 0.2% proof strength ( $f_y$ )

$n$  is an index of non-linearity behavior

The degree of non-linearity of the stress-strain curve is characterized by the index  $n$ ; lower  $n$  values imply a greater degree of non-linearity, see Figure 2-3

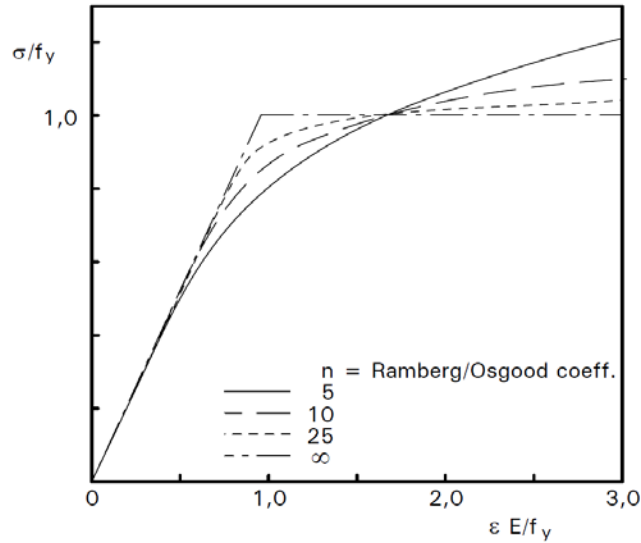


Figure 2-3 : Effect of the parameter  $n$  on the non-linearity of the stress-strain curve

The value of  $n$  may be obtained from the ratio of the stress at the limit of proportionality (conventionally the 0,01% proof strength,  $\sigma_{0,01}$ ) to the 0,2% proof strength,  $\sigma_{0,2}$ , as follows :

$$n = \frac{\ln(0.2/0.01)}{\ln(\sigma_{0,2}/\sigma_{0,01})} \tag{2.2}$$

Ramberg-Osgood formulation gives excellent approach with experimental stress-strain data up to the 0,2% proof strength, but at higher strains the model generally over estimates the stress corresponding to a given level of strain.

Mirambell and Real [2][27], proposed the use of two adjoining Ramberg-Osgood curves to achieve improved modeling accuracy at strains above the 0,2% proof strength. The basic Ramberg-Osgood expression is used up to the 0,2% proof stress, then a modified expression re-defines the origin for the second curve as the point of 0,2% proof stress, and ensures continuity of gradients.

Figure 2-4 expressed the improved accuracy at higher strains of this compound Ramberg-Osgood expression.

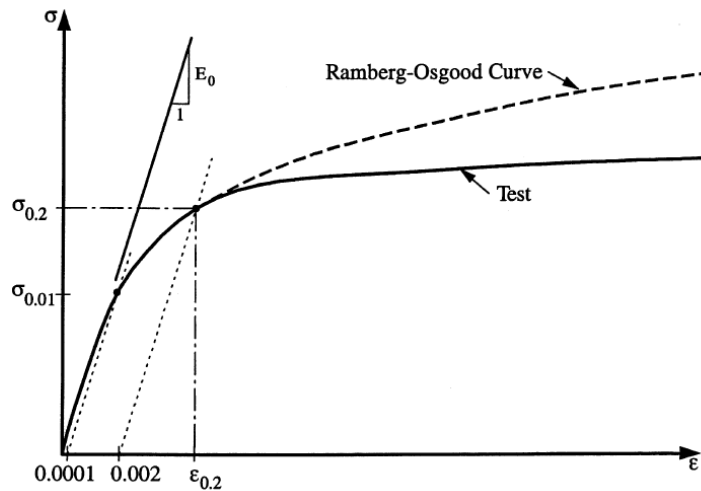


Figure 2-4 : Comparison between compound and basic Ramberg-Osgood models

Mirambell and Real’s model to describe compressive stress strain behavior express with the formula.

$$\varepsilon = 0.002 + \frac{\sigma_{0.2}}{E_0} + \frac{\sigma - \sigma_{0.2}}{E_{0.2}} + \varepsilon_{pl,u} \left[ \frac{\sigma - \sigma_{0.2}}{\sigma_u - \sigma_{0.2}} \right]^m \quad (2.3)$$

Parameters :

$E_0$  is Young’s modulus of stainless steel material

$E_{0.2}$  is the stiffness at the 0.2% proof stress.

$$E_{0.2} = \frac{E_0}{1 + 0.002 n \frac{E_0}{\sigma_{0.2}}} \quad (2.4)$$

$\sigma_{0.2}$  is the 0.2% proof strength ( $f_y$ )

$\sigma_u$  is the ultimate material strength

$\varepsilon_{pl,u}$  is the plastic strain at ultimate strength

$$\varepsilon_{pl,u} = 1 - \frac{\sigma_{0.2}}{\sigma_u} \quad (2.5)$$

$m$  is a strain hardening exponent that can be determined from the ultimate strength and another intermediate point

$$m = 1 + 3.5 \frac{\sigma_{0.2}}{\sigma_u} \quad (2.6)$$

L. Gardner [2][28] has proposed a modification to Mirambell and Real’s model to describe compressive stress strain behavior, but since lack of experimental parametric study data, therefore it will not be consider in this thesis.

### 3. Structural Member Cross section

#### 3.1. Class Classification

In principle, stainless steel cross-sections classify the same as carbon steel. Sections are classified as Class 1, 2, or 3 depending on the limits set out in Table 5.2 of EN 1993-1-4, and the sections which do not meet the criteria for Class 3 sections are classified as Class 4. In this thesis, class classification represent refer to the EN 1993-1-4 enhancement recommendation taken from L. Gardner & Theofanous’s research [21].

Internal compression parts				
Class	Part subject to bending	Part subject to compression	Part subject to bending and axial force	
1	$c/t \leq 72,0\epsilon$	$c/t \leq 33,0\epsilon$	when $\alpha > 0,5$ : $c/t \leq \frac{396\epsilon}{13\alpha - 1}$ when $\alpha \leq 0,5$ : $c/t \leq \frac{36\epsilon}{\alpha}$	
2	$c/t \leq 76,0\epsilon$	$c/t \leq 35,0\epsilon$	when $\alpha > 0,5$ : $c/t \leq \frac{420\epsilon}{13\alpha - 1}$ when $\alpha \leq 0,5$ : $c/t \leq \frac{38\epsilon}{\alpha}$	
3	$c/t \leq 90,0\epsilon$	$c/t \leq 37,0\epsilon$	$c/t \leq 18,5\epsilon \sqrt{k_\sigma}$ For $k_\sigma$ see EN 1993-1-5	
$\epsilon = \left[ \frac{235}{f_y} \frac{E}{210\,000} \right]^{0,5}$	Grade	1.4301	1.4401	1.4462
	$f_y$ (N/mm <sup>2</sup> )	210	220	460
	$\epsilon$	1,03	1,01	0,698
Note: For hollow sections, c may conservatively be taken as (h-2t) or (b-2t).				

Figure 3-1 : Maximum width-to-thickness ratios for compression parts – Internal parts

Outstand flanges					
Class	Section type	Part subject to compression	Part subject to bending and axial force		
			Tip in compression	Tip in tension	
1	Cold formed and welded	$c/t \leq 9,0\varepsilon$	$c/t \leq \frac{9,0\varepsilon}{\alpha}$	$c/t \leq \frac{9,0\varepsilon}{\alpha\sqrt{\alpha}}$	
2	Cold formed and welded	$c/t \leq 10,0\varepsilon$	$c/t \leq \frac{10,0\varepsilon}{\alpha}$	$c/t \leq \frac{10,0\varepsilon}{\alpha\sqrt{\alpha}}$	
3	Cold formed and welded	$c/t \leq 14,0\varepsilon$	$c/t \leq 21,0\varepsilon\sqrt{k_\sigma}$ For $k_\sigma$ see EN 1993-1-5		
$\varepsilon = \left[ \frac{235}{f_y} \frac{E}{210\,000} \right]^{0,5}$		Grade	1.4301	1.4401	1.4462
		$f_y$ (N/mm <sup>2</sup> )	210	220	460
		$\varepsilon$	1,03	1,01	0,698

Figure 3-2 : Maximum width-to-thickness ratios for compression parts – Outstand flanges

### 3.2. Effective width in class 4 cross-section

The effective widths and effective cross-sections are applied for Class 4 cross-sections only. The effective width is normally found by applying a reduction factor,  $\rho$ , to the full width. The reduction factor  $\rho$  may be calculated as follows:

Cold formed or welded internal elements:

$$\rho = \frac{0.772}{\bar{\lambda}_p} - \frac{0.125}{\bar{\lambda}_p^2} \quad \text{but } \leq 1 \tag{3.1}$$

Cold formed outstand elements:

$$\rho = \frac{1}{\bar{\lambda}_p} - \frac{0.231}{\bar{\lambda}_p^2} \quad \text{but } \leq 1 \quad (3.2)$$

Welded outstand elements:

$$\rho = \frac{1}{\bar{\lambda}_p} - \frac{0.242}{\bar{\lambda}_p^2} \quad \text{but } \leq 1 \quad (3.3)$$

where  $\bar{\lambda}_p$  is the element slenderness defined as:

$$\bar{\lambda}_p = \frac{\bar{b}/t}{28.4 \varepsilon \sqrt{k_\sigma}} \quad (3.4)$$

Where :

t is the relevant thickness

$k_\sigma$  is the buckling factor corresponding to the stress ratio  $\gamma$  and boundary conditions from Table 4.1 or Table 4.2 in EN 1993-1-5 as appropriate

$\bar{b}$  is the relevant width as follows:

$\bar{b} = d$  for webs (except RHS)

$\bar{b} =$  flat element width for webs of RHS, which can conservatively be taken as  $h-2t$

$\bar{b} = b$  for internal flange elements (except RHS)

$\bar{b} =$  flat element width for RHS flanges, which can conservatively be taken as  $b-2t$

$\bar{b} = c$  for outstand flanges

$\bar{b} = h$  for equal leg angles and unequal leg angles

$\varepsilon$  is the material factor defined in formula :

$$\varepsilon = \sqrt{\frac{235}{f_y} \frac{E}{210\,000}} \quad (3.5)$$

### 3.3. Cross section subject to compression

The resistance of a cross-section subject to compression are adopted from Carbon steel (EN1993-1-1),  $N_{c,Rd}$ , may be taken as:

$$N_{c,Rd} = A f_y / \gamma_{M0} \quad (3.6)$$

And the buckling resistance of the member due to uniaxial compression,  $N_{b,Rd}$ , should be taken as :

$$N_{b,Rd} = \chi A f_y / \gamma_{M1} \quad (3.7)$$

A Cross section area, where for class 1,2, or 3 use gross cross section area ( $A_g$ ), and Effective cross section area ( $A_{eff}$ ) applied for class 4 cross section area

$\gamma_{M0}$  Partial factor for resistance of cross sections ( $\gamma_{M0} = 1.1$  Recommended in EN1993-1-4)

$\gamma_{M1}$  Partial factor for resistance of members to instability assessed by member check ( $\gamma_{M1} = 1.1$  Recommended in EN1993-1-4)

$\chi$  Reduction factor for relevant buckling mode.

$$\chi = \frac{1}{\varphi + \sqrt{[\varphi^2 - \bar{\lambda}^2]}} \quad \text{but } \chi \leq 1 \quad (3.8)$$

$$\varphi = 0,5 [1 + \alpha(\lambda - \bar{\lambda}_0) + \bar{\lambda}^2] \quad (3.9)$$

Where Relative slenderness ( $\bar{\lambda}$ ), may be obtained from :

$$\bar{\lambda} = \sqrt{\frac{A f_y}{N_{cr}}} \quad (3.10)$$

$N_{cr}$  is the elastic critical force for the relevant buckling mode based on the gross cross sectional properties

$$N_{cr} = \frac{\pi^2 EI}{L_{cr}^2} \quad (3.11)$$

$L_{cr}$  is the buckling length in the buckling plane considered, determined taking into account the boundary conditions.

$\alpha$  is an imperfection factor

$\bar{\lambda}_0$  is limiting slenderness

Values for  $\alpha$  and  $\bar{\lambda}_0$  should be obtained from table 5.3 of EN1993-1-4 as summarize in table 3.1 as follow:

Buckling Mode	Type of member	$\alpha$	$\bar{\lambda}_0$
Flexural	Cold formed open section, and Hollow sections (welded and seamless)	0.49	0.40
	Welded open sections (major axis)	0.49	0.20
	Welded open sections (minor axis)	0.76	0.20
Torsional and torsional-flexural	All members	0.34	0.20

Table 3.1 : Value for  $\alpha$  and  $\bar{\lambda}_0$  EN 1993-1-4



### 3.4. Cross section subject to bending moment

The design moment resistance of a cross-section subject to a uniaxial moment should be taken as:

$$M_{c,Rd} = W_y f_y / \gamma_{M0} \quad (3.12)$$

And, for the design buckling resistance moment of a laterally unrestrained beam should be taken as :

$$M_{b,Rd} = \chi_{LT} W_y f_y / \gamma_{M1} \quad (3.13)$$

Where  $W_y$  is the appropriate section modulus as follows :

- $W_y = W_{pl}$  for Class 1, 2 cross-sections
- $W_y = W_{el,min}$  for Class 3 cross-sections
- $W_y = W_{eff,min}$  for Class 4 cross-sections

$W_{pl}$  is the plastic section modulus

$W_{el,min}$  is the elastic section modulus corresponding to the fiber with the maximum elastic stress.

$W_{eff,min}$  is the elastic modulus of effective section corresponding to the fiber with the maximum elastic stress.

$\chi_{LT}$  Reduction factor for lateral-torsional buckling.

$$\chi_{LT} = \frac{1}{\varphi_{LT} + \sqrt{[\varphi_{LT}^2 - \bar{\lambda}_{LT}^2]}} \quad \text{but } \chi_{LT} \leq 1 \quad (3.14)$$

$$\varphi_{LT} = 0,5 [1 + \alpha_{LT}(\bar{\lambda}_{LT} - \bar{\lambda}_0) + \bar{\lambda}_{LT}^2] \quad (3.15)$$

Where lateral-torsional buckling slenderness ( $\bar{\lambda}_{LT}$ ), may be obtained from :

$$\bar{\lambda}_{LT} = \sqrt{\frac{W_y f_y}{M_{cr}}} \quad (3.16)$$

$M_{cr}$  is the elastic critical moment for lateral torsional buckling.

$\alpha_{LT}$  is an imperfection factor

= 0.34 for cold formed sections and hollow sections (welded and seamless)

= 0.72 for welded open sections and other sections for which no data is available.

### 3.5. Interaction of axial compression and bending moment (Eurocode EN1993-1-4)

The interaction behavior under the combined effects of axial compression and bending moment proposed by Eurocode EN 1993-1-4 expressed as follows:

#### Axial compression and uniaxial major axis moment:

To prevent premature buckling about the major axis:

$$\frac{N_{Ed}}{(N_{b,Rd})_{\min}} + k_y \left( \frac{M_{y,Ed} + N_{Ed} e_{Ny}}{\beta_{w,y} W_{pl,y} f_y / \gamma_{M1}} \right) \leq 1 \quad (3.17)$$

#### Axial compression and uniaxial minor axis moment:

To prevent premature buckling about the minor axis:

$$\frac{N_{Ed}}{(N_{b,Rd})_{\min}} + k_z \left( \frac{M_{z,Ed} + N_{Ed} e_{Nz}}{\beta_{w,z} W_{pl,z} f_y / \gamma_{M1}} \right) \leq 1 \quad (3.18)$$

#### Axial compression and biaxial moments:

All members should satisfy:

$$\frac{N_{Ed}}{(N_{b,Rd})_{\min}} + k_y \left( \frac{M_{y,Ed} + N_{Ed} e_{Ny}}{\beta_{w,y} W_{pl,y} f_y / \gamma_{M1}} \right) + k_z \left( \frac{M_{z,Ed} + N_{Ed} e_{Nz}}{\beta_{w,z} W_{pl,z} f_y / \gamma_{M1}} \right) \leq 1 \quad (3.19)$$

In the above expressions:

- $(N_{b,Rd})_{\min}$  is the smallest value of  $N_{b,Rd}$  for the following four buckling modes: flexural buckling about the y axis, flexural buckling about the z axis, torsional buckling and torsional-flexural buckling.
- $(N_{b,Rd})_{\min1}$  is the smallest value of  $N_{b,Rd}$  for the following three buckling modes: flexural buckling about the z axis, torsional buckling and torsional-flexural buckling.
- $\beta_{w,y}$  and  $\beta_{w,z}$  are the values of  $\beta_w$  determined for the y and z axes respectively in which
  - $\beta_w = 1$  for Class 1 or 2 cross-sections
  - $\beta_w = W_{el}/W_{pl}$  for Class 3 cross-sections
  - $\beta_w = W_{eff}/W_{pl}$  for Class 4 cross-sections
- $W_{pl,y}$  and  $W_{pl,z}$  are the plastic moduli for the y and z axes respectively
- $k_y, k_z$  are the interaction factors

Interaction factor recommended by Eurocode EN1993-1-4 may be taken from :

$$k_y = 1.0 + 2(\bar{\lambda}_y - 0.5) \frac{N_{Ed}}{N_{b,Rd,y}} \quad \text{but } 1.2 \leq k_y \leq 1.2 + 2 \frac{N_{Ed}}{N_{b,Rd,y}} \quad (3.20)$$

$$k_z = 1.0 + 2(\bar{\lambda}_z - 0.5) \frac{N_{Ed}}{(N_{b,Rd})_{\min 1}} \quad \text{but } 1.2 \leq k_y \leq 1.2 + 2 \frac{N_{Ed}}{(N_{b,Rd})_{\min 1}} \quad (3.21)$$

### 3.6. Interaction of axial compression and bending moment (Eurocode EN1993-1-1)

General format of interaction formula given by EN1993-1-1 :

$$\frac{N_{Ed}}{N_{b,y,Rd}} + k_{yy} \left( \frac{M_{y,Ed} + N_{Ed} e_{Ny}}{M_{b,y,Rd}} \right) + k_{yz} \left( \frac{M_{z,Ed} + N_{Ed} e_{Nz}}{M_{z,Rk}/\gamma_{M1}} \right) \leq 1 \quad (3.22)$$

$$\frac{N_{Ed}}{N_{b,y,Rd}} + k_{zy} \left( \frac{M_{y,Ed} + N_{Ed} e_{Ny}}{M_{b,y,Rd}} \right) + k_{zz} \left( \frac{M_{z,Ed} + N_{Ed} e_{Nz}}{M_{z,Rk}/\gamma_{M1}} \right) \leq 1 \quad (3.23)$$

The parameters:

$e_{Ny}$  and  $e_{Nz}$  are the shifts in the neutral axes when the cross-section is subject to uniform compression

$N_{Ed}$ ,  $M_{y,Ed}$  and  $M_{z,Ed}$  are the design values of the compression force and the maximum moments about the y-y and z-z axis along the member, respectively

$M_{b,Rd}$  is the lateral-torsional buckling resistance

$M_{Rk}$  is member characteristic resistance

$k_{yy}$ ,  $k_{yz}$ ,  $k_{zy}$ ,  $k_{zz}$  are the interaction factors

The interaction factors have been derived from two alternative approaches. Value of this factors may be obtained from Annex A (Method 1) and Annex B (Method 2) of Eurocode 3 Part 1-1 [24][22][23]

### 3.7. Interaction of axial compression and bending moment (Lopes, Real, & Silva – 2009)

Combined axial force and bending moment proposed by Lopes, Real, & Silva – 2009 [15] still using the same general assembly formula as describe in Chapter 3.5 equation (3.17), (3.18) and (3.19)

Specifically for flexural buckling without Lateral Torsional Buckling, will have to satisfy formula (3.17) and (3.19) with interaction factor should be taken from :

$$k_y = 1.0 - \frac{\mu_y N_{Ed}}{N_{b,Rd,y}}, \quad \text{with } k_y \leq 1.5 \text{ and } k_y \geq \mu_y - 0.7 \quad (3.24)$$

$$k_z = 1.0 - \frac{\mu_z N_{Ed}}{N_{b,Rd,z}}, \quad \text{with } k_z \leq 1.5 \text{ and } k_z \geq \mu_z - 0.7 \quad (3.25)$$

To determine the  $\mu_y$  and  $\mu_z$  values, the following equations should be used.

$$\mu_y = (0.97 \beta_{M,y} - 2.11) \bar{\lambda}_y + 0.44 \beta_{M,y} + 0.09, \quad \text{if } \bar{\lambda}_y \leq 0.3 \text{ then } \mu_y \leq 1.0 \text{ else } \mu_y \leq 0.9 \quad (3.26)$$

$$\mu_z = (1.09 \beta_{M,y} - 2.32) \bar{\lambda}_z + 0.29 \beta_{M,z} + 0.48, \quad \text{if } \bar{\lambda}_y \leq 0.3 \text{ then } \mu_y \leq 1.0 \text{ else } \mu_y \leq 0.9 \quad (3.27)$$

The equivalent uniform moment factor  $\beta_{M,y}$  and  $\beta_{M,z}$  can be determined in function of the bending diagram shape, according to the expression :

$$\beta_{M,i} = 1.8 - 0.7 \psi_i \quad (3.28)$$

### 3.8. Interaction of axial compression and bending moment (R. Greiner & M Kettler – 2008)

Interaction of axial compression and bending moment formula which proposed by R. Greiner & M Kettler – 2008 [13] were adopted and modified from EN1993-1-1 Method 2 with uniaxial bending moment but limited to class 1 and 2 only.

**Insusceptible to torsional deformation (Pure flexural buckling) formula:**

$$\frac{N_{Ed}}{\chi_y N_{pl,Rd}} + k_y \left( \frac{C_{my} M_{y,Ed}}{M_{pl,y,Rd}} \right) \leq 1 \quad (3.29)$$

$$\frac{N_{Ed}}{\chi_z N_{pl,Rd}} + 0.6 k_y \left( \frac{C_{my} M_{y,Ed}}{M_{pl,y,Rd}} \right) \leq 1 \quad (3.30)$$

The interaction factor depends on the section shape of structural members.

Open I-Section, the interaction factor shall be taken from :

$$k_y = 0.9 + 2.2 \bar{n}_y (\bar{\lambda}_y - 0.4) \leq 0.9 + 2.42 \bar{n}_y \quad (3.31)$$

$$k_z = 1.2 + 1.5 \bar{n}_z (\bar{\lambda}_z - 0.7) \leq 1.2 + 1.95 \bar{n}_z \quad (3.32)$$

And for Hollow Section, the interaction factor shall be taken from :

$$k_y^* = 0.9 + 2.2 \bar{n}_y (\bar{\lambda}_y - 0.4) \leq 0.9 + 2.42 \bar{n}_y \quad (\text{CHS, Welded box-sections RHS – annealed}) \quad (3.33)$$

$$k_y^* = 0.9 + 3.5 (\bar{n}_y)^{1.8} (\bar{\lambda}_y - 0.5) \leq 0.9 + 1.75 (\bar{n}_y)^{1.8} \quad (\text{RHS – cold formed}) \quad (3.34)$$

Note : \*)  $k_y$  formula for hollow section is also applicable for calculating  $k_z$  by replacing the terms  $\bar{n}_y$  and  $\bar{\lambda}_y$  by  $\bar{n}_z$  and  $\bar{\lambda}_z$ .

Where :

$$\bar{n}_y = \frac{N_{Ed}}{\chi_y N_{pl,Rd}}; \quad \bar{n}_z = \frac{N_{Ed}}{\chi_z N_{pl,Rd}} \quad (3.35)$$

And  $C_{my}$  will be accordance to EN1993-1-1 Annex B Table B3.

### 3.9. Interaction of axial compression and bending moment (ENV 1993-1-1 and Talja - Salmi – 1995)

General formula for Bending and axial compression based on ENV 1993-1-1 [20] describe as follow:

$$\frac{N_{Ed}}{\chi_{min} A f_y / \gamma_{M1}} + k_y \left( \frac{M_{y,Ed}}{W_y f_y / \gamma_{M1}} \right) \leq 1 \quad (3.36)$$

Where :

$\chi_{min}$  is the lesser of the reduction factor  $\chi_y$  and  $\chi_z$  for buckling

A is cross section area. Effective area ( $A_{Eff}$ ) is used for uniform compression, otherwise Gross section area applied ( $A_g$ )

$W_y$  is appropriate section modulus as describe in chapter 3.4.

$k_y$  is magnification factor of second order effects of the bending moment

$$k_y = 1.0 - \frac{\mu_y N_{Ed}}{N_{b,Rd,y}}, \quad \text{but } k_y \leq 1.5 \quad (3.37)$$

Talja and Salmi [17] were also using the same general approach as in ENV 1993-1-1 equation (3.36), but they proposed the  $k_y$  value **not to be limited**.

$$k_y = 1.0 - \frac{\mu_y N_{Ed}}{N_{b,Rd,y}}, \quad (\text{Talja and Salmi improvement for } k_y) \quad (3.38)$$

$$\mu_y = \bar{\lambda}_y (2 \beta_{M,y} - 4) \quad \text{but } \mu_y \leq 0.9 \quad (\text{For elastic design}) \quad (3.39)$$

$$\mu_y = \bar{\lambda}_y (2 \beta_{M,y} - 4) + \left( \frac{W_{pl,y}}{W_{el,y}} - 1 \right) \quad \text{but } \mu_y \leq 0.9 \quad (\text{For plastic design}) \quad (3.40)$$

$$\beta_{M,y} = 1.8 - 0.7 \psi_i \quad (3.41)$$

### 3.10. Interaction of axial compression and bending moment (EN 1999-1-1)

Aluminium material stress-strain diagram shows the non-linearity behavior and the graph-trend follow the Ramberg-Osgood rules as describe in EN 1999-1-1. This behavior is typically the same as stainless steel behavior, therefore it is interesting to observe the correlation of interaction axial compression and bending moment formula for Aluminium corresponds to stainless steel parametric study result.

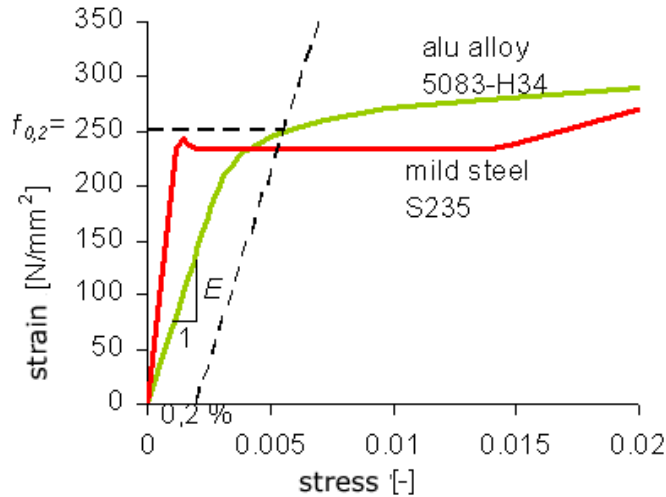


Figure 3-3 : Compare stress strain diagram Aluminium and Carbon steel

1. The interaction axial compression and bending moment for a member with open doubly symmetric cross section (solid cross section) for flexural buckling accordance to EN 1999-1-1 :

For major axis bending :

$$\left(\frac{N_{Ed}}{\chi_y \omega_x N_{Rd}}\right)^{\xi_{yc}} + \left(\frac{M_{y,Ed}}{\omega_0 M_{y,Rd}}\right) \leq 1.0 \tag{3.42}$$

For minor axis bending :

$$\left(\frac{N_{Ed}}{\chi_z \omega_x N_{Rd}}\right)^{\eta_c} + \left(\frac{M_{z,Ed}}{\omega_0 M_{z,Rd}}\right)^{\xi_{zc}} \leq 1.0 \tag{3.43}$$

Where :

$\eta_c = 0.8$  or may alternatively be taken as  $\eta_c = \eta_0 \chi_z$ , but  $\eta_c \geq 0.8$

$\xi_{yc} = 0.8$  or may alternatively be taken as  $\xi_{yc} = \xi_0 \chi_y$ , but  $\xi_{yc} \geq 0.8$

$\xi_{zc} = 0.8$  or may alternatively be taken as  $\xi_{zc} = \xi_0 \chi_z$ , but  $\xi_{zc} \geq 0.8$

$\eta_0 = 1.0$  or may alternatively be taken as  $\eta_0 = \alpha_z^2 \alpha_y^2$ , but  $1 \leq \eta_0 \leq 2$

$\xi_0 = 1.0$  or may alternatively be taken as  $\xi_0 = \alpha_y^2$ , but  $1 \leq \xi_0 \leq 1.56$

$\alpha_z, \alpha_y$  are the shape factors for bending about the y and x axis based on EN 1999-1-1

Cross section class	Without welds
1 / 2	$W_{pl} / W_{el}$
3	$W_{el} / W_{el} = 1$
4	$W_{eff} / W_{el}$

Table 3.2 : Value for  $\alpha_y$  and  $\alpha_z$  shape factor EN 1999-1-1

The formulas above were taken only from the equation of without welds and non-reinforced part cross section for Aluminium. This based on the assumption that Stainless steel section do not have reduction strength factor due to welds.

$\omega_x = \omega_0 = 1$  for beam – columns without localized welds and with equal end moments, otherwise then shall be calculated.

Based on EN 1999-1-1, Members subjected to combined axial force and unequal end moments and/or transverse loads, different section along the beam-column may use the interaction expressions as follow :

$$\omega_x = \frac{1}{\chi + (1 - \chi) \sin \frac{\pi x_s}{l_c}} \tag{3.44}$$

$$\omega_{x.LT} = \frac{1}{\chi_{LT} + (1 - \chi_{LT}) \sin \frac{\pi x_s}{l_c}} \tag{3.45}$$

Where  $x_s$  is the distance from studied section to a simple support or point of contra flexure of the deflection curve for elastic buckling of axial force only.

For end moments  $M_{Ed,1} > M_{Ed,2}$  only, the distance  $x_s$  can be then calculated :

$$\cos \left( \frac{x_s \pi}{l_c} \right) = \frac{(M_{Ed,1} - M_{Ed,2})}{M_{Rd}} \cdot \frac{N_{Rd}}{N_{Ed}} \cdot \frac{1}{\pi(1/\chi - 1)} \quad \text{but } x_s \geq 0 \tag{3.46}$$

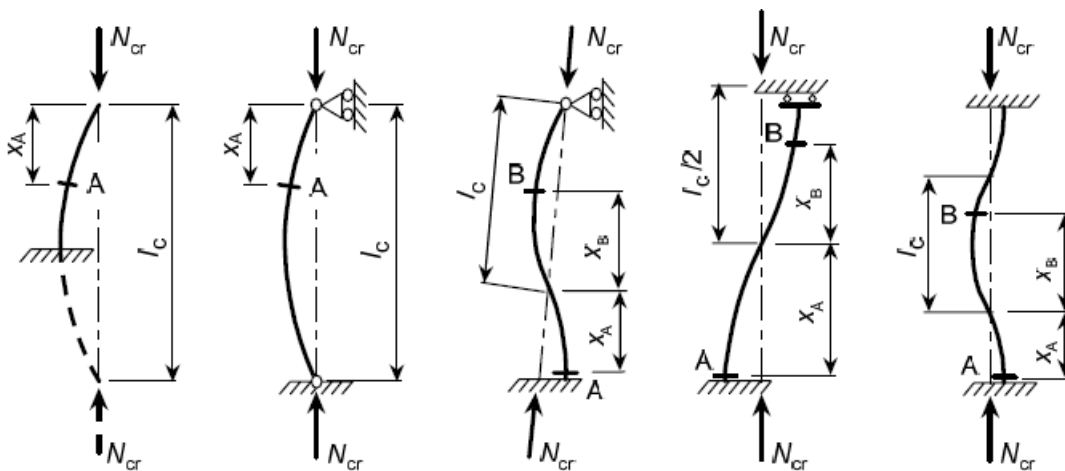


Figure 3-4 : Buckling length  $l_c$  (critical length) and definition of  $x_s$  ( $=x_A$  or  $x_B$ )

- 2. Hollow cross sections and tubes for flexural buckling accordance to EN 1999-1-1 should satisfy the following equation :**

$$\left(\frac{N_{Ed}}{\chi_{min}\omega_x N_{Rd}}\right)^{\psi_c} + \frac{1}{\omega_0} \left[ \left(\frac{M_{y,Ed}}{M_{y,Rd}}\right)^{1.7} + \left(\frac{M_{z,Ed}}{M_{z,Rd}}\right)^{1.7} \right]^{0.6} \leq 1.0 \quad (3.47)$$

Where :

$\psi_c = 0.8$  or may alternatively be taken as :

$$\psi_c = 1.3 \chi_y \text{ or } 1.3 \chi_z \quad , \text{ but } \psi_c \geq 0.8 \quad (3.48)$$

Depending on direction of buckling.

$$\chi_{min} = \min(\chi_y, \chi_z) \quad , \text{ but } \psi_c \geq 0.8 \quad (3.49)$$



#### 4. Stainless steel materials grade of published test report

The analyses begin with Identification the stainless steel materials grade and various section types which have been extracted from several published test reports [14], [16], [17], to be modelled and analyzed in ABAQUS.

The observed mechanical properties were based on flat test coupon types and base values of stainless steel material without considering any strain hardening and strength enhancement due to manufacturing process of the material.

Two kind of observed sections in this analysis are;

1. Rectangular Hollow Section (RHS) Cold formed
2. Open I Section

The various material properties range for each type of materials for Rectangular Hollow Section (RHS) tabulated as follow [16], [17].

For Austenitic Stainless steel grade (1.4301) :

Material Grade	E <sub>0</sub> (Gpa)	σ <sub>0,2</sub> (Mpa)	σ <sub>u</sub> (Mpa)	n
1.4301	195.2	431	676	4.8
1.4301	191.6	437	689	4.5
1.4301	188	606	781	4.49
1.4301	182	526	725	5.14
1.4301	180	571	691	3.72
1.4301	182	489	646	4.41
1.4301	177	591	793	4.6
1.4301	191	497	728	4.74
1.4301	195	304	630	5.96
1.4301	199	288	624	5.8
1.4301	190	403	668	5.85
1.4301	196	296	639	7.87
1.4301	194	388	693	4.52
1.4301	201	275	651	5.53

Table 4.1 : RHS - Austenitic grade mechanical properties

And by using the Ramberg – Osgood equation, then the graph σ-ε relationship can be obtained as illustrated below :

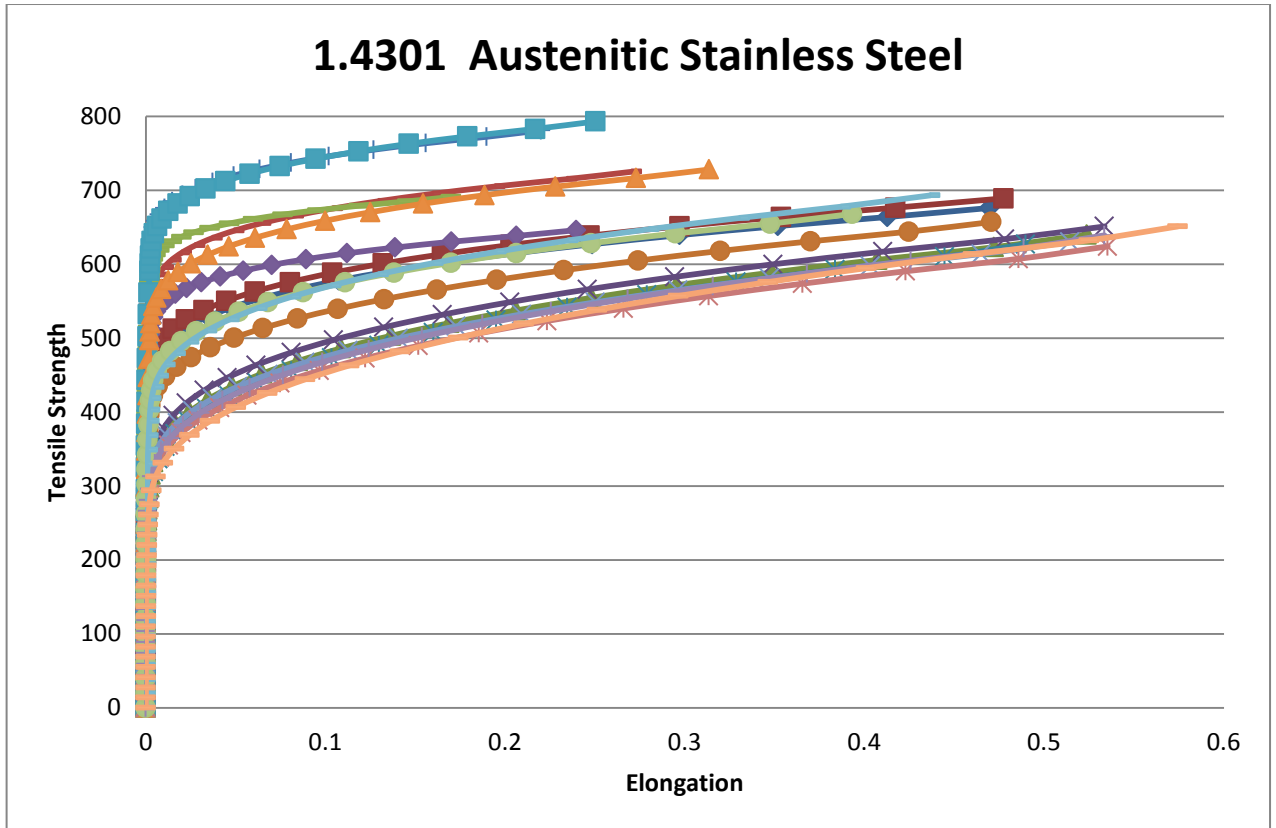


Figure 4-1 :  $\sigma$ - $\epsilon$  diagram for Austenitic Stainless Steel (1.4301)

For Ferritic Stainless steel grade (1.4003) tabulated as follow :

Material Grade	$E_0$ (Gpa)	$\sigma_{0,2}$ (Mpa)	$\sigma_u$ (Mpa)	n
1.4003	193.7	381	450	7.9
1.4003	201	471	490	7.6
1.4003	191.4	411	455	13.9
1.4003	189.2	466	483	8.3

Table 4.2 : RHS - Ferritic grade mechanical properties

And with the same Ramberg – Osgood approach, the  $\sigma$ - $\epsilon$  relationship can be charted as shown in the following picture:

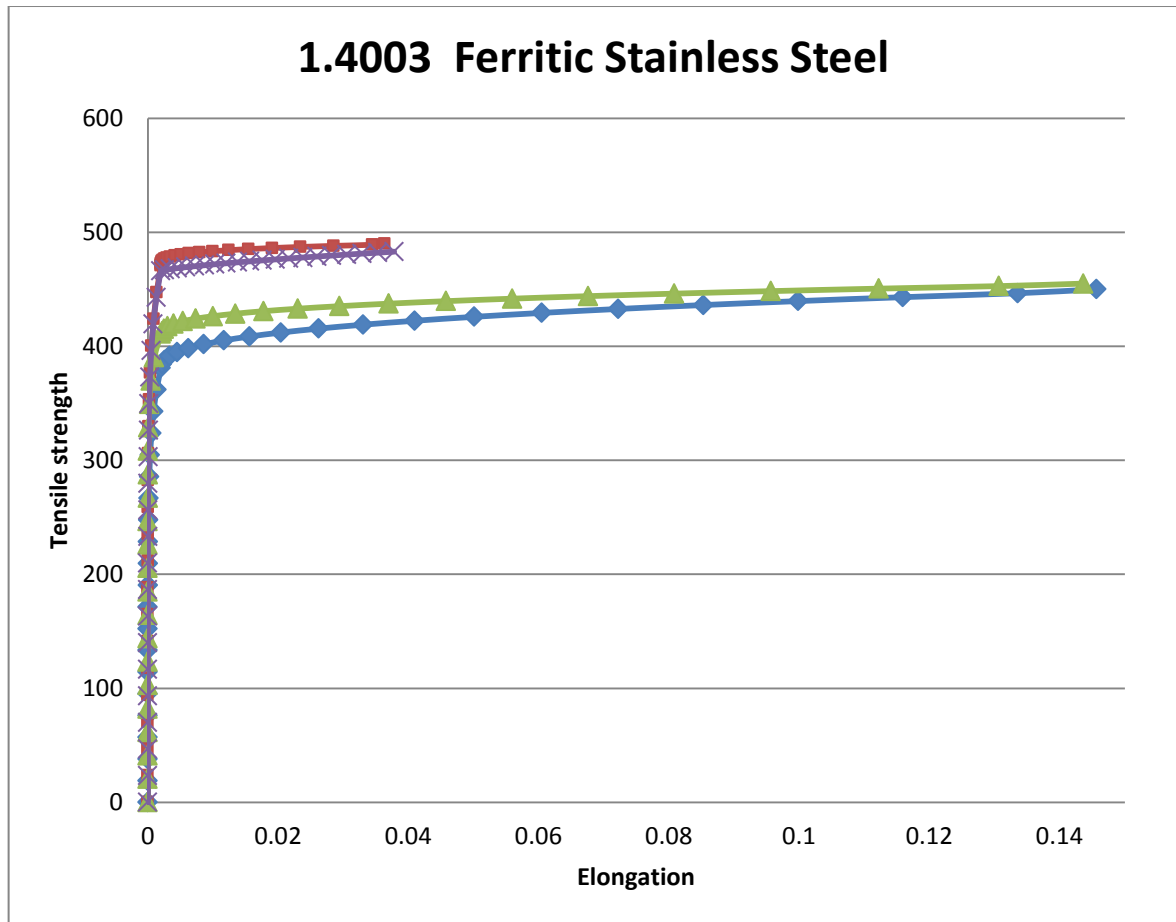


Figure 4-2 :  $\sigma$ - $\epsilon$  diagram for Ferritic Stainless Steel 1.4003

Duplex stainless steel grade (1.4462) material properties were populated in table :

Material Grade	$E_0$ (Gpa)	$\sigma_{0,2}$ (Mpa)	$\sigma_u$ (Mpa)	n
1.4462	191.2	544	744	6.6
1.4462	189.4	551	768	6.4

Table 4.3 : RHS - Duplex grade material properties

And with the same approach (Ramberg – Osgood), the stress and strain diagram for duplex (1.4462) can be drafted as follow:

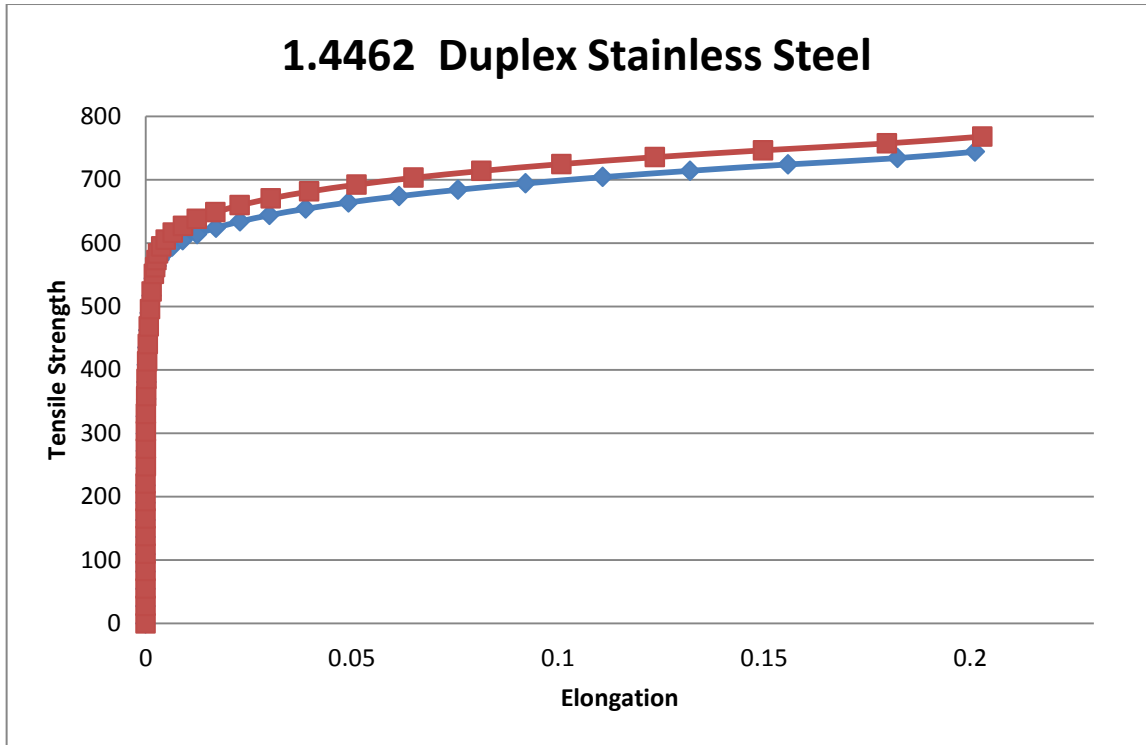


Figure 4-3 :  $\sigma$ - $\epsilon$  diagram for Duplex Stainless Steel (1.4301)

The I – section, since the I – Section fabricated as welded I – Section, therefore the material properties were divided into two parts; web and flange parts. But, due to lack of experimental data, I-Section material properties were only observed for Austenitic and Duplex material and were taken from average of experimental data [14].

Material Grade	Parts	$E_0$ (Gpa)	$\sigma_{0,2}$ (Mpa)	$\sigma_u$ (Mpa)	n
1.4462	Web	202	524	778	4.6
1.4462	Flange	202	522	756	5.4
1.4301	Web	198	300	624	6.4
1.4301	Flange	201	300.778	611.444	5.494

Table 4.4 : I-Section material properties

By using the Ramberg – Osgood formula, the relationship for stress – strain of the material can be then illustrated in graph as follow:

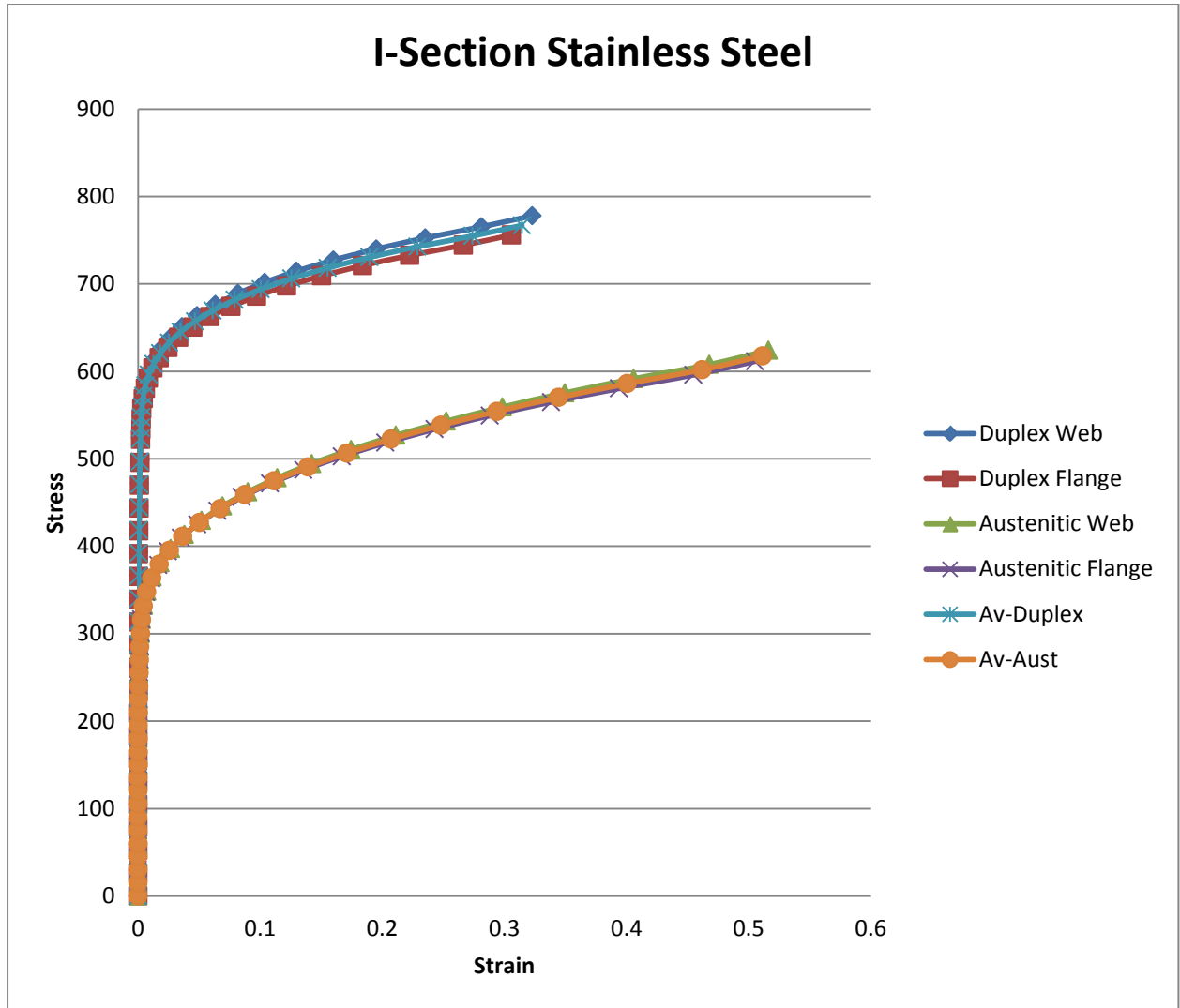


Figure 4-4 :  $\sigma$ - $\epsilon$  diagram for I-Section materials

With the wide range variety of mechanical properties of stainless steel materials, therefore the analysis in validation study will be based on particular experimental test value of material properties which corresponds to the comparing both experimental test result and finite element modelling in Abaqus.

## 5. Conventions of member axis

In general, the convention for member axes is:

x-x along the length of the member.

y-y cross-section axis perpendicular to web, or perpendicular to the larger leg in the case of angle sections.

z-z cross-section axis parallel to web, or parallel to the larger leg in the case of angle sections.

The y-y axis will normally be the major axis of the section and the z-z axis will normally be the minor axis. And for angle sections, the major and minor axes (u-u and v-v) are inclined to the y-y and z-z axes, see Figure.2-1.

For example, for an I-section bending moment acting in the plane of the web is denoted  $M_y$  because it acts about the cross-section axis perpendicular to the web.

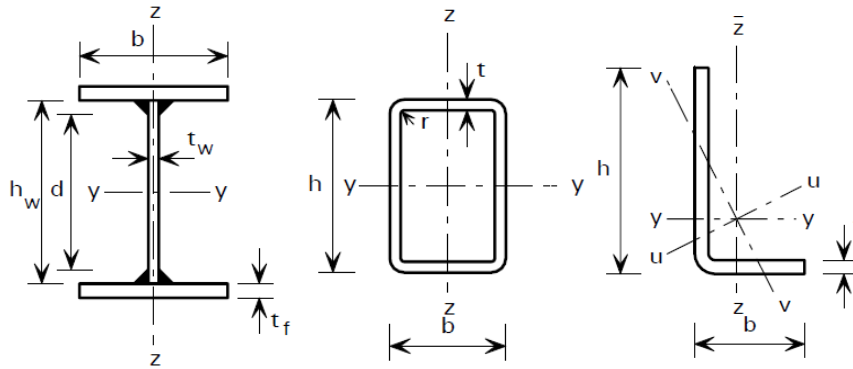


Figure 5-1 : Dimension and axis of cross section members

## 6. I-Section validation study and experimental investigation

The experimental test data were taken from Heiko Stangenberg & Richard A Weber’s technical report [14], the report covers the test results of concentric test and column-beam (eccentric) test. These results then will be comparing to the finite element model result for both type of test (concentric and eccentric compression test).

### 6.1. Concentric compression experimental buckling test – major axis

Nine welded I-section members were taken for concentric compression test. All of the specimens had a nominal section depth of 160 mm, but with different section width and mechanical properties. Table 6.1 summaries the measured geometric and mechanical properties of tested columns.

Specimen reference name	I 160X80-C1/MAJOR	I 160X80-C2/MAJOR	I 160X80-C3/MAJOR	I 160X160-C1/MAJOR	I 160X160-C2/MAJOR	I 160X160-C3/MAJOR	I 160X160 DUPLEX-C1/MAJOR	I 160X160 DUPLEX-C2/MAJOR	I 160X160 DUPLEX-C3/MAJOR
Steel Grade material	1.4301	1.4301	1.4301	1.4301	1.4301	1.4301	1.4462	1.4462	1.4462
Specimen length, L (mm)	2048	3343	5031	2050	3348	5045	2050	3348	5046
Section depth, H (mm)	157	157.6	158.5	158.3	158.4	158	162.7	161.4	160.4
Section width, B (mm)	79.4	79	80.1	160	159.9	159.2	159.1	159.5	161
Web thickness, $t_w$ (mm)	6	6	6	6	6	6	6.8	6.8	6.8
Web yield strength, $f_{y,w}$ (N/mm <sup>2</sup> )	300	300	300	300	300	300	524	524	524
Web ultimate strength, $f_{u,w}$ (N/mm <sup>2</sup> )	624	624	624	624	624	624	778	778	778
Web modulus of elasticity $E_w$ (kN/mm <sup>2</sup> )	198	198	198	198	198	198	202	202	202
Ramberg-Osgood coefficient, $n_w$	6.4	6.4	6.4	6.4	6.4	6.4	4.6	4.6	4.6
Flange thickness, $t_f$ (mm)	9.86	9.86	9.86	9.94	9.94	9.9	10.06	10.06	10.06
Flange yield strength, $f_{y,f}$ (N/mm <sup>2</sup> )	299	299	299	300	300	300	522	522	522
Flange ultimate strength, $f_{u,f}$ (N/mm <sup>2</sup> )	610	610	610	610	610	610	756	756	756
Flange modulus of elasticity $E_f$ (kN/mm <sup>2</sup> )	202	202	202	198	198	200	202	202	202
Ramberg-Osgood coefficient, $n_f$	5.4	5.4	5.4	5.3	5.3	5.4	5.4	5.4	5.4

Table 6.1 : Geometric and material properties of the I-section column specimens subject to major axis flexural buckling

The test were using pinned-pinned boundary condition as illustrated in schematic test representation

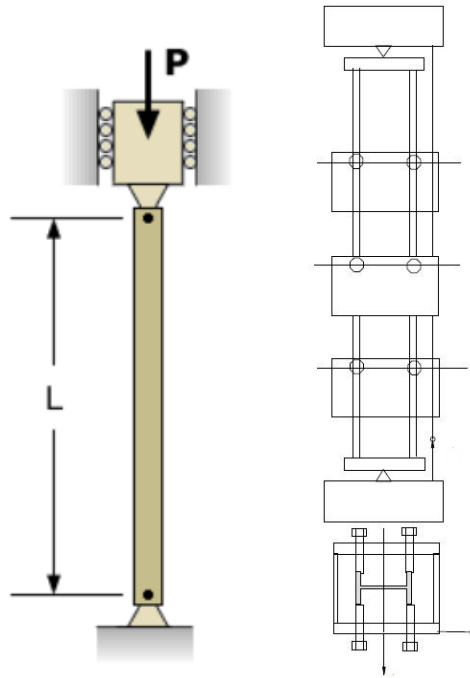


Figure 6-1 : Schematic representation of the flexural buckling test

## 6.2. Concentric compression test result and numerical investigation

Data given will be then modelled and simulate the test in finite element calculation with ABAQUS. All nine section members will be modelled based on its geometry and mechanical properties.

The section members modelled with full length of the column and applied boundary condition where simulate pinned-pinned condition as in the test. And lateral restraints also applied at flange for both ends to avoid torsional and minor buckling.

The Abaqus model used shell element with four nodes, known as element S4, and were modelled consist of three parts, web part, upper and bottom flange. The section materials in Abaqus were independent and different for web and flange (upper and bottom part) as suggested in Heiko Stangenberg & Richard A Weber test report [14]. And only axial forces were applied on end column section member as illustrated in picture 6-1.

Initial imperfections also introduced in the model in order to find the maximum capacity of the section members under non-linearity behaviour. But since the initial imperfection were literary written in the test report [14], therefore the comparison in this thesis also considering the initial imperfection value from the report.



No	Type of imperfection	Initial imperfection	Remarks
1	Global	$L/1000$	General initial imperfection commonly used (reference to EN 1993-1-5, Real-Lopes [15], and Talja [17])
	Local (web)	$c/200$	
2	Global	$L/400$	Initial imperfection suggested in Heiko Stangenberg & Richard A Weber's test report [14]
	Local (web)	$c/800$	
	Local (flange)	$d/500$	
3	Global	$L/400$	Modified Initial imperfection suggested in Heiko Stangenberg & Richard A Weber's test report [14], but only taken from the severe value amplitude result
	Local (web)	$d/500$	

Table 6.2 : Initial imperfection used for the I-Section concentric compression analysis

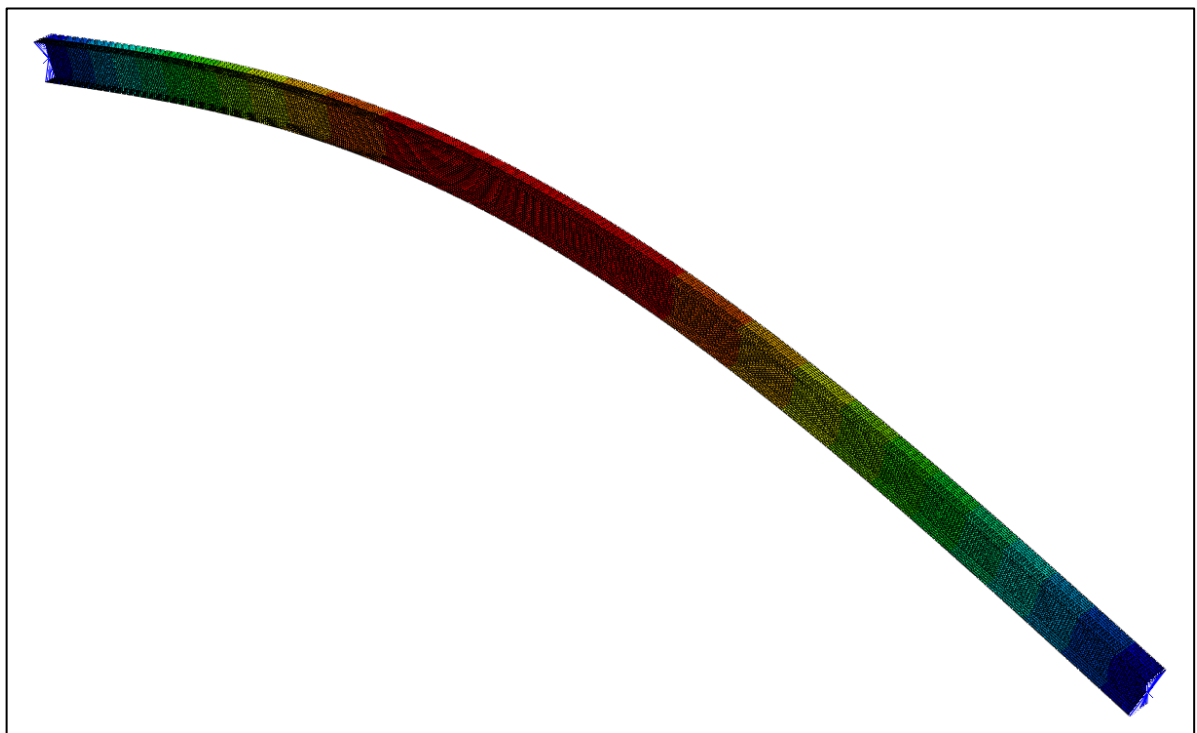


Figure 6-2 : I-Section global imperfection mode – Abaqus visualitation

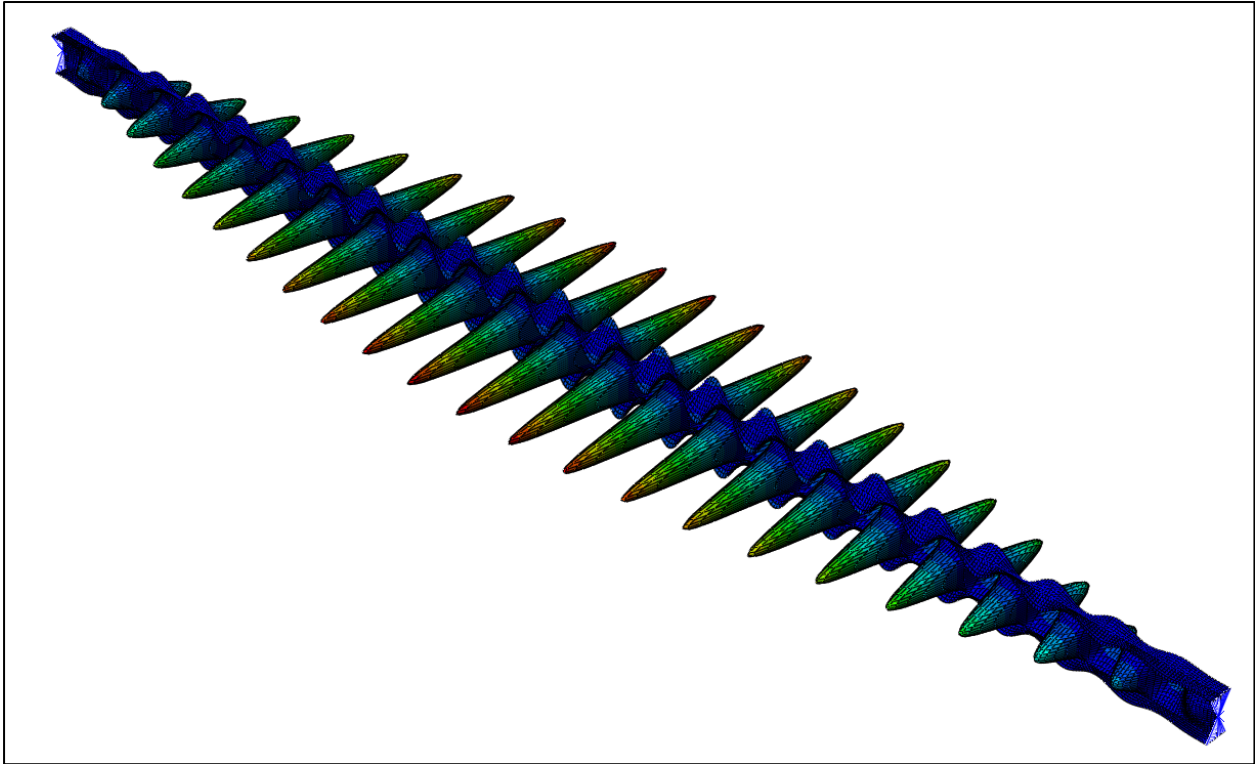


Figure 6-3 : I-Section local imperfection (web and flange imperfection) mode – Abaqus visualization

The finite element results (maximum loads) for each initial imperfection are summarized and compared to test result report [14]

Specimen reference name	I 160X80-C1/MAJOR	I 160X80-C2/MAJOR	I 160X80-C3/MAJOR	I 160X160-C1/MAJOR	I 160X160-C2/MAJOR	I 160X160-C3/MAJOR	I 160X160 DUPLEX-C1/MAJOR	I 160X160 DUPLEX-C2/MAJOR	I 160X160 DUPLEX-C3/MAJOR
Section class	1	1	1	2	2	1	3	3	3
$N_{cr, FEM}$ (kN)	4487.6	1762.6	806.61	7851.2	3181.5	1433.1	8728.6	3460.6	1552.4
$E_{average}$ (kN/mm <sup>2</sup> )	200	200	200	198	198	199	202	202	202
$f_{y, average}$ (N/mm <sup>2</sup> )	299.5	299.5	299.5	300	300	300	523	523	523
$\lambda_{Theory}$	0.399	0.637	0.946	0.392	0.615	0.913	0.500	0.794	1.189
$X_{b,y}$ EN 1993-1-4	0.898	0.763	0.572	0.902	0.777	0.592	0.843	0.666	0.439

Table 6.3 : Section classification and slenderness – concentric compression test

The table 6.3 shows the section class classification differently as in the experimental report [14], this is because of consideration of new proposal cross section class classification [21] as describe in chapter (3.1).

Specimen reference name	I 160X80-C1/MAJOR	I 160X80-C2/MAJOR	I 160X80-C3/MAJOR	I 160X160-C1/MAJOR	I 160X160-C2/MAJOR	I 160X160-C3/MAJOR	I 160X160 DUPLEX-C1/MAJOR	I 160X160 DUPLEX-C2/MAJOR	I 160X160 DUPLEX-C3/MAJOR
$N_{b,Rd, FEM}$ - imperfection 1 (kN)	666.224	530.199	406.413	1131.84	908.025	688.451	2294.32	1540.99	1229.51
$N_{b,Rd, FEM}$ - imperfection 2 (kN)	635.122	495.345	367.05	1078.66	848.894	623.729	1919.58	1434.2	963.198
$N_{b,Rd, FEM}$ - imperfection 3 (kN)	634.06	495.145	366.986	1078.66	848.772	623.653	1919.58	1433.91	963.068
Maximum Experimental Load, $N_u$ (kN)	664	535	402	1108	860	725	1930	1490	990
$N_{b,Rd, FEM}/N_u$ - imperfection 1	1.003	0.991	1.011	1.022	1.056	0.950	1.189	1.034	1.242
$N_{b,Rd, FEM}/N_u$ - imperfection 2	0.957	0.926	0.913	0.974	0.987	0.860	0.995	0.963	0.973
$N_{b,Rd, FEM}/N_u$ - imperfection 3	0.955	0.926	0.913	0.974	0.987	0.860	0.995	0.962	0.973

Table 6.4 : Comparison of FE results with experimental test – concentric compression test

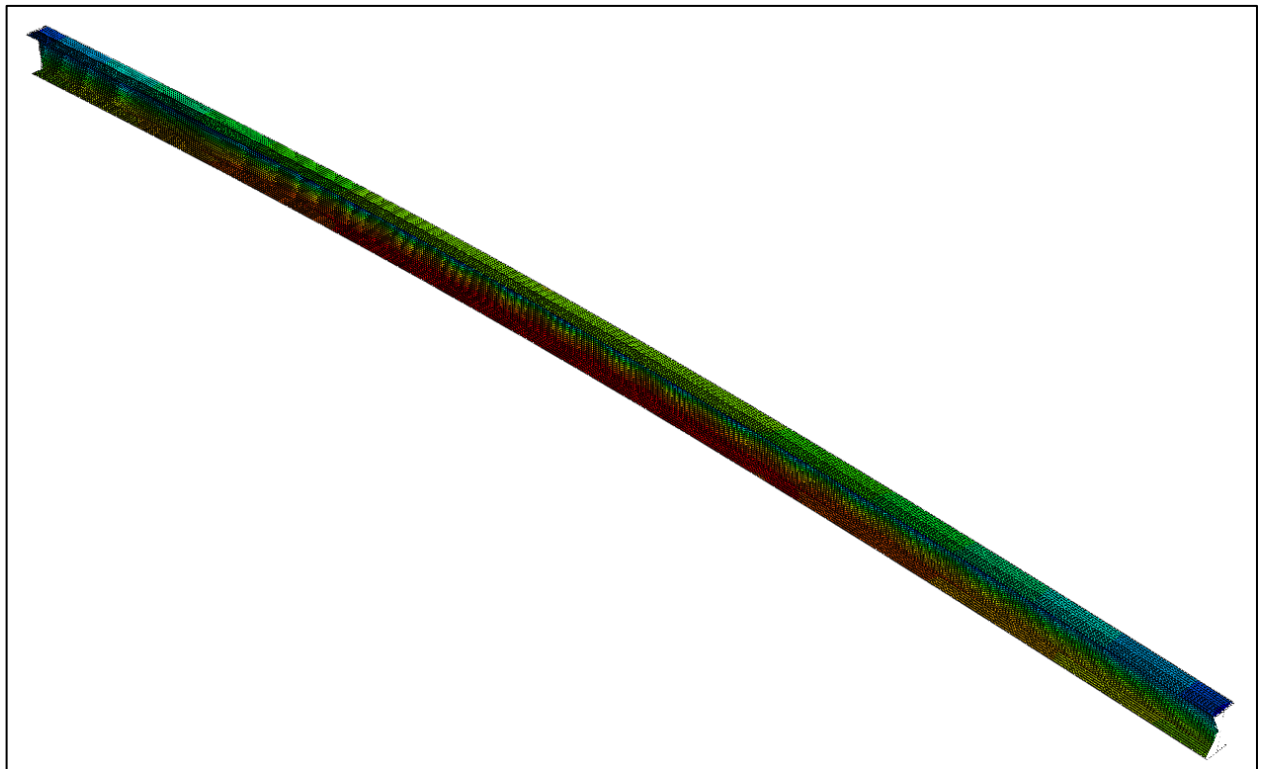


Figure 6-4 : I-Section Abaqus geometry non linearity result visualitation

### 6.3. Eccentric compression test

Six I-section members were taken for beam-columns (eccentric compression) test. The test set up was typically the same as figure 6.1 but the groove positioned in the centerline of the flange. Table 6.5 summaries the measured geometric and mechanical properties of tested beam-columns.

Specimen reference name	I 160X80-EC1	I 160X80-EC2	I 160X80-EC3	I 160X160-EC1	I 160X160-EC2	I 160X160-EC3
Steel Grade material	1.4301	1.4301	1.4301	1.4301	1.4301	1.4301
Specimen length, L (mm)	2045	3339	5041	2048	3345	5043
Section depth, H (mm)	160.3	158.9	158.7	159	158.5	159.5
Section width, B (mm)	79.5	79.2	80.9	160.9	160.2	160.5
Web thickness, $t_w$ (mm)	6	6	6	6	6	6
Web yield strength, $f_{y,w}$ (N/mm <sup>2</sup> )	300	300	300	300	300	300
Web ultimate strength, $f_{u,w}$ (N/mm <sup>2</sup> )	624	624	624	624	624	624
Web modulus of elasticity $E_w$ (kN/mm <sup>2</sup> )	198	198	198	198	198	198
Ramberg-Osgood coefficient, $n_w$	6.4	6.4	6.4	6.4	6.4	6.4
Flange thickness, $t_f$ (mm)	9.86	9.86	9.86	9.86	9.86	9.94
Flange yield strength, $f_{y,f}$ (N/mm <sup>2</sup> )	299	299	299	299	299	300
Flange ultimate strength, $f_{u,f}$ (N/mm <sup>2</sup> )	610	610	610	610	610	610
Flange modulus of elasticity $E_f$ (kN/mm <sup>2</sup> )	202	202	202	202	202	198
Ramberg-Osgood coefficient, $n_f$	5.3	5.3	5.3	5.3	5.3	5.3

Table 6.5 : Geometric and material properties of the I-section column specimens subject to eccentric compression

### 6.4. Eccentric compression test result and numerical investigation

With the same procedure for numerical analysis as in concentric compression analysis, all six sections modelled and simulated refer to its geometry and mechanical properties as describe in table 6.5.

The Abaqus model has the same element type as in concentric test which is four nodes shell element (S4 element), and other conditions (boundary condition, and lateral restraint) were typically the same. Material will be, again, independent for three parts (web, upper and bottom flange), but the material the properties will be different to concentric section member test. The material will refer to Heiko Stangenberg & Richard A Weber eccentric test report [14].

Since the groove for compression test was positioned in the centerline of the flange, therefore the applied load will have eccentricity effect caused bending moment accordingly. Hence, the applied will be combined axial load and bending moment due to eccentricity.

Since in the report [14] were not specifically describe the initial imperfection applied for particular eccentric compression test, therefore in this thesis, the analysis will introduced the initial imperfection as applied in concentric compression test, which is :

- Global initial imperfection :  $L/1000$
- Local initial imperfection (web) :  $c/200$

The finite element results (maximum loads) are summarized and compared to experimental result report [14]

Specimen reference name	I 160X80-EC1	I 160X80-EC2	I 160X80-EC3	I 160X160-EC1	I 160X160-EC2	I 160X160-EC3
Section class	1	1	1	2	1	2
$N_{cr, FEM}$ (kN)	4705.7	1799.5	812.73	8043.4	3246.1	1471.1
$E_{average}$ (kN/mm <sup>2</sup> )	200	200	200	200	200	198
$f_{y,average}$ (N/mm <sup>2</sup> )	299.5	299.5	299.5	299.5	299.5	300
$\lambda_{Theory}$	0.392	0.632	0.946	0.386	0.607	0.906
$X_{b,y}$ EN 1993-1-4	0.902	0.766	0.572	0.905	0.781	0.596

Table 6.6 : Section classification and slenderness – eccentric compression test

The table 6.6 has described different result as in the experimental test [14] for section class classification, as explain previously in chapter 6.2, this is because of consideration of new proposal cross section class classification [21] as explain in chapter (3.1) and also because of the calculation using the actual section members geometry as summarized in table 6.5.

Specimen reference name	I 160X80-EC1	I 160X80-EC2	I 160X80-EC3	I 160X160-EC1	I 160X160-EC2	I 160X160-EC3
$N_{b,Rd, FEM}$ (kN)	343.694	277.124	215.464	576.153	477.287	377.818
Maximum Experimental Load, $N_u$ (kN)	338	270	222	540	454	356
$N_{b,Rd, FEM}/N_u$	1.017	1.026	0.971	1.067	1.051	1.061

Table 6.7 : Comparison of FE results with experimental test – eccentric compression test

### 7. Rectangular Hollow Section (RHS) validation study and experimental investigation

The experimental test data and results were presented in VTT Research publishing [17] as one of research study ever published for roll-formed stainless steel rectangular hollow sections (RHS). The test covers of the result of concentric compression, eccentric compression, and bending and web crippling, but this thesis will be focused on only concentric and eccentric compression to study the RHS stainless steel section members' behavior under flexural buckling and compare the test result with Abaqus simulation result.

The material grade for this test were Austenitic stainless steel (1.4301) only, and the mechanical properties were taken from the tensile test coupon of longitudinal cuts of Rectangular Hollow Section named as (W) means wide face and (N) means narrow face. Narrow face coupon means the part which opposite to the welded seam and wide face means the part which beside the welded seam.

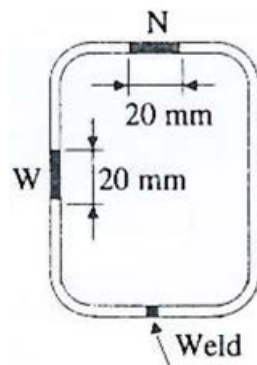


Figure 7-1 : Test coupon location in RHS cross section

The section members use in this test were Square Hollow Section (SHS) and Rectangular Hollow Section (RHS) as summarize in the table

Section	Depth (H) mm	Width (B) mm	Thickness mm
RHS-1	60	60	5
RHS-2	150	100	3
RHS-3	150	100	6

Table 7.1 : Nominal geometry for test section members

And with length variation of the section members, resulted different maximum experimental axial load as tabulated in table 7.2. CC means concentric compression and EC means eccentric compression.

Test Name	RHS - 1		RHS - 2		RHS - 3	
	length - mm	Max. Force F - kN	length - mm	Max. Force F - kN	length - mm	Max. Force F - kN
CC-2	1050	417	2700	349	2700	830
CC-3	1700	235	4350	254	4350	488
CC-4	2350	137	6000	189	6000	306
EC-2	1050	210	2700	173	2700	403
EC-3	1700	125	4350	134	4350	267
EC-4	2350	83	6000	95	6000	192

Table 7.2 : Nominal column lengths and measured maximum axial forces.

The test arrangement illustrated in the picture 7.2 :

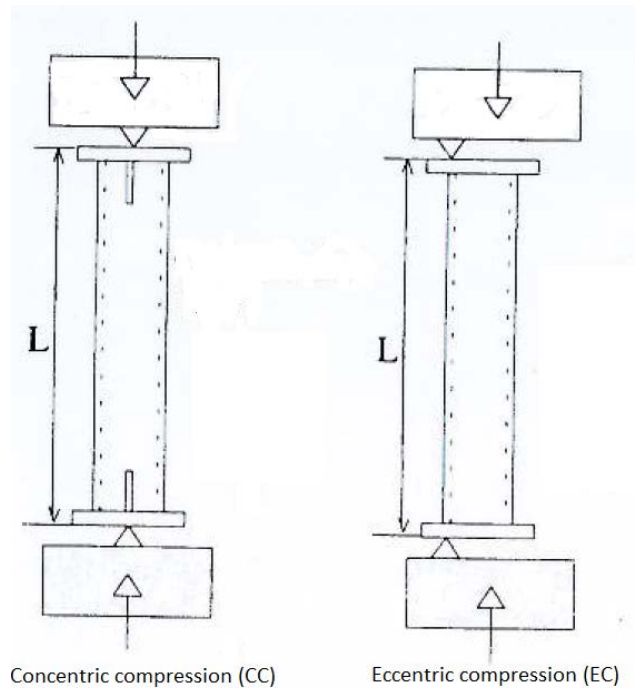


Figure 7-2 : Arrangement of column test : concentric compression and eccentric compression

**7.1. Concentric compression experimental buckling test – major axis**

There were forty two (42) section members in concentric compression test with different measured dimension and length. Table 7.3 summaries the measured geometric and mechanical properties of tested columns for all length variations and type of tests.

Section	RHS-1a/ST-1N	RHS-1a/ST-1W	RHS-1b/ST-1N	RHS-1b/ST-1W	RHS-1c/ST-1N	RHS-1c/ST-1W	RHS-2/ST-1N	RHS-2/ST-2N	RHS-2/ST-1W	RHS-2/ST-2W
<b>Test name : CC-2</b>										
Specimen length, L (mm)	1000	1000	1000	1000	1000	1000	2648	2648	2648	2648
Section depth, H (mm)	59.74	59.74	59.74	59.74	59.74	59.74	150.23	150.23	150.23	150.23
Section width, B (mm)	59.56	59.56	59.56	59.56	59.56	59.56	100.31	100.31	100.31	100.31
Thickness, t (mm)	4.83	4.84	4.9	4.88	4.7	4.71	2.79	3.04	2.79	3.04
inside radius, r (mm)	3	3	3	3	3	3	3	3	3	3
Yield strength, $f_y$ (N/mm <sup>2</sup> )	612	532	571	489	591	497	293	312	288	286
Ultimate strength, $f_u$ (N/mm <sup>2</sup> )	780	731	691	646	793	728	614	635	617	627
Modulus of elasticity E (kN/mm <sup>2</sup> )	188	182	180	182	177	191	199	190	201	197
Ramberg-Osgood coefficient, n	4.49	5.14	3.72	4.41	4.6	4.74	6.59	5.33	4.89	6.71
<b>Test name : CC-3</b>										
Specimen length, L (mm)	1650	1650	1650	1650	1650	1650	4304	4304	4304	4304
Section depth, H (mm)	59.76	59.76	59.76	59.76	59.76	59.76	150.12	150.12	150.12	150.12
Section width, B (mm)	59.63	59.63	59.63	59.63	59.63	59.63	100.33	100.33	100.33	100.33
Thickness, t (mm)	4.83	4.84	4.9	4.88	4.7	4.71	2.79	3.04	2.79	3.04
inside radius, r (mm)	3	3	3	3	3	3	3	3	3	3
Yield strength, $f_y$ (N/mm <sup>2</sup> )	612	532	571	489	591	497	293	312	288	286
Ultimate strength, $f_u$ (N/mm <sup>2</sup> )	780	731	691	646	793	728	614	635	617	627
Modulus of elasticity E (kN/mm <sup>2</sup> )	188	182	180	182	177	191	199	190	201	197
Ramberg-Osgood coefficient, n	4.49	5.14	3.72	4.41	4.6	4.74	6.59	5.33	4.89	6.71
<b>Test name : CC-4</b>										
Specimen length, L (mm)	2300	2300	2300	2300	2300	2300	5952	5952	5952	5952
Section depth, H (mm)	59.86	59.86	59.86	59.86	59.86	59.86	150.42	150.42	150.42	150.42
Section width, B (mm)	59.67	59.67	59.67	59.67	59.67	59.67	100.38	100.38	100.38	100.38
Thickness, t (mm)	4.83	4.84	4.9	4.88	4.7	4.71	2.79	3.04	2.79	3.04
inside radius, r (mm)	3	3	3	3	3	3	3	3	3	3
Yield strength, $f_y$ (N/mm <sup>2</sup> )	612	532	571	489	591	497	293	312	288	286
Ultimate strength, $f_u$ (N/mm <sup>2</sup> )	780	731	691	646	793	728	614	635	617	627
Modulus of elasticity E (kN/mm <sup>2</sup> )	188	182	180	182	177	191	199	190	201	197
Ramberg-Osgood coefficient, n	4.49	5.14	3.72	4.41	4.6	4.74	6.59	5.33	4.89	6.71

Table 7.3 : Geometric and material properties of the rectangular hollow section column specimens subject to concentric compression (RHS-1 and RHS-2)



Section	RHS-3a/ST-1N	RHS-3a/ST-2W	RHS-3b/ST-1N	RHS-3b/ST-1W
<b>Test name : CC-2</b>				
Specimen length, L (mm)	2650	2650	2650	2650
Section depth, H (mm)	149.86	149.86	149.86	149.86
Section width, B (mm)	100.14	100.14	100.14	100.14
Thickness, t (mm)	5.78	5.75	5.87	5.83
inside radius, r (mm)	5	5	5	5
Yield strength, $f_y$ (N/mm <sup>2</sup> )	402	297	388	275
Ultimate strength, $f_u$ (N/mm <sup>2</sup> )	661	638	693	651
Modulus of elasticity E (kN/mm <sup>2</sup> )	190	196	194	201
Ramberg-Osgood coefficient, n	5.85	7.87	4.52	5.53
<b>Test name : CC-3</b>				
Specimen length, L (mm)	4300	4300	4300	4300
Section depth, H (mm)	150.77	150.77	150.77	150.77
Section width, B (mm)	100.65	100.65	100.65	100.65
Thickness, t (mm)	5.78	5.75	5.87	5.83
inside radius, r (mm)	6	6	6	6
Yield strength, $f_y$ (N/mm <sup>2</sup> )	402	297	388	275
Ultimate strength, $f_u$ (N/mm <sup>2</sup> )	661	638	693	651
Modulus of elasticity E (kN/mm <sup>2</sup> )	190	196	194	201
Ramberg-Osgood coefficient, n	5.85	7.87	4.52	5.53
<b>Test name : CC-4</b>				
Specimen length, L (mm)	5950	5950	5950	5950
Section depth, H (mm)	150.6	150.6	150.6	150.6
Section width, B (mm)	100.61	100.61	100.61	100.61
Thickness, t (mm)	5.78	5.75	5.87	5.83
inside radius, r (mm)	5.5	5.5	5.5	5.5
Yield strength, $f_y$ (N/mm <sup>2</sup> )	402	297	388	275
Ultimate strength, $f_u$ (N/mm <sup>2</sup> )	661	638	693	651
Modulus of elasticity E (kN/mm <sup>2</sup> )	190	196	194	201
Ramberg-Osgood coefficient, n	5.85	7.87	4.52	5.53

Table 7.4 : Geometric and material properties of the rectangular hollow section column specimens subject to concentric compression (RHS-3)

## 7.2. Concentric compression test result and numerical investigation

The finite element section members were modelled as its measured dimension and mechanical properties as describe in table 7.3 and table 7.4. The full length model of column and boundary condition applied to simulate pinned-pinned condition as in the tests as in figure 7.2. Lateral restraints also applied at the both ends of RHS to avoid torsional and minor buckling.

Abaqus model were using shell elements with nine nodes (known as S9R5), and material considered homogenous in all sections but independent for each test coupon result.

The stress enhancements at the corner of the section as manufacture rolled effect were also ignored in the finite element model. In concentric compression, the model will applied axial force only as illustrated in figure 7-2 compression test.

Initial imperfections also introduced in the model in order to find the maximum capacity of the section members, which is :

- Global initial imperfection :  $L/1000$
- Local initial imperfection (web) :  $c/200$



Figure 7-3 : RHS-Section global imperfection mode – Abaqus visualitation

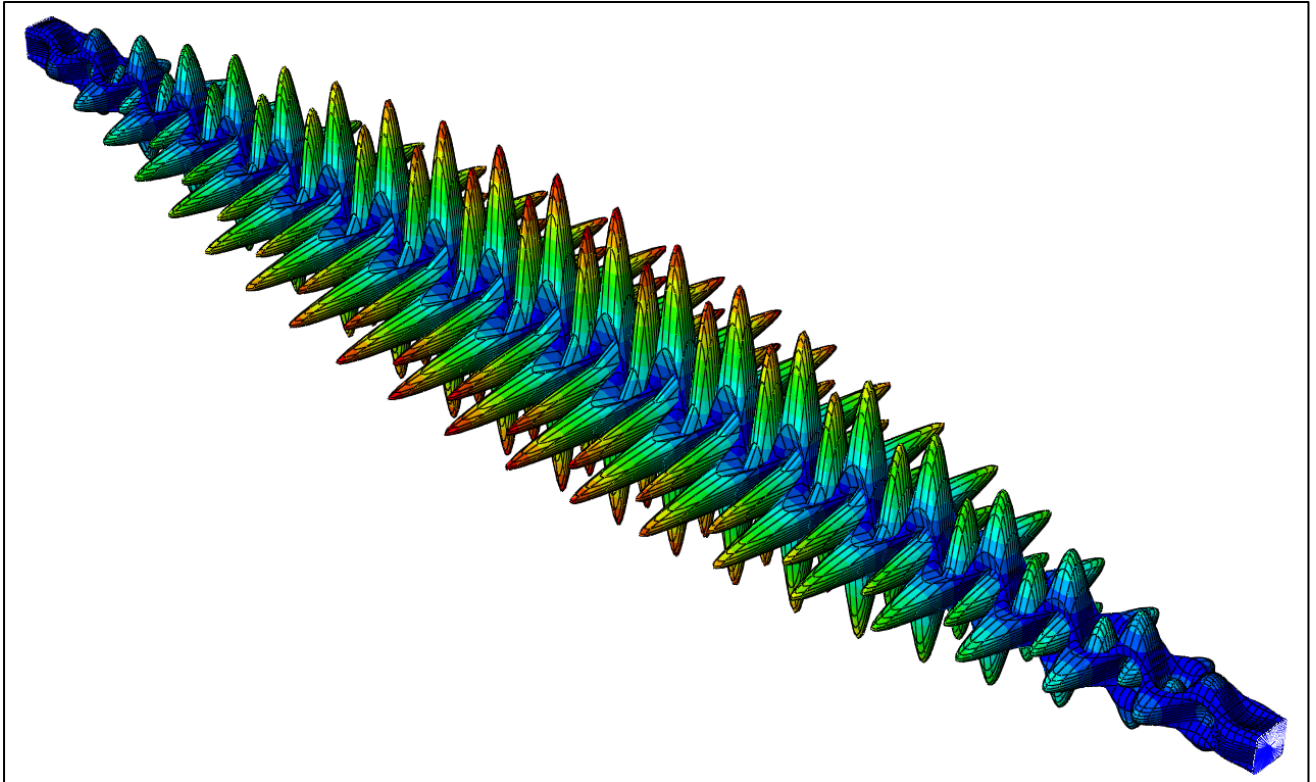


Figure 7-4 : RHS-Section local imperfection (web and flange imperfection) mode – Abaqus visualitation

From the result table 7.6, RHS-2 (RHS 150 x 100 thickness 3 mm) classified as class 4 section which required to define the effective cross section area ( $A_{eff}$ ) for calculating the effective compression member resistance ( $N_{Rd,eff}$ ). The effective cross section area can be obtained using Abaqus by adding boundary conditions to the normal compression test model in order to restrict the global buckling phenomenon. The maximum load will be then considered as effective compression member resistance ( $N_{Rd,eff}$ ).

The Abaqus model can be modelled from the section which has the longest in length as representative for all RHS-2 class 4 sections, therefore the Abaqus model geometry and length for effective area calculation will be taken from CC-4 test.

Section	RHS-1a/ST-1N	RHS-1a/ST-1W	RHS-1b/ST-1N	RHS-1b/ST-1W	RHS-1c/ST-1N	RHS-1c/ST-1W
<b>Test name : CC-2</b>						
Section class	1	1	1	1	1	1
$N_{cr, FEM}$ (kN)	894.21	866.88	864.86	871.94	825.8	892.46
$A_{eff}$ (mm <sup>2</sup> )	1014.22	1016.085	1027.252	1023.534	989.8907	991.768
$\lambda_{Theory}$	0.833	0.790	0.824	0.758	0.842	0.743
$\chi_{b,y}$ EN 1993-1-4	0.706	0.739	0.713	0.762	0.700	0.773
$N_{b,Rd, FEM}$ (kN)	444.095	395.141	421.012	372.05	416.615	368.992
Maximum Experimental Load, $N_u$ (kN)	417	417	417	417	417	417
$N_{b,Rd, FEM}/N_u$	1.065	0.948	1.010	0.892	0.999	0.885

Table 7.5 : RHS-1 Section classification, slenderness, and comparison of FE results with experimental test – concentric compression test (CC-2)

Section	RHS-2/ST-1N	RHS-2/ST-2N	RHS-2/ST-1W	RHS-2/ST-2W
<b>Test name : CC-2</b>				
Section class	4	4	4	4
$N_{cr, FEM}$ (kN)	1182.8	1222.8	1194.7	1267.9
$A_{eff}$ (mm <sup>2</sup> )	1211.72	1353.901	1222.108	1362.014
$\lambda_{Theory}$	0.548	0.588	0.543	0.554
$\chi_{b,y}$ EN 1993-1-4	0.909	0.883	0.913	0.905
$N_{b,Rd, FEM}$ (kN)	264.091	308.741	254.049	294.135
Maximum Experimental Load, $N_u$ (kN)	349	349	349	349
$N_{b,Rd, FEM}/N_u$	0.757	0.885	0.728	0.843

Table 7.6 : RHS-2 Section classification, slenderness, and comparison of FE results with experimental test – concentric compression test (CC-2)

Section	RHS-3a/ST-1N	RHS-3a/ST-2W	RHS-3b/ST-1N	RHS-3b/ST-1W
<b>Test name : CC-2</b>				
Section class	1	1	1	1
$N_{cr, FEM}$ (kN)	2120.6	2177.8	2193.5	2259.4
$A_{eff}$ (mm <sup>2</sup> )	2678.072	2665.01	2717.206	2699.823
$\lambda_{Theory}$	0.713	0.603	0.693	0.573
$\chi_{b,y}$ EN 1993-1-4	0.796	0.873	0.810	0.893
$N_{b,Rd, FEM}$ (kN)	800.37	617.603	786.64	578.39
Maximum Experimental Load, $N_u$ (kN)	830	830	830	830
$N_{b,Rd, FEM}/N_u$	0.964	0.744	0.948	0.697

Table 7.7 : RHS-3 Section classification, slenderness, and comparison of FE results with experimental test – concentric compression test (CC-2)

Section	RHS-1a/ST-1N	RHS-1a/ST-1W	RHS-1b/ST-1N	RHS-1b/ST-1W	RHS-1c/ST-1N	RHS-1c/ST-1W
<b>Test name : CC-3</b>						
Section class	1	1	1	1	1	1
$N_{cr, FEM}$ (kN)	335.3	325.08	324.31	326.95	309.64	334.66
$A_{eff}$ (mm <sup>2</sup> )	1015.089	1016.956	1028.134	1024.412	990.7367	992.6158
$\lambda_{Theory}$	1.361	1.290	1.345	1.238	1.375	1.214
$\chi_{b,y}$ EN 1993-1-4	0.382	0.415	0.389	0.441	0.376	0.454
$N_{b,Rd, FEM}$ (kN)	267.948	253.034	247.941	237.193	251.121	240.947
Maximum Experimental Load, $N_u$ (kN)	235	235	235	235	235	235
$N_{b,Rd, FEM}/N_u$	1.140	1.077	1.055	1.009	1.069	1.025

Table 7.8 : RHS-1 Section classification, slenderness, and comparison of FE results with experimental test – concentric compression test (CC-3)

Section	RHS-2/ST-1N	RHS-2/ST-2N	RHS-2/ST-1W	RHS-2/ST-2W
<b>Test name : CC-3</b>				
Section class	4	4	4	4
$N_{cr, FEM}$ (kN)	454.13	469.44	458.7	486.71
$A_{eff}$ (mm <sup>2</sup> )	1211.72	1353.901	1222.108	1362.014
$\lambda_{Theory}$	0.884	0.949	0.876	0.895
$X_{b,y}$ EN 1993-1-4	0.668	0.621	0.674	0.660
$N_{b,Rd, FEM}$ (kN)	216.688	238.79	203.158	235.895
Maximum Experimental Load, $N_u$ (kN)	254	254	254	254
$N_{b,Rd, FEM}/N_u$	0.853	0.940	0.800	0.929

Table 7.9 : RHS-2 Section classification, slenderness, and comparison of FE results with experimental test – concentric compression test (CC-3)

Section	RHS-3a/ST-1N	RHS-3a/ST-2W	RHS-3b/ST-1N	RHS-3b/ST-1W
<b>Test name : CC-3</b>				
Section class	2	1	1	1
$N_{cr, FEM}$ (kN)	826.28	848.72	854.82	880.4
$A_{eff}$ (mm <sup>2</sup> )	2684.564	2671.469	2723.799	2706.371
$\lambda_{Theory}$	1.143	0.967	1.112	0.919
$X_{b,y}$ EN 1993-1-4	0.494	0.608	0.512	0.642
$N_{b,Rd, FEM}$ (kN)	543.98	469.277	517.559	421.938
Maximum Experimental Load, $N_u$ (kN)	488	488	488	488
$N_{b,Rd, FEM}/N_u$	1.115	0.962	1.061	0.865

Table 7.10 : RHS-3 Section classification, slenderness, and comparison of FE results with experimental test – concentric compression test (CC-3)

Section	RHS-1a/ST-1N	RHS-1a/ST-1W	RHS-1b/ST-1N	RHS-1b/ST-1W	RHS-1c/ST-1N	RHS-1c/ST-1W
<b>Test name : CC-4</b>						
Section class	1	1	1	1	1	1
$N_{cr, FEM}$ (kN)	174.31	169.02	168.59	169.97	160.95	173.99
$A_{eff}$ (mm <sup>2</sup> )	1016.442	1018.311	1029.506	1025.779	992.0527	993.9346
$\lambda_{Theory}$	1.889	1.790	1.867	1.718	1.909	1.685
$\chi_{b,y}$ EN 1993-1-4	0.222	0.244	0.226	0.261	0.218	0.270
$N_{b,Rd, FEM}$ (kN)	156.143	150.425	146.109	144.752	145.157	148.177
Maximum Experimental Load, $N_u$ (kN)	137	137	137	137	137	137
$N_{b,Rd, FEM}/N_u$	1.140	1.098	1.066	1.057	1.060	1.082

Table 7.11 : RHS-1 Section classification, slenderness, and comparison of FE results with experimental test – concentric compression test (CC-4)

Section	RHS-2/ST-1N	RHS-2/ST-2N	RHS-2/ST-1W	RHS-2/ST-2W
<b>Test name : CC-4</b>				
Section class	4	4	4	4
$N_{cr, FEM}$ (kN)	239.81	247.79	242.14	256.97
$A_{eff}$ (mm <sup>2</sup> )	1211.72	1353.901	1222.108	1362.014
$\lambda_{Theory}$	1.217	1.306	1.206	1.231
$\chi_{b,y}$ EN 1993-1-4	0.452	0.408	0.458	0.445
$N_{b,Rd, FEM}$ (kN)	165.979	175.08	154.087	179.226
Maximum Experimental Load, $N_u$ (kN)	189	189	189	189
$N_{b,Rd, FEM}/N_u$	0.878	0.926	0.815	0.948

Table 7.12 : RHS-2 Section classification, slenderness, and comparison of FE results with experimental test – concentric compression test (CC-4)

Section	RHS-3a/ST-1N	RHS-3a/ST-2W	RHS-3b/ST-1N	RHS-3b/ST-1W
<b>Test name : CC-4</b>				
Section class	2	1	1	1
$N_{cr, FEM}$ (kN)	433.56	445.32	448.44	461.8
$A_{eff}$ (mm <sup>2</sup> )	2687.098	2673.99	2726.372	2708.927
$\lambda_{Theory}$	1.578	1.335	1.536	1.270
$X_{b,y}$ EN 1993-1-4	0.301	0.394	0.315	0.425
$N_{b,Rd, FEM}$ (kN)	359.926	341.196	347.647	311.897
Maximum Experimental Load, $N_u$ (kN)	306	306	306	306
$N_{b,Rd, FEM}/N_u$	1.176	1.115	1.136	1.019

Table 7.13 : RHS-3 Section classification, slenderness, and comparison of FE results with experimental test – concentric compression test (CC-4)

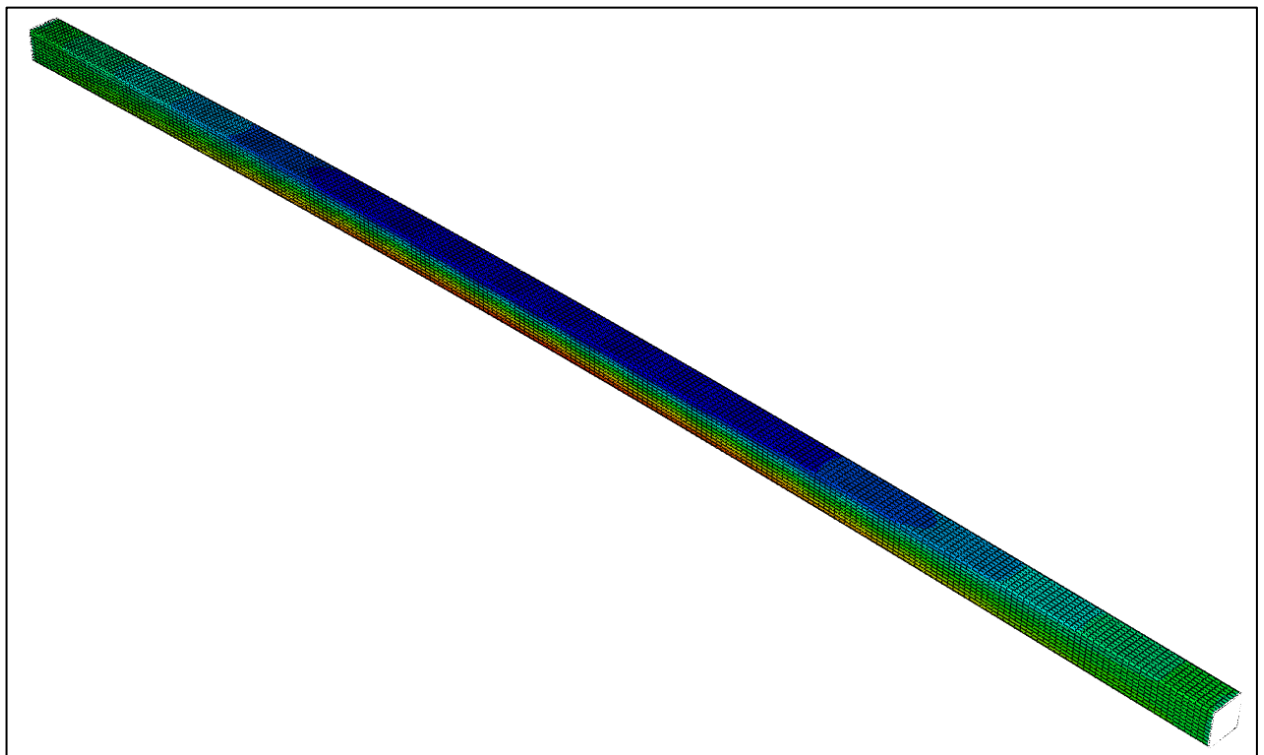


Figure 7-5 : RHS-Section Abaqus geometry non linearity result visualitation

### 7.3. Eccentric compression test

There were another forty two (42) section members for eccentric compression test which has typical dimension and length. However, in order to have reliable simulation of actual test, the numerical analysis will be modelled as its measured dimension and length. Table 7.14 summaries the measured geometric and mechanical properties of tested columns for all length variations and type of tests.



Section	RHS-1a/ST-1N	RHS-1a/ST-1W	RHS-1b/ST-1N	RHS-1b/ST-1W	RHS-1c/ST-1N	RHS-1c/ST-1W	RHS-2/ST-1N	RHS-2/ST-2N	RHS-2/ST-1W	RHS-2/ST-2W
<b>Test name : EC-2</b>										
Specimen length, L (mm)	1000	1000	1000	1000	1000	1000	2650	2650	2650	2650
Section depth, H (mm)	59.75	59.75	59.75	59.75	59.75	59.75	150.21	150.21	150.21	150.21
Section width, B (mm)	59.56	59.56	59.56	59.56	59.56	59.56	100.31	100.31	100.31	100.31
Thickness, t (mm)	4.83	4.84	4.9	4.88	4.7	4.71	2.79	3.04	2.79	3.04
inside radius, r (mm)	3	3	3	3	3	3	2.5	2.5	2.5	2.5
Yield strength, $f_y$ (N/mm <sup>2</sup> )	612	532	571	489	591	497	293	312	288	286
Ultimate strength, $f_u$ (N/mm <sup>2</sup> )	780	731	691	646	793	728	614	635	617	627
Modulus of elasticity E (kN/mm <sup>2</sup> )	188	182	180	182	177	191	199	190	201	197
Ramberg-Osgood coefficient, n	4.49	5.14	3.72	4.41	4.6	4.74	6.59	5.33	4.89	6.71
<b>Test name : EC-3</b>										
Specimen length, L (mm)	1649	1649	1649	1649	1649	1649	4297	4297	4297	4297
Section depth, H (mm)	59.76	59.76	59.76	59.76	59.76	59.76	150.62	150.62	150.62	150.62
Section width, B (mm)	59.42	59.42	59.42	59.42	59.42	59.42	100.36	100.36	100.36	100.36
Thickness, t (mm)	4.83	4.84	4.9	4.88	4.7	4.71	2.79	3.04	2.79	3.04
inside radius, r (mm)	3.5	3.5	3.5	3.5	3.5	3.5	2.5	2.5	2.5	2.5
Yield strength, $f_y$ (N/mm <sup>2</sup> )	612	532	571	489	591	497	293	312	288	286
Ultimate strength, $f_u$ (N/mm <sup>2</sup> )	780	731	691	646	793	728	614	635	617	627
Modulus of elasticity E (kN/mm <sup>2</sup> )	188	182	180	182	177	191	199	190	201	197
Ramberg-Osgood coefficient, n	4.49	5.14	3.72	4.41	4.6	4.74	6.59	5.33	4.89	6.71
<b>Test name : EC-4</b>										
Specimen length, L (mm)	2300	2300	2300	2300	2300	2300	5950	5950	5950	5950
Section depth, H (mm)	59.79	59.79	59.79	59.79	59.79	59.79	150.23	150.23	150.23	150.23
Section width, B (mm)	59.44	59.44	59.44	59.44	59.44	59.44	100.23	100.23	100.23	100.23
Thickness, t (mm)	4.83	4.84	4.9	4.88	4.7	4.71	2.79	3.04	2.79	3.04
inside radius, r (mm)	3	3	3	3	3	3	3	3	3	3
Yield strength, $f_y$ (N/mm <sup>2</sup> )	612	532	571	489	591	497	293	312	288	286
Ultimate strength, $f_u$ (N/mm <sup>2</sup> )	780	731	691	646	793	728	614	635	617	627
Modulus of elasticity E (kN/mm <sup>2</sup> )	188	182	180	182	177	191	199	190	201	197
Ramberg-Osgood coefficient, n	4.49	5.14	3.72	4.41	4.6	4.74	6.59	5.33	4.89	6.71

Table 7.14 : Geometric and material properties of the rectangular hollow section column specimens subject to eccentric compression (RHS-1 and RHS-2)

Section	RHS-3a/ST-1N	RHS-3a/ST-2W	RHS-3b/ST-1N	RHS-3b/ST-1W
<b>Test name : EC-2</b>				
Specimen length, L (mm)	2649	2649	2649	2649
Section depth, H (mm)	149.44	149.44	149.44	149.44
Section width, B (mm)	100.12	100.12	100.12	100.12
Thickness, t (mm)	5.78	5.75	5.87	5.83
inside radius, r (mm)	5	5	5	5
Yield strength, $f_y$ (N/mm <sup>2</sup> )	402	297	388	275
Ultimate strength, $f_u$ (N/mm <sup>2</sup> )	661	638	693	651
Modulus of elasticity E (kN/mm <sup>2</sup> )	190	196	194	201
Ramberg-Osgood coefficient, n	5.85	7.87	4.52	5.53
<b>Test name : EC-3</b>				
Specimen length, L (mm)	4296	4296	4296	4296
Section depth, H (mm)	150.45	150.45	150.45	150.45
Section width, B (mm)	100.63	100.63	100.63	100.63
Thickness, t (mm)	5.78	5.75	5.87	5.83
inside radius, r (mm)	5.5	5.5	5.5	5.5
Yield strength, $f_y$ (N/mm <sup>2</sup> )	402	297	388	275
Ultimate strength, $f_u$ (N/mm <sup>2</sup> )	661	638	693	651
Modulus of elasticity E (kN/mm <sup>2</sup> )	190	196	194	201
Ramberg-Osgood coefficient, n	5.85	7.87	4.52	5.53
<b>Test name : EC-4</b>				
Specimen length, L (mm)	5948	5948	5948	5948
Section depth, H (mm)	150.57	150.57	150.57	150.57
Section width, B (mm)	100.58	100.58	100.58	100.58
Thickness, t (mm)	5.78	5.75	5.87	5.83
inside radius, r (mm)	6.5	6.5	6.5	6.5
Yield strength, $f_y$ (N/mm <sup>2</sup> )	402	297	388	275
Ultimate strength, $f_u$ (N/mm <sup>2</sup> )	661	638	693	651
Modulus of elasticity E (kN/mm <sup>2</sup> )	190	196	194	201
Ramberg-Osgood coefficient, n	5.85	7.87	4.52	5.53

Table 7.15 : Geometric and material properties of the rectangular hollow section column specimens subject to eccentric compression (RHS-3)

#### 7.4. Eccentric compression test result and numerical investigation

The same procedure for numerical analysis as in chapter 7.2, all the section members modelled and simulated as its geometry and mechanical properties in table 7.14 and table 7.15.

The full length model of column and boundary condition were applied to simulate pinned-pinned condition as actual experimental test condition as shown in figure 7.2. Lateral restraints also applied at the both ends of RHS to avoid torsional and minor buckling.

The Abaqus model has the same element type as in concentric test which is nine nodes shell elements (element S9R5), and material considered homogenous in all sections and neglecting the stress enhancements at the corner of the section.

The groove for compression test was positioned at the edge of the section, therefore the applied load will have eccentricity effect leads to bending moment accordingly. Hence, the applied will be combined axial load and bending moment due to eccentricity

Initial imperfections applied the same as in concentric compression test (chapter 7.2), which is:

- Global initial imperfection :  $L/1000$
- Local initial imperfection (web) :  $c/200$

The result table 7.1 shows that RHS-2 (RHS 150 x 100 thickness 3 mm) classified as class 4 section. Therefore the effective cross section area ( $A_{eff}$ ) will be defined by calculating the effective compression member resistance ( $N_{Rd,eff}$ ). The effective member resistance can be obtained using Abaqus by applying the concentric compression only to the section members and adding boundary conditions to the model in order to restrict the global buckling phenomenon. The maximum load will be then considered as effective compression member resistance ( $N_{Rd,eff}$ ).

The Abaqus model can be modelled from the section which has the longest in length as representative for all RHS-2 class 4 sections, therefore the Abaqus model geometry and length for effective area calculation will be taken from EC-4 test, but with concentric compressions were applied.

Section	RHS-1a/ST-1N	RHS-1a/ST-1W	RHS-1b/ST-1N	RHS-1b/ST-1W	RHS-1c/ST-1N	RHS-1c/ST-1W
<b>Test name : EC-2</b>						
Section class	1.00	1.00	1.00	1.00	1.00	1.00
$N_{cr, FEM}$ (kN)	894.61	867.40	865.27	872.50	826.05	892.72
$A_{eff}$ (mm <sup>2</sup> )	1014.32	1016.18	1027.35	1023.63	989.98	991.86
$\lambda_{Theory}$	0.83	0.79	0.82	0.76	0.84	0.74
$\chi_{b,y}$ EN 1993-1-4	0.71	0.74	0.71	0.76	0.70	0.77
$N_{b,Rd, FEM}$ (kN)	218.23	196.08	205.20	183.52	205.42	183.33
Maximum Experimental Load, $N_u$ (kN)	210.00	210.00	210.00	210.00	210.00	210.00
$N_{b,Rd, FEM}/N_u$	1.04	0.93	0.98	0.87	0.98	0.87

Table 7.16 : RHS-1 Section classification, slenderness, and comparison of FE results with experimental test – concentric compression test (EC-2)

Section	RHS-2/ST-1N	RHS-2/ST-2N	RHS-2/ST-1W	RHS-2/ST-2W
<b>Test name : EC-2</b>				
Section class	4.00	4.00	4.00	4.00
$N_{cr, FEM}$ (kN)	1184.20	1224.40	1196.10	1269.50
$A_{eff}$ (mm <sup>2</sup> )	1209.71	849.42	964.38	747.20
$\lambda_{Theory}$	0.55	0.47	0.48	0.41
$\chi_{b,y}$ EN 1993-1-4	0.91	0.96	0.95	0.99
$N_{b,Rd, FEM}$ (kN)	124.22	146.42	121.60	139.51
Maximum Experimental Load, $N_u$ (kN)	173.00	173.00	173.00	173.00
$N_{b,Rd, FEM}/N_u$	0.72	0.85	0.70	0.81

Table 7.17 : RHS-2 Section classification, slenderness, and comparison of FE results with experimental test – concentric compression test (EC-2)

Section	RHS-3a/ST-1N	RHS-3a/ST-2W	RHS-3b/ST-1N	RHS-3b/ST-1W
<b>Test name : EC-2</b>				
Section class	1.00	1.00	1.00	1.00
$N_{cr, FEM}$ (kN)	2107.20	2164.40	2180.20	2245.50
$A_{eff}$ (mm <sup>2</sup> )	2672.99	2659.95	2712.04	2694.69
$\lambda_{Theory}$	0.71	0.60	0.69	0.57
$\chi_{b,y}$ EN 1993-1-4	0.79	0.87	0.81	0.89
$N_{b,Rd, FEM}$ (kN)	382.93	298.91	376.61	282.04
Maximum Experimental Load, $N_u$ (kN)	403.00	403.00	403.00	403.00
$N_{b,Rd, FEM}/N_u$	0.95	0.74	0.93	0.70

Table 7.18 : RHS-3 Section classification, slenderness, and comparison of FE results with experimental test – concentric compression test (EC-2)

Section	RHS-1a/ST-1N	RHS-1a/ST-1W	RHS-1b/ST-1N	RHS-1b/ST-1W	RHS-1c/ST-1N	RHS-1c/ST-1W
<b>Test name : EC-3</b>						
Section class	1.00	1.00	1.00	1.00	1.00	1.00
$N_{cr, FEM}$ (kN)	332.32	322.27	321.42	324.05	306.88	331.71
$A_{eff}$ (mm <sup>2</sup> )	1008.91	1010.77	1021.87	1018.17	984.73	986.59
$\lambda_{Theory}$	1.36	1.29	1.35	1.24	1.38	1.22
$\chi_{b,y}$ EN 1993-1-4	0.38	0.41	0.39	0.44	0.38	0.45
$N_{b,Rd, FEM}$ (kN)	144.21	132.24	135.67	124.94	135.02	125.37
Maximum Experimental Load, $N_u$ (kN)	125.00	125.00	125.00	125.00	125.00	125.00
$N_{b,Rd, FEM}/N_u$	1.15	1.06	1.09	1.00	1.08	1.00

Table 7.19 : RHS-1 Section classification, slenderness, and comparison of FE results with experimental test – concentric compression test (EC-3)

Section	RHS-2/ST-1N	RHS-2/ST-2N	RHS-2/ST-1W	RHS-2/ST-2W
<b>Test name : EC-3</b>				
Section class	4.00	4.00	4.00	4.00
$N_{cr, FEM}$ (kN)	460.73	476.31	465.36	493.82
$A_{eff}$ (mm <sup>2</sup> )	1209.71	849.42	964.38	747.20
$\lambda_{Theory}$	0.88	0.75	0.77	0.66
$X_{b,y}$ EN 1993-1-4	0.67	0.77	0.75	0.83
$N_{b,Rd, FEM}$ (kN)	105.04	119.16	101.30	116.06
Maximum Experimental Load, $N_u$ (kN)	134.00	134.00	134.00	134.00
$N_{b,Rd, FEM}/N_u$	0.78	0.89	0.76	0.87

Table 7.20 : RHS-2 Section classification, slenderness, and comparison of FE results with experimental test – concentric compression test (EC-3)

Section	RHS-3a/ST-1N	RHS-3a/ST-2W	RHS-3b/ST-1N	RHS-3b/ST-1W
<b>Test name : EC-3</b>				
Section class	2.00	1.00	1.00	1.00
$N_{cr, FEM}$ (kN)	826.20	848.52	854.51	880.44
$A_{eff}$ (mm <sup>2</sup> )	2685.60	2672.49	2724.85	2707.41
$\lambda_{Theory}$	1.14	0.97	1.11	0.92
$X_{b,y}$ EN 1993-1-4	0.49	0.61	0.51	0.64
$N_{b,Rd, FEM}$ (kN)	278.17	230.57	271.45	215.41
Maximum Experimental Load, $N_u$ (kN)	267.00	267.00	267.00	267.00
$N_{b,Rd, FEM}/N_u$	1.04	0.86	1.02	0.81

Table 7.21 : RHS-3 Section classification, slenderness, and comparison of FE results with experimental test – concentric compression test (EC-3)

Section	RHS-1a/ST-1N	RHS-1a/ST-1W	RHS-1b/ST-1N	RHS-1b/ST-1W	RHS-1c/ST-1N	RHS-1c/ST-1W
<b>Test name : EC-4</b>						
Section class	1.00	1.00	1.00	1.00	1.00	1.00
$N_{cr, FEM}$ (kN)	173.18	167.95	167.55	168.87	159.99	172.87
$A_{eff}$ (mm <sup>2</sup> )	1013.54	1015.41	1026.57	1022.85	989.23	991.11
$\lambda_{Theory}$	1.89	1.79	1.87	1.72	1.91	1.69
$X_{b,y}$ EN 1993-1-4	0.22	0.24	0.23	0.26	0.22	0.27
$N_{b,Rd, FEM}$ (kN)	99.33	93.11	92.84	88.23	92.80	89.35
Maximum Experimental Load, $N_u$ (kN)	83.00	83.00	83.00	83.00	83.00	83.00
$N_{b,Rd, FEM}/N_u$	1.20	1.12	1.12	1.06	1.12	1.08

Table 7.22 : RHS-1 Section classification, slenderness, and comparison of FE results with experimental test – concentric compression test (EC-4)

Section	RHS-2/ST-1N	RHS-2/ST-2N	RHS-2/ST-1W	RHS-2/ST-2W
<b>Test name : EC-4</b>				
Section class	4.00	4.00	4.00	4.00
$N_{cr, FEM}$ (kN)	239.16	247.15	241.51	256.29
$A_{eff}$ (mm <sup>2</sup> )	1209.71	849.42	964.38	747.20
$\lambda_{Theory}$	1.22	1.04	1.07	0.91
$X_{b,y}$ EN 1993-1-4	0.45	0.56	0.54	0.65
$N_{b,Rd, FEM}$ (kN)	84.61	92.71	80.49	92.34
Maximum Experimental Load, $N_u$ (kN)	95.00	95.00	95.00	95.00
$N_{b,Rd, FEM}/N_u$	0.89	0.98	0.85	0.97

Table 7.23 : RHS-2 Section classification, slenderness, and comparison of FE results with experimental test – concentric compression test (EC-4)

Section	RHS-3a/ST-1N	RHS-3a/ST-2W	RHS-3b/ST-1N	RHS-3b/ST-1W
<b>Test name : EC-4</b>				
Section class	2.00	1.00	1.00	1.00
$N_{cr, FEM}$ (kN)	430.45	442.17	445.32	458.82
$A_{eff}$ (mm <sup>2</sup> )	2676.48	2663.43	2715.59	2698.22
$\lambda_{Theory}$	1.58	1.34	1.54	1.27
$X_{b,y}$ EN 1993-1-4	0.30	0.39	0.31	0.42
$N_{b,Rd, FEM}$ (kN)	202.42	177.28	196.06	164.81
Maximum Experimental Load, $N_u$ (kN)	192.00	192.00	192.00	192.00
$N_{b,Rd, FEM}/N_u$	1.05	0.92	1.02	0.86

Table 7.24 : RHS-3 Section classification, slenderness, and comparison of FE results with experimental test – concentric compression test (EC-4)

### 8. Summary of comparison FE results and experimental test

The I-section comparison results, both concentric and eccentric test, showed that the finite element simulation and experimental test result were giving typically the same results as summarize in table 8.1.

	Average	Standard Deviation
$N_{b,Rd, FEM}/N_u$ - imperfection 1	1.055	0.096
$N_{b,Rd, FEM}/N_u$ - imperfection 2	0.950	0.043
$N_{b,Rd, FEM}/N_u$ - imperfection 3	0.949	0.043

Table 8.1 : I-Section comparison result (Average and standard deviation)

Table 8.1 shows the average and standard deviation of overall finite element result of  $N_{b,Rd, FEM}/N_u$ , where  $N_u$  is maximum experimental load, have reasonable results for all applied initial imperfections. However, individual comparison shows imperfection 1 (table 6.2) were more acceptable and applicable for the finite element simulation as it is giving more reliable imperfection value for global and local imperfection of section members as also applied in standard code EN 1993-1-5.

As highlighted also in this simulation, the Duplex section members 160 x 160, the ratio  $N_{b,Rd, FEM}/N_u$  have better resistance for imperfection 1, as in other hand imperfection 2 and imperfection 3 giving low ratio  $N_{b,Rd, FEM}/N_u$ .

The finite element models for I-Section material were split independently for flange (upper and bottom flange) and web, and ignored the residual stress due to welding. Hence the web and flange material modelled with based material properties from the test as shown in table 6.1 and table 6.5.



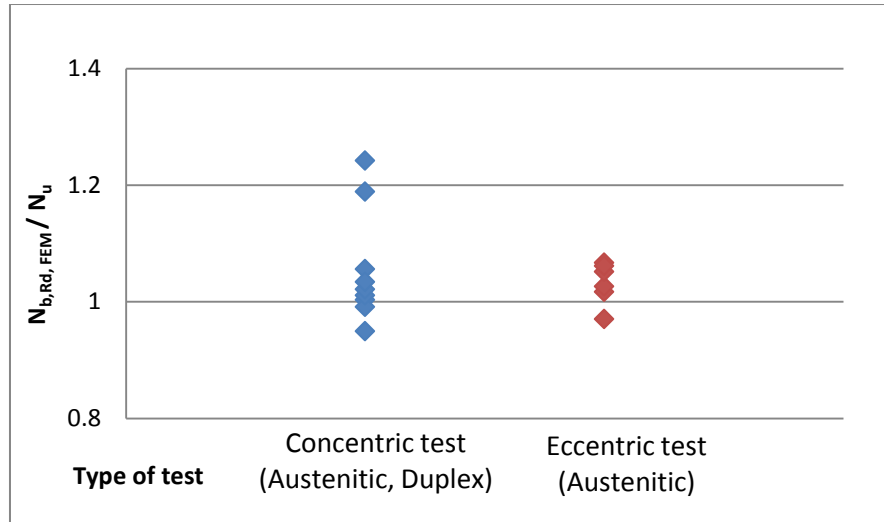


Figure 8-1 : I-Section comparison data distribution (Axial force ratio Vs Concentric and Eccentric test)

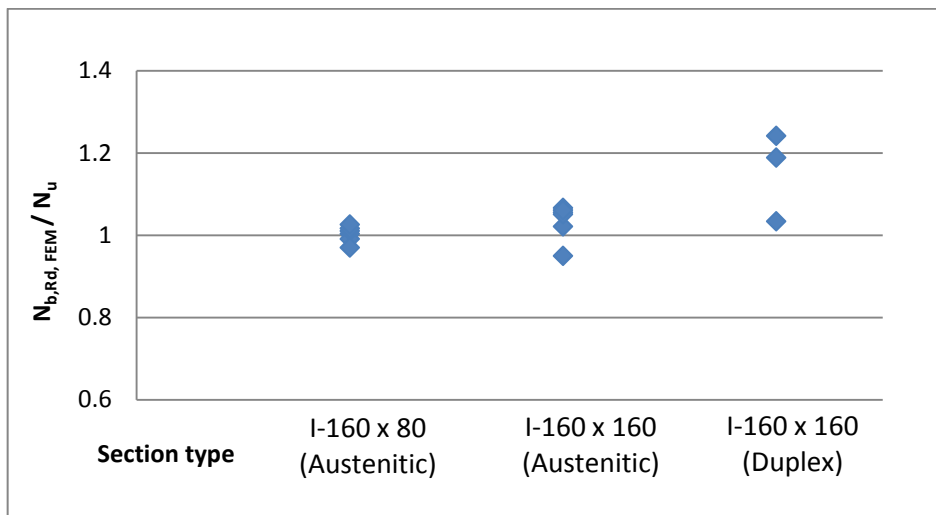


Figure 8-2 : I-Section comparison data distribution (Axial force ratio Vs Section member type)

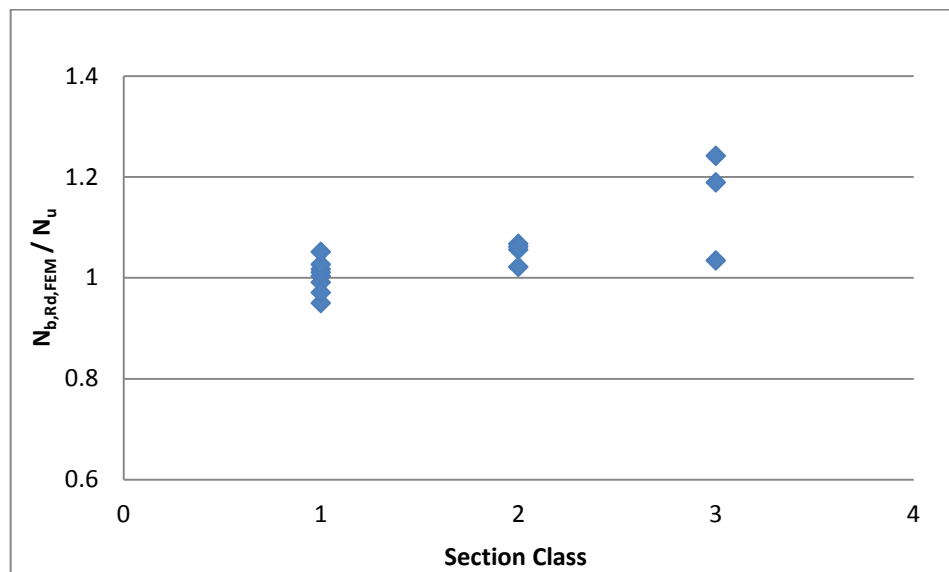


Figure 8-3 : I-Section comparison data distribution (Axial force ratio Vs Section class)

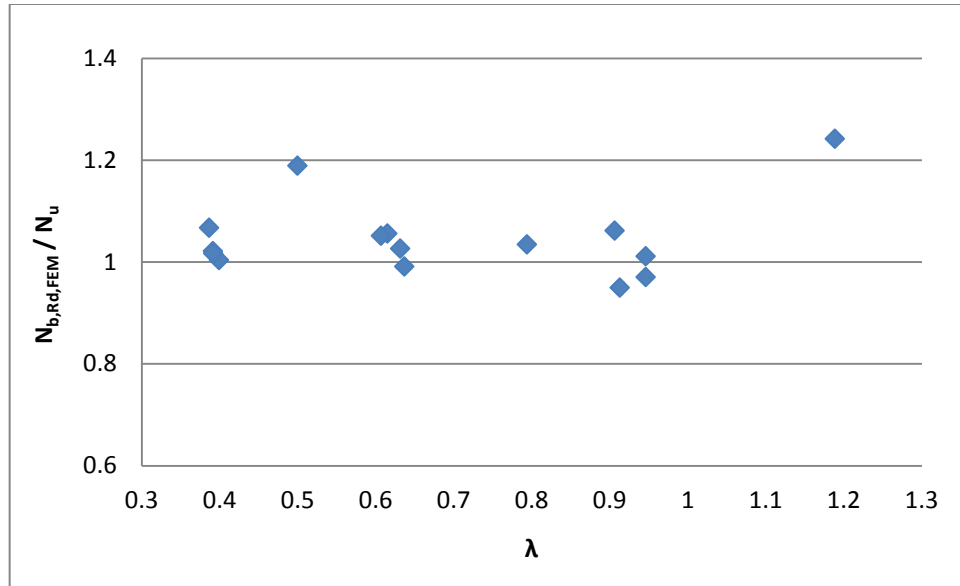


Figure 8-4 : I-Section comparison data distribution (Axial force ratio Vs slenderness,  $\lambda$ )

For Rectangular Hollow Section (RHS section members) test, the comparison finite element simulation and experimental test summarize in table 8.2.

Section	RHS-1	RHS-2	RHS-3	Test type
Average Nb,Rd, FEM (kN)	402.98	280.25	695.75	CC2
Average of Maximum Experimental Load, Nu (kN)	417.00	349.00	830.00	
$N_{b,Rd, FEM} / N_u$	0.97	0.80	0.84	
Average Nb,Rd, FEM (kN)	249.70	223.63	488.19	CC3
Average of Maximum Experimental Load, Nu (kN)	235.00	254.00	488.00	
$N_{b,Rd, FEM} / N_u$	1.06	0.88	1.00	
Average Nb,Rd, FEM (kN)	148.46	168.59	340.17	CC4
Average of Maximum Experimental Load, Nu (kN)	137.00	189.00	306.00	
$N_{b,Rd, FEM} / N_u$	1.08	0.89	1.11	
Average Nb,Rd, FEM (kN)	198.63	132.94	335.12	EC2
Average of Maximum Experimental Load, Nu (kN)	210.00	173.00	403.00	
$N_{b,Rd, FEM} / N_u$	0.95	0.77	0.83	
Average Nb,Rd, FEM (kN)	132.91	110.39	248.90	EC3
Average of Maximum Experimental Load, Nu (kN)	125.00	134.00	267.00	
$N_{b,Rd, FEM} / N_u$	1.06	0.82	0.93	
Average Nb,Rd, FEM (kN)	92.61	87.54	185.14	EC4
Average of Maximum Experimental Load, Nu (kN)	83.00	95.00	192.00	
$N_{b,Rd, FEM} / N_u$	1.12	0.92	0.96	

Table 8.2 : RHS comparison of Average FE results with experimental test

In modelling rectangular hollow section (RHS) for comparing the finite element simulation and the experimental test result [17], there are some highlights which impact to the result of comparison:

1. The RHS members were modelled using base material properties and measured thickness which presented in table 7.3, table 7.4, table 7.14, and table 7.15 which originally extracted from appendix 1/1 of tensile experimental test report [17], and the finite element models also ignored the stress enhancement at the corner of RHS sections as effect of cold or rolled formed manufacturing process.
2. The material properties considered homogenous and independent, therefore each test coupons of material properties (narrow and wide face) considered as different type of section members.
3. The maximum experimental load tests for comparison study were singular test value as tabulated in table 7.2 which mean that either the test result value were taken from single test result or average of maximum experimental load.
4. In this thesis, refer to point 1 and point 2 regarding material properties, RHS-1 modelled in six (6) variations of materials, RHS-2 modelled in four (4) variations of materials, and RHS-3 modelled in four (4) variations of materials. And these variation models were applied for both Concentric Test and Eccentric Test. So there were forty two (42) models for each test types, and in total eighty four (84) models.
5. The finite element models also ignored the residual stress effect of the welding of RHS manufacturing process.

The mentioned modelling conditions have merely influenced the validity of comparison study for rectangular hollow section (RHS). However, considering the factors above, the difference variance can be considered that the finite element simulation and experimental test tends to give nearly the same results.

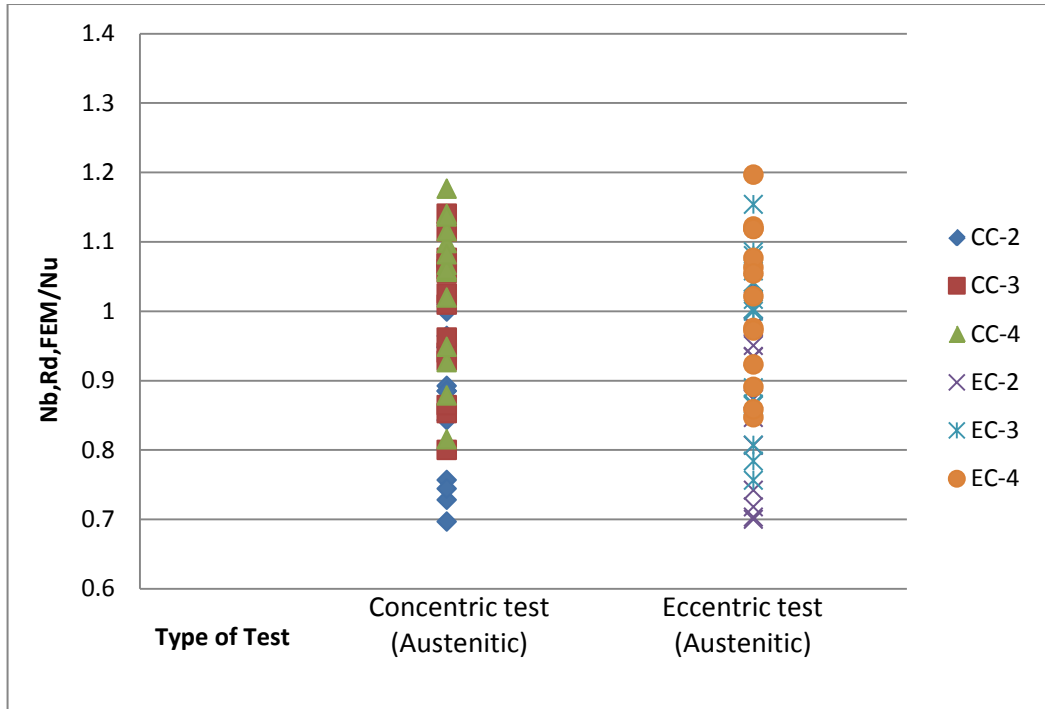


Figure 8-5 : RHS-Section comparison data distribution (Axial force ratio Vs Concentric and Eccentric test)

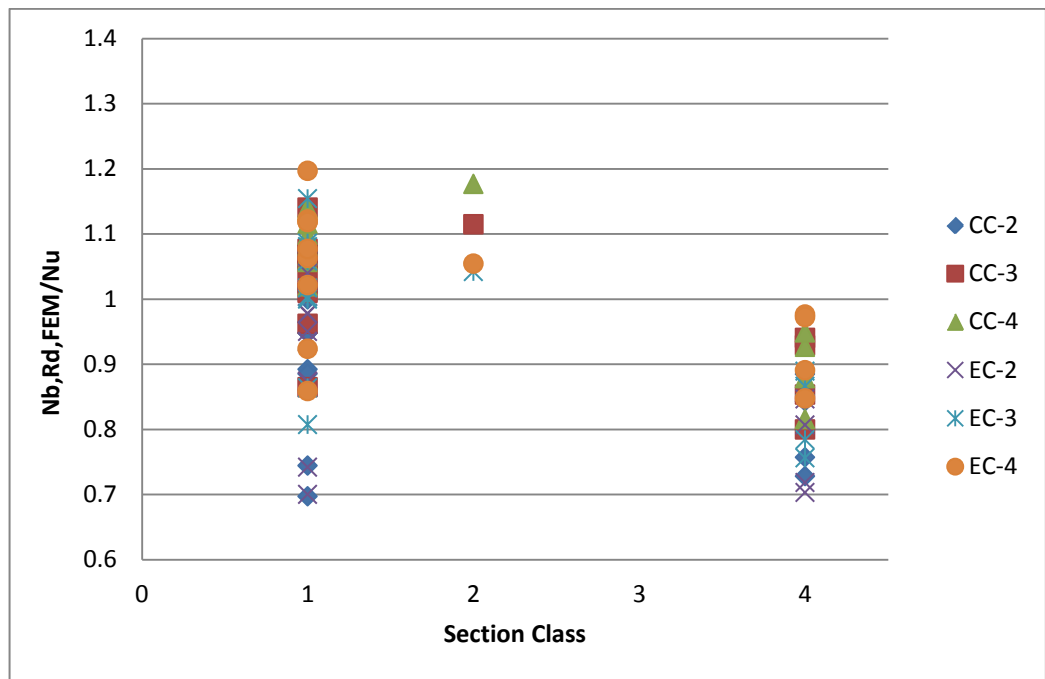


Figure 8-6 : RHS-Section comparison data distribution (Axial force ratio Vs Section class)

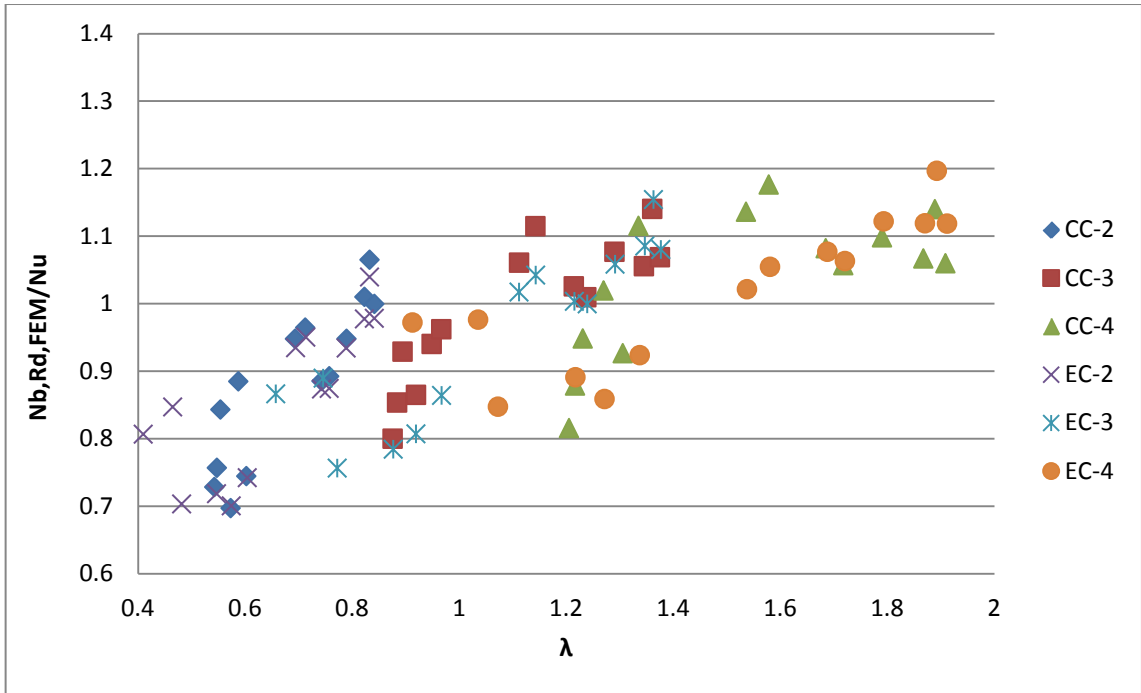


Figure 8-7 : RHS-Section comparison data distribution (Axial force ratio Vs slenderness,  $\lambda$ )

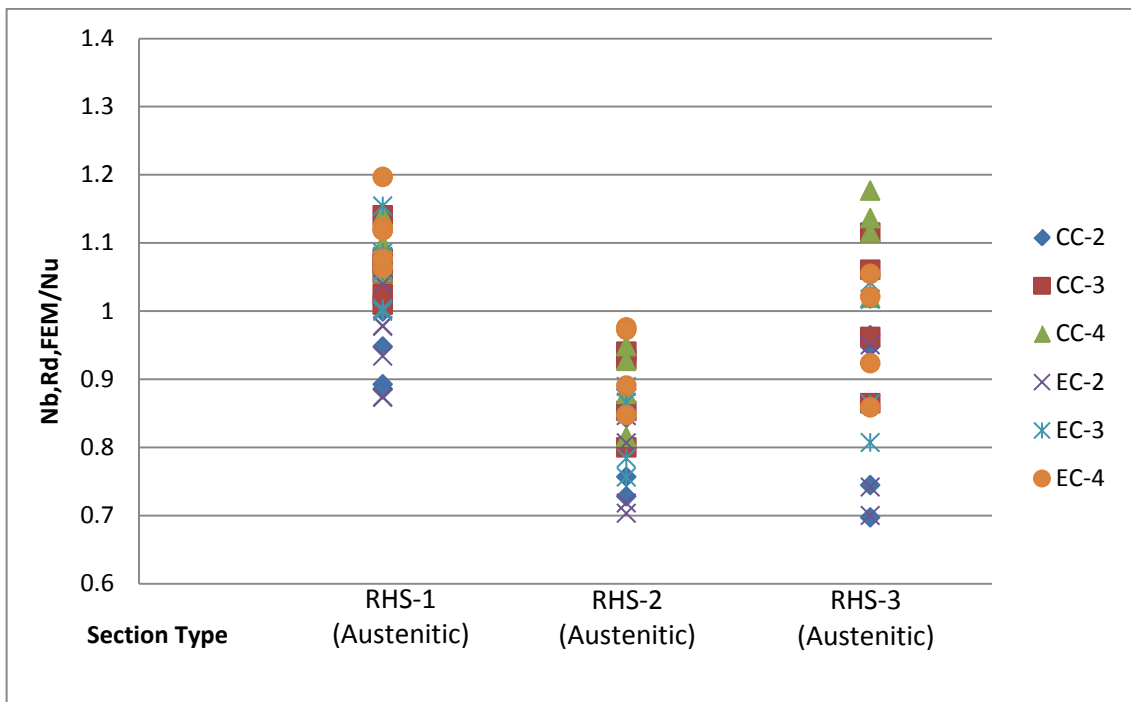


Figure 8-8 : RHS-Section comparison data distribution (Axial force ratio Vs Section member type)

## 9. Parametric study

In order to have more detailed data for axial force and bending moment interaction relation of stainless steel members, a parametric study was carried out. In this parametric study, the activities cover:

- a. The finite element simulations for investigating various relative slenderness in particular material properties (austenitic, ferritic, and duplex), as parameters in order to have the axial force and bending interaction relation.
- b. Comparison the parametric results with some axial force and bending interaction relation formulas proposed by standard codes (Eurocode) and some researcher's approaches (published journals)
  - Eurocode EN 1993-1-4
  - Eurocode EN 1993-1-1 Method 1
  - Eurocode EN 1993-1-1 Method 2
  - ENV 1993-1-1
  - Lopes, Real, and Silva proposed approach interaction formula [15]
  - Greiner and Kettler proposed approach interaction formula [13]
  - Talja and Salmi proposed approach interaction formula [17]
- c. As stainless steel material properties have similar rounded  $\sigma$ - $\epsilon$  relation diagram as aluminium, investigating and comparing the parametric results using aluminium interaction formula would be necessary, in order to find the correlation of interaction axial compression and bending moment equation for aluminium corresponds to stainless steel parametric study result.
  - Aluminium 1, General Aluminium formula with calculated for the variables as describe in Chapter 3.10 ( $\xi_{yc} = \xi_0 \chi_y$ , and  $\psi_c = 1.3 \chi_y$ )
  - Aluminium 2, General Aluminium formula, but using the constant values for the variables ( $\psi_c = 0.8$ , and  $\xi_{yc} = 0.8$ )

The material properties used in this parametric study will be the same for all section members and all type of test (compression, eccentric, and bending simulation test).

The material considered homogenous for all sections (web and flange for I-section and for RHS section). The material properties based on EN 1993-1-4 and enhancement amendment recommendation from Afshan, Rossi and Gardner research journal [19]

Material	Grade	E <sub>0</sub> (Gpa)	σ <sub>0,2</sub> (Mpa)	σ <sub>u</sub> (Mpa)	n
Austenitic	1.4301	200	230	540	5.6
Ferritic	1.4003	200	280	450	7.9
Duplex	1.4462	200	480	660	7.2

Table 9.1 : Material properties for parametric study

The finite element models were based on typical section members' geometric for both I-Sections and RHS sections as summarize in table 9.2, table 9.3, table 9.4, and table 9.5.

Section	SHS 60 X 60 X 5	SHS 60 X 60 X 5	SHS 60 X 60 X 5	SHS 60 X 60 X 5	SHS 60 X 60 X 5	SHS 60 X 60 X 5	SHS 60 X 60 X 5	SHS 60 X 60 X 5	SHS 60 X 60 X 5
Steel material	Austenitic	Austenitic	Austenitic	Ferritic	Ferritic	Ferritic	Duplex	Duplex	Duplex
Steel Grade material	1.4301	1.4301	1.4301	1.4003	1.4003	1.4003	1.4462	1.4462	1.4462
Load variation, ψ	1	1	1	1	1	1	1	1	1
Specimen length, L (mm)	1050	1700	2350	1050	1700	2350	1050	1700	2350
Section depth, H (mm)	59.78	59.78	59.78	59.78	59.78	59.78	59.78	59.78	59.78
Section width, B (mm)	59.55	59.55	59.55	59.55	59.55	59.55	59.55	59.55	59.55
Thickness, t (mm)	4.81	4.81	4.81	4.81	4.81	4.81	4.81	4.81	4.81
internal corner radius, r <sub>i</sub> (mm)	3	3	3	3	3	3	3	3	3

Table 9.2 : Dimension of SHS 60 x 60 x 5 column specimens (ψ = 1)

Section	SHS 60 X 60 X 5	SHS 60 X 60 X 5	SHS 60 X 60 X 5	SHS 60 X 60 X 5	SHS 60 X 60 X 5	SHS 60 X 60 X 5
Steel material	Austenitic	Austenitic	Austenitic	Austenitic	Austenitic	Austenitic
Steel Grade material	1.4301	1.4301	1.4301	1.4301	1.4301	1.4301
Load variation, ψ	0	0	0	-1	-1	-1
Specimen length, L (mm)	1050	1700	2350	1050	1700	2350
Section depth, H (mm)	59.78	59.78	59.78	59.78	59.78	59.78
Section width, B (mm)	59.55	59.55	59.55	59.55	59.55	59.55
Thickness, t (mm)	4.81	4.81	4.81	4.81	4.81	4.81
internal corner radius, r <sub>i</sub> (mm)	3	3	3	3	3	3

Table 9.3 : Dimension of SHS 60 x 60 x 5 column specimens (ψ = 0 and ψ = -1)

Section	RHS 150 X 100 X 3	RHS 150 X 100 X 3	RHS 150 X 100 X 3	RHS 150 X 100 X 3	RHS 150 X 100 X 3	RHS 150 X 100 X 3	RHS 150 X 100 X 3	RHS 150 X 100 X 3	RHS 150 X 100 X 3
Steel material	Austenitic	Austenitic	Austenitic	Ferritic	Ferritic	Ferritic	Duplex	Duplex	Duplex
Steel Grade material	1.4301	1.4301	1.4301	1.4003	1.4003	1.4003	1.4462	1.4462	1.4462
Load variation, $\psi$	1	1	1	1	1	1	1	1	1
Specimen length, L (mm)	2700	4350	6000	2700	4350	6000	2700	4350	6000
Section depth, H (mm)	150.31	150.31	150.31	150.31	150.31	150.31	150.31	150.31	150.31
Section width, B (mm)	100.34	100.34	100.34	100.34	100.34	100.34	100.34	100.34	100.34
Thickness, t (mm)	2.92	2.92	2.92	2.92	2.92	2.92	2.92	2.92	2.92
internal corner radius, $r_i$ (mm)	3	3	3	3	3	3	3	3	3

Table 9.4 : Dimension of RHS 150 x 100 x 3 column specimens ( $\psi = 1$ )

Section	I 160 X 80	I 160 X 80	I 160 X 80	I 160 X 80	I 160 X 80	I 160 X 80	I 160 X 80	I 160 X 80	I 160 X 80
Steel material	Austenitic	Austenitic	Austenitic	Ferritic	Ferritic	Ferritic	Duplex	Duplex	Duplex
Steel Grade material	1.4301	1.4301	1.4301	1.4003	1.4003	1.4003	1.4462	1.4462	1.4462
Load variation, $\psi$	1	1	1	1	1	1	1	1	1
Specimen length, L (mm)	3000	6000	9500	3000	6000	9500	3000	6000	9500
Section depth, H (mm)	159	159	159	159	159	159	159	159	159
Section width, B (mm)	79.8	79.8	79.8	79.8	79.8	79.8	79.8	79.8	79.8
Web thickness, $t_w$ (mm)	6	6	6	6	6	6	6	6	6
Flange thickness, $t_f$ (mm)	9.86	9.86	9.86	9.86	9.86	9.86	9.86	9.86	9.86

Table 9.5 : Dimension of I - 160 x 80 column specimens ( $\psi = 1$ )



**9.1. SHS 60 X 60 X 5 ( $\psi = 1$ ) Comparison result**

Section	SHS 60 X 60 X 5	SHS 60 X 60 X 5	SHS 60 X 60 X 5	SHS 60 X 60 X 5	SHS 60 X 60 X 5	SHS 60 X 60 X 5	SHS 60 X 60 X 5	SHS 60 X 60 X 5	SHS 60 X 60 X 5
Steel material	Aust	Aust	Aust	Fert	Fert	Fert	Dupl	Dupl	Dupl
Steel Grade material	1.4301	1.4301	1.4301	1.4003	1.4003	1.4003	1.4462	1.4462	1.4462
Specimen length, L (mm)	1050	1700	2350	1050	1700	2350	1050	1700	2350
Section class	1	1	1	1	1	1	1	1	1
$N_{cr, FEM}$ (kN)	864.19	335.15	176.31	864.19	335.15	176.31	864.19	335.15	176.31
$A_{eff}$ (mm <sup>2</sup> )	1010.78	1010.78	1010.78	1010.78	1010.78	1010.78	1010.78	1010.78	1010.78
$\lambda_{FEM}$	0.519	0.833	1.148	0.572	0.919	1.267	0.749	1.203	1.659
$X_{b,y}$ EN 1993-1-4	0.790	0.618	0.461	0.792	0.637	0.462	0.748	0.530	0.324

Table 9.6 : Parametric result of SHS 60 x 60 x 5 column specimens ( $\psi = 1$ )

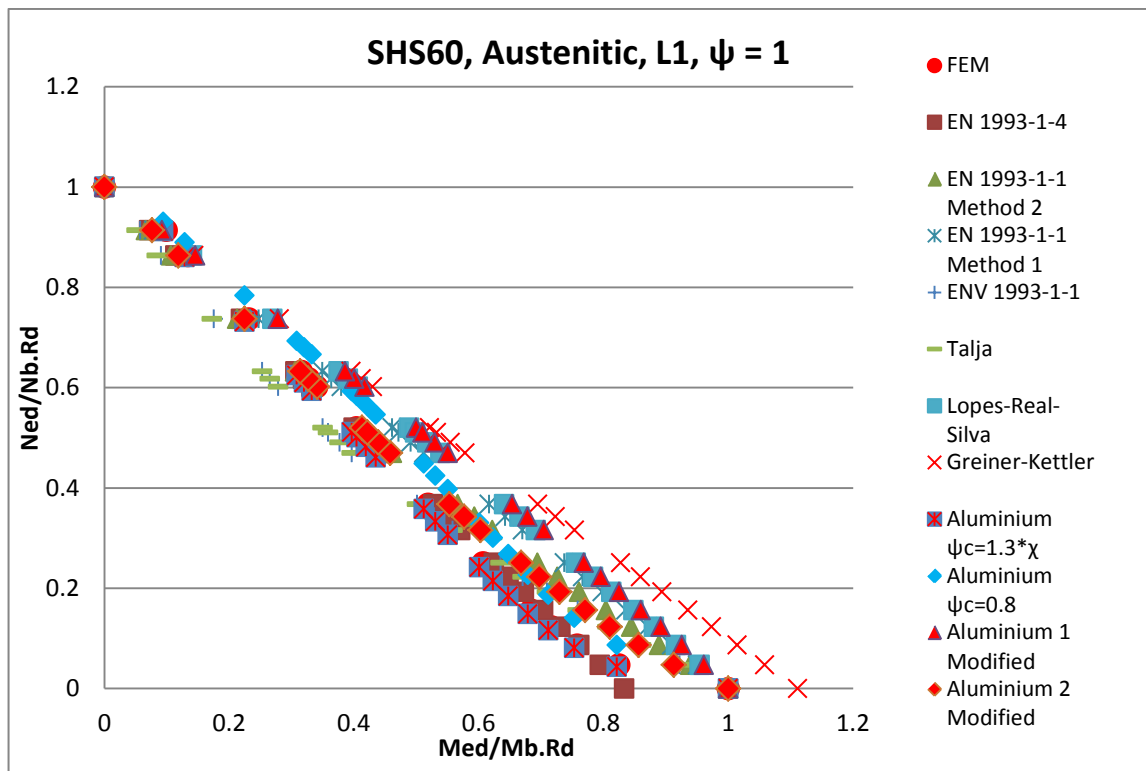


Figure 9-1 : SHS 60 x 60 x 5 Interaction axial force and bending moment diagram comparison, Austenitic, L=1050 mm,  $\psi = 1$

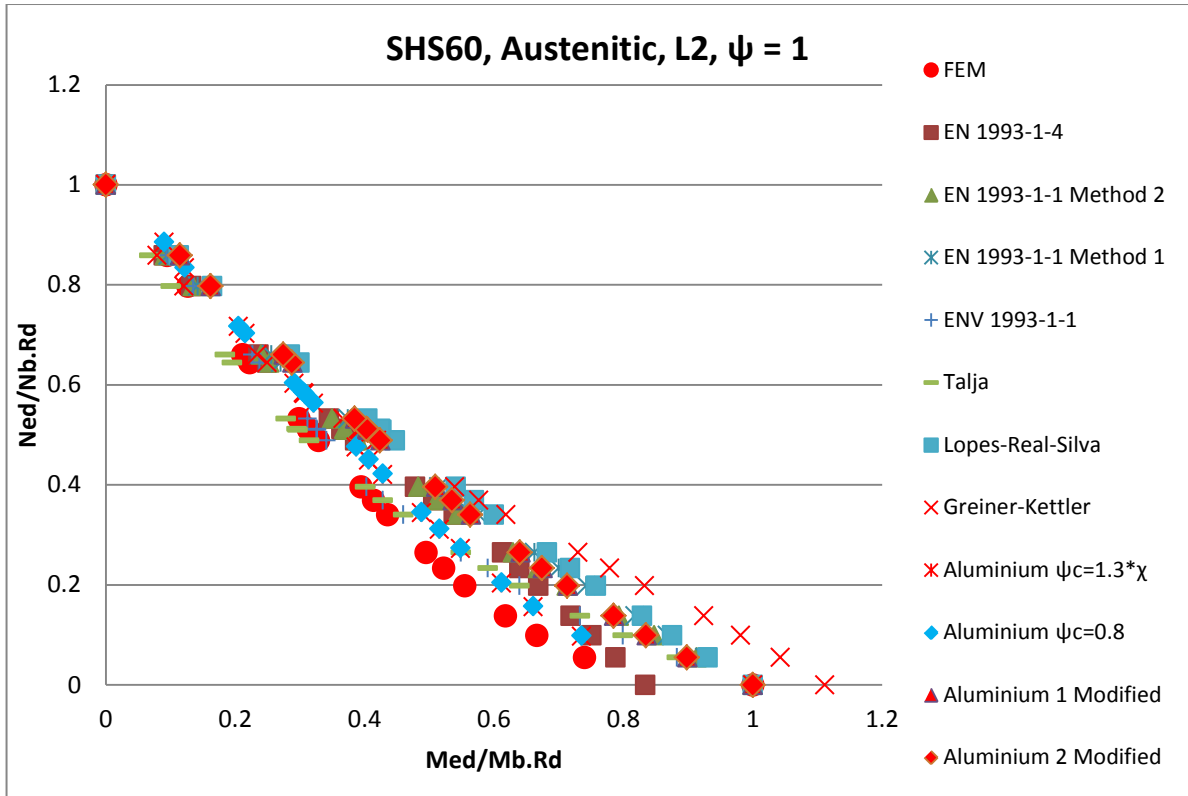


Figure 9-2 : SHS 60 x 60 x 5 Interaction axial force and bending moment diagram comparison, Austenitic, L=1700 mm,  $\psi = 1$

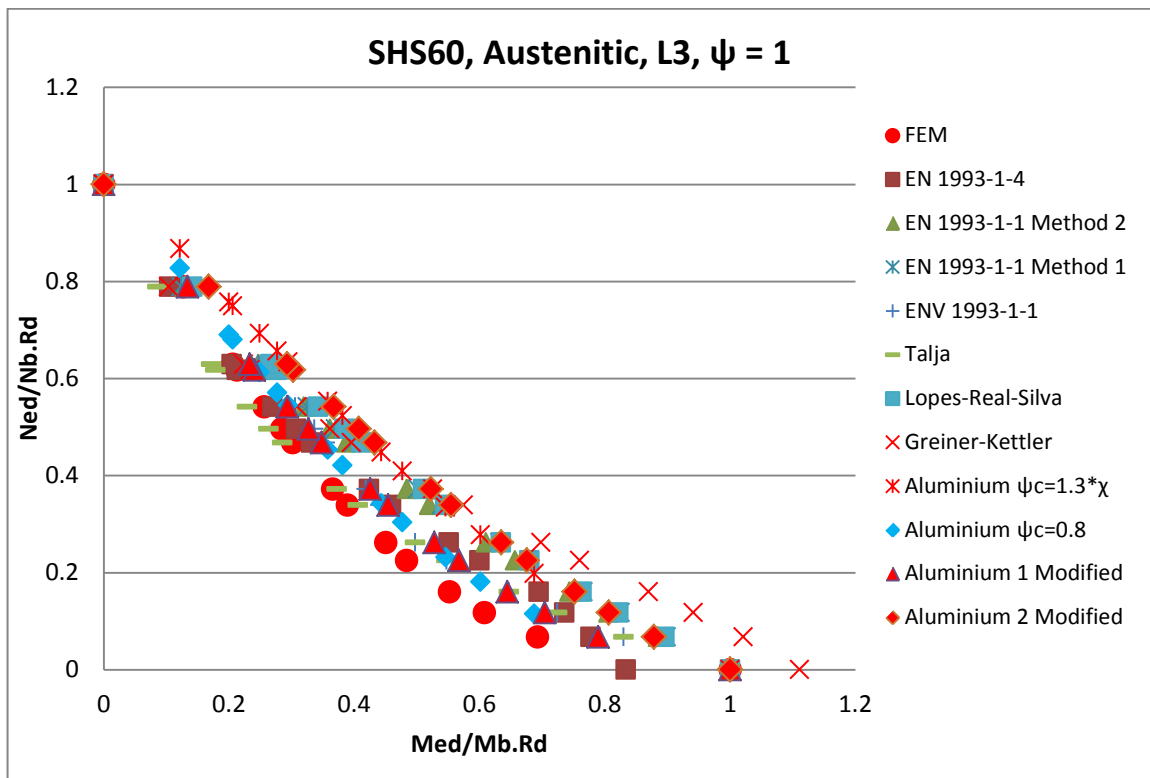


Figure 9-3 : SHS 60 x 60 x 5 Interaction axial force and bending moment diagram comparison, Austenitic, L=2350 mm,  $\psi = 1$

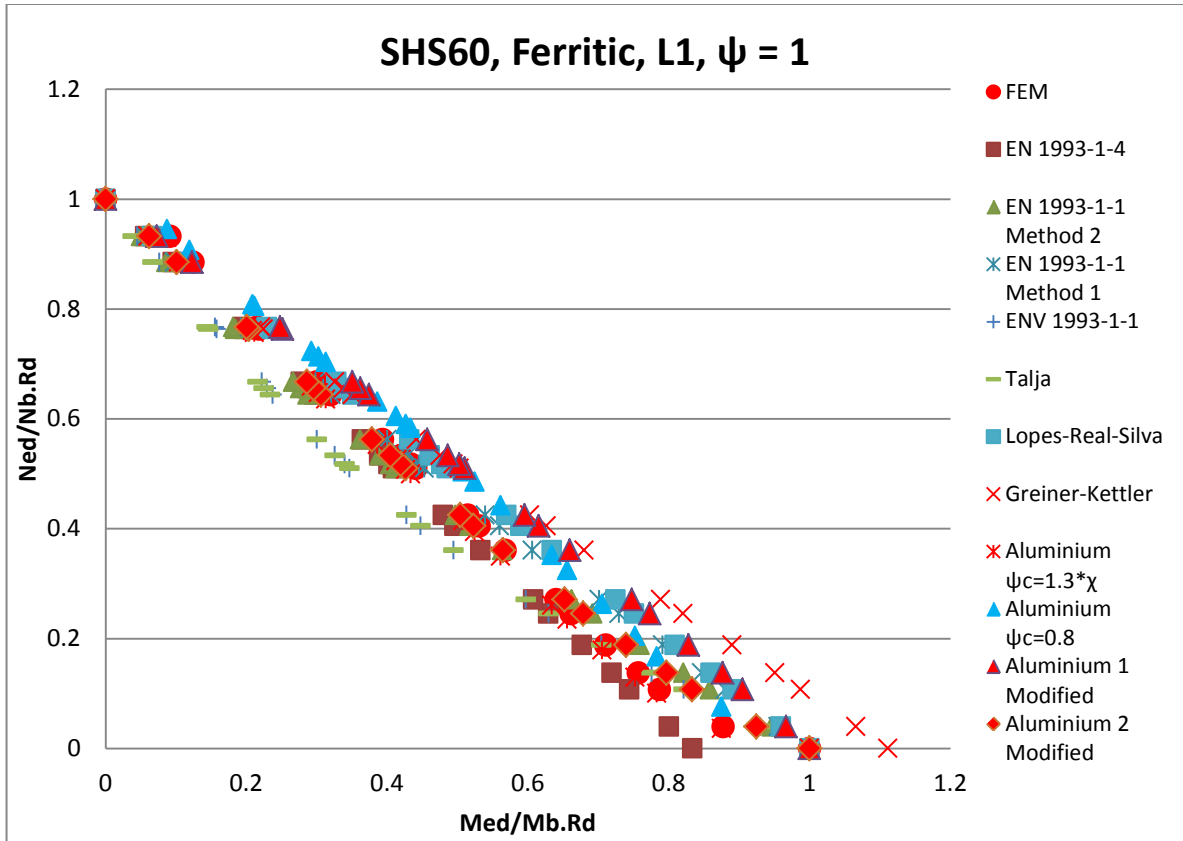


Figure 9-4 : SHS 60 x 60 x 5 Interaction axial force and bending moment diagram comparison, Ferritic, L=1050 mm,  $\psi = 1$

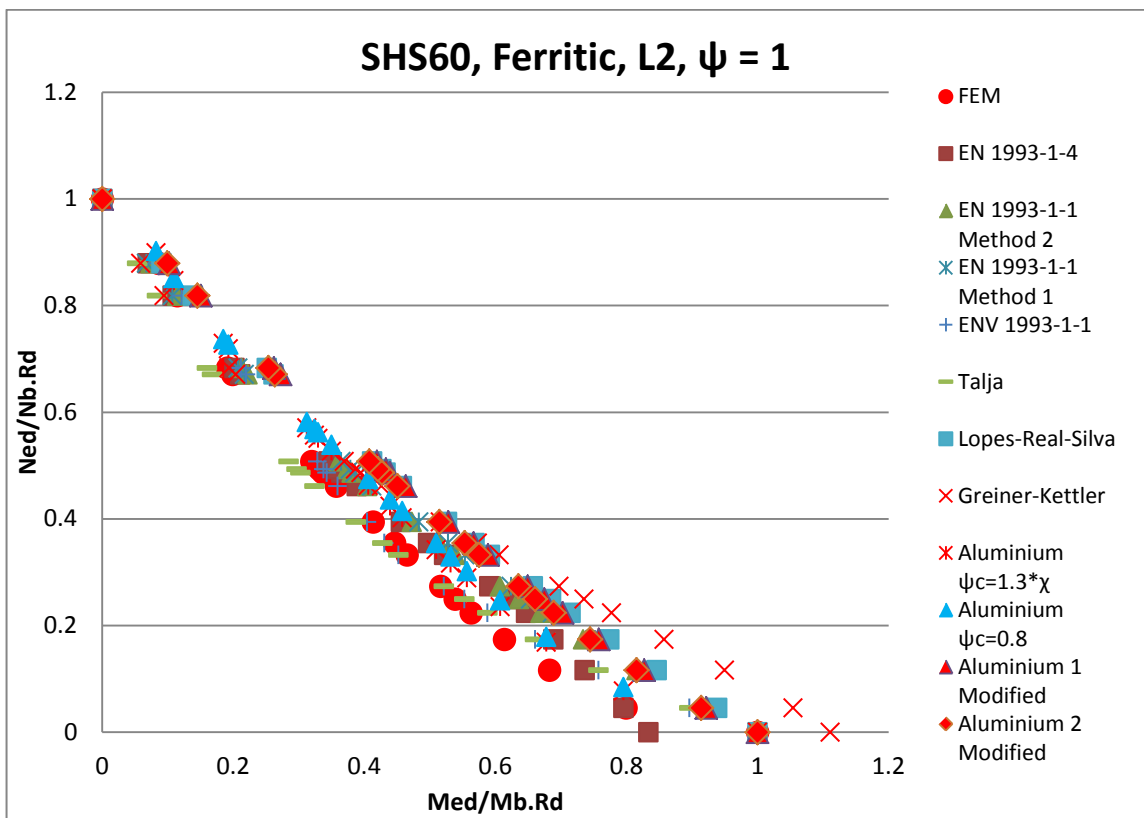


Figure 9-5 : SHS 60 x 60 x 5 Interaction axial force and bending moment diagram comparison, Ferritic, L=1700 mm,  $\psi = 1$

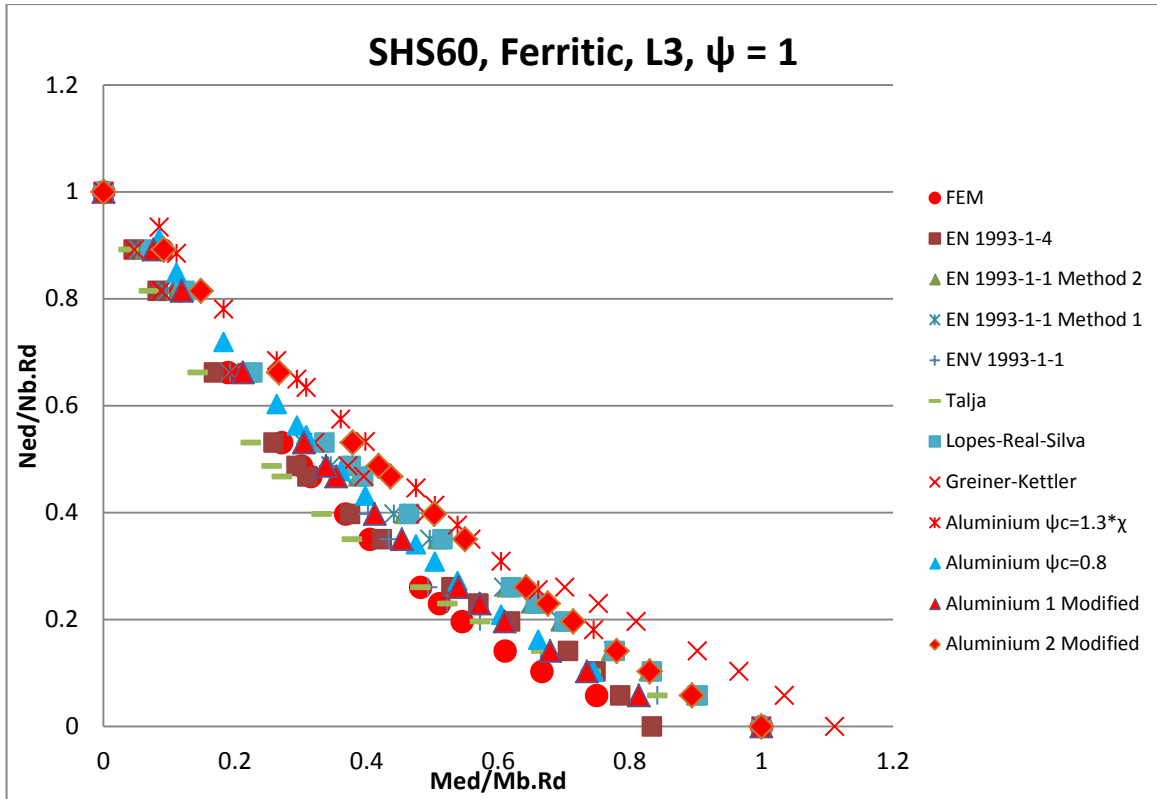


Figure 9-6 : SHS 60 x 60 x 5 Interaction axial force and bending moment diagram comparison, Ferritic, L=2350 mm,  $\psi = 1$

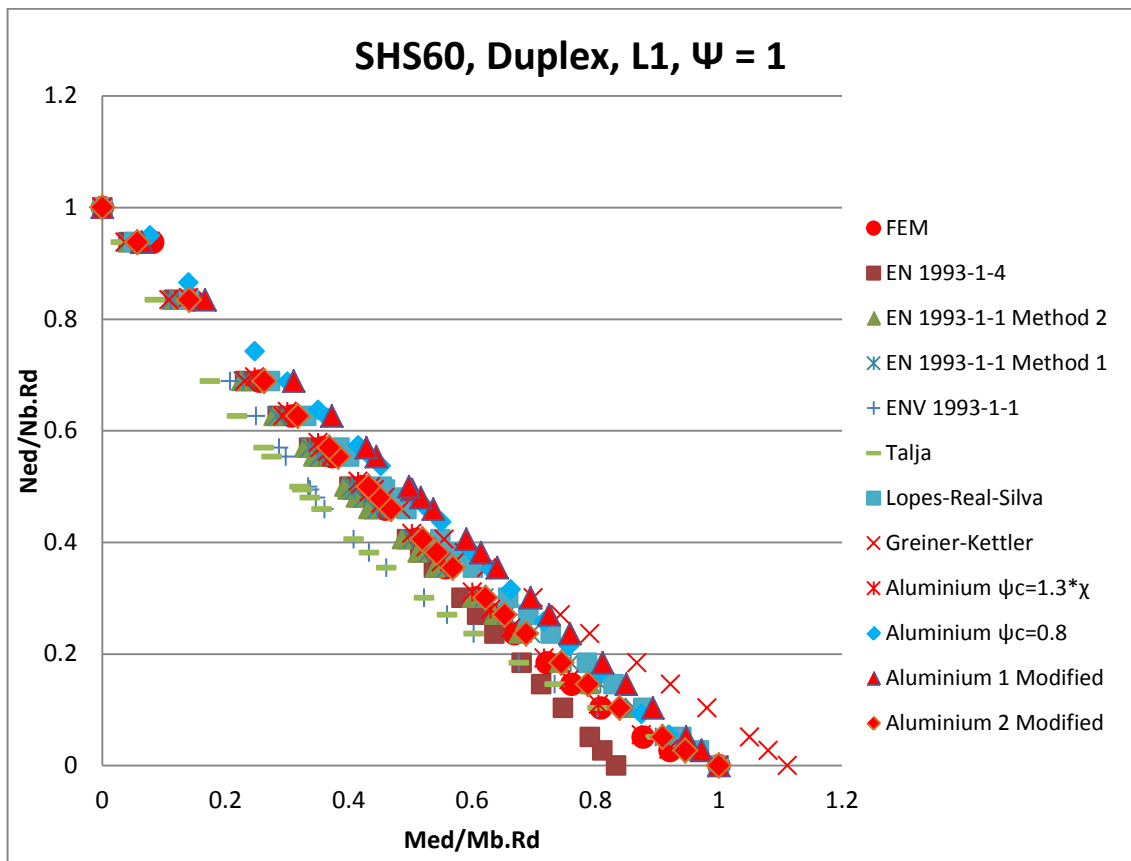


Figure 9-7 : SHS 60 x 60 x 5 Interaction axial force and bending moment diagram comparison, Duplex, L=1050 mm,  $\psi = 1$

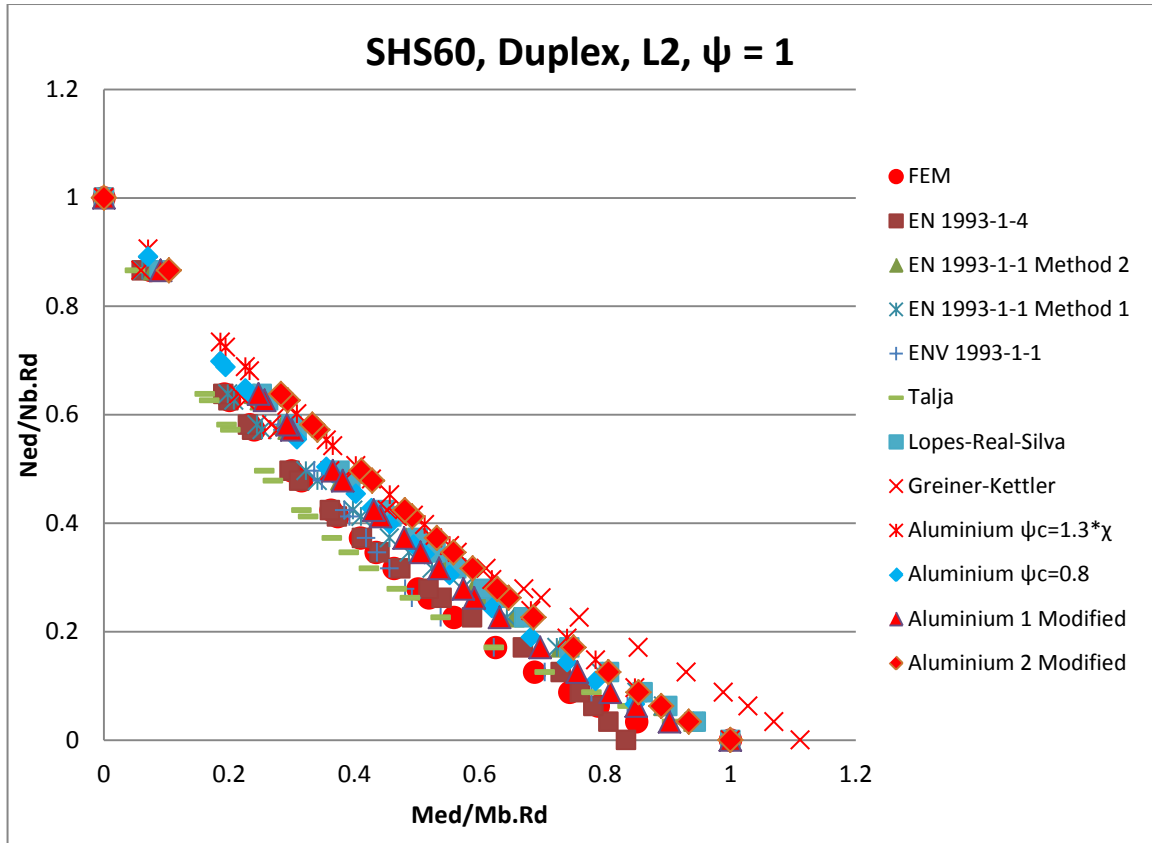


Figure 9-8 : SHS 60 x 60 x 5 Interaction axial force and bending moment diagram comparison, Duplex, L=1700 mm,  $\psi = 1$

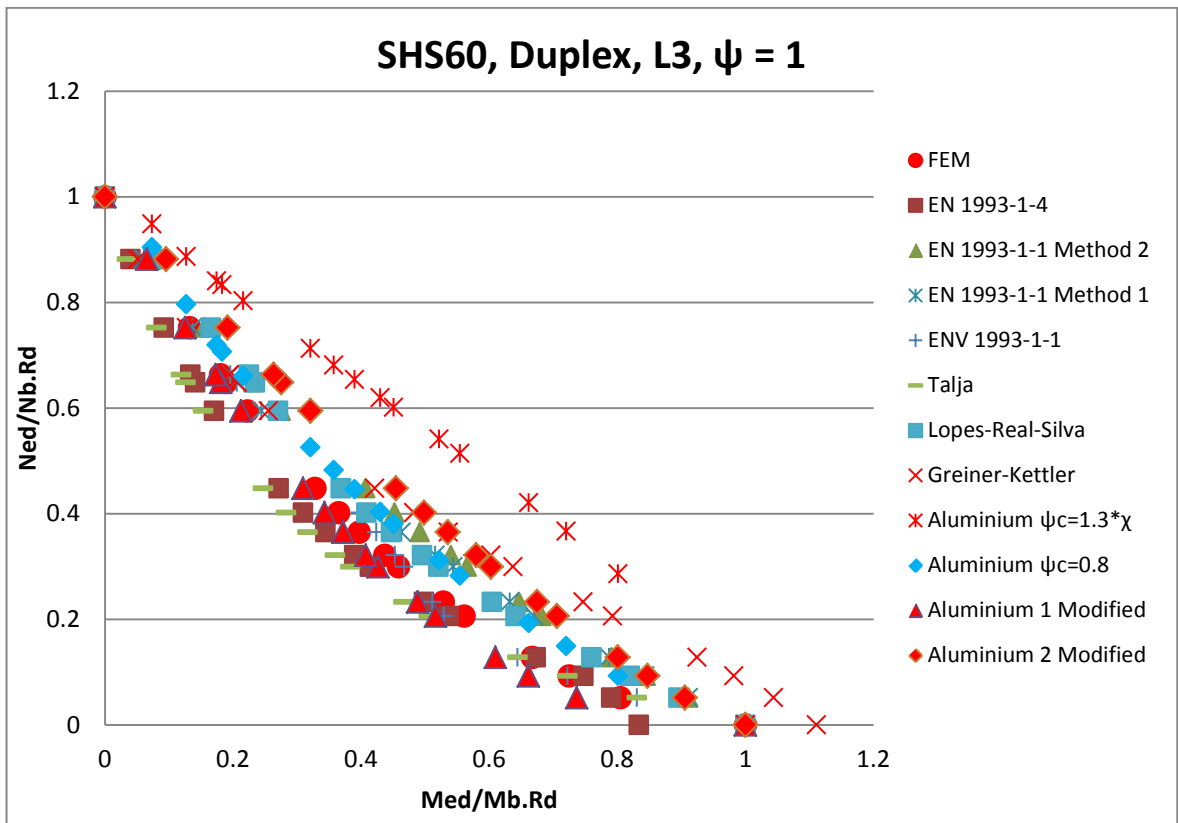


Figure 9-9 : SHS 60 x 60 x 5 Interaction axial force and bending moment diagram comparison, Duplex, L=2350 mm,  $\psi = 1$

From the graph comparison for SHS 60 x 60 x 5, physically seen that all the approaches were tends to follow the FEM graph. And it is clearly seen that Greiner-Kettler approach tends to overestimate under low axial force and high bending moment.

The mean and standard deviation of the ratio  $k_y$  of the proposed by standard codes or research journals and with  $k_y$  Finite Element (FEM) result ( $k_y/k_{y,FEM}$  summarize in table 9.7, table 9.8 and table 9.9.

SHS 60 X 60 X 5, Austenitic, L = 1050 mm, $\psi = 1$									
	EN 1993-1-4	EN 1993-1-1 Method 2	EN 1993-1-1 Method 1	ENV 1993-1-1	Talja [17]	Lopes-Real [15]	Greiner-Kettler [13]	Modif. Aluminium 1	Modif. Aluminium 2
$k_y/k_{y,FEM}$ Mean (Average)	0.989	0.933	0.852	1.054	1.069	0.813	0.756	0.796	0.927
$k_y/k_{y,FEM}$ Standard Deviation	0.242	0.256	0.215	0.315	0.344	0.197	0.190	0.192	0.227
SHS 60 X 60 X 5, Austenitic, L = 1700 mm, $\psi = 1$									
	EN 1993-1-4	EN 1993-1-1 Method 2	EN 1993-1-1 Method 1	ENV 1993-1-1	Talja [17]	Lopes-Real [15]	Greiner-Kettler [13]	Modif. Aluminium 1	Modif. Aluminium 2
$k_y/k_{y,FEM}$ Mean (Average)	0.843	0.803	0.765	0.879	0.961	0.721	0.755	0.751	0.753
$k_y/k_{y,FEM}$ Standard Deviation	0.226	0.208	0.200	0.219	0.277	0.186	0.231	0.189	0.190
SHS 60 X 60 X 5, Austenitic, L = 2350 mm, $\psi = 1$									
	EN 1993-1-4	EN 1993-1-1 Method 2	EN 1993-1-1 Method 1	ENV 1993-1-1	Talja [17]	Lopes-Real [15]	Greiner-Kettler [13]	Modif. Aluminium 1	Modif. Aluminium 2
$k_y/k_{y,FEM}$ Mean (Average)	0.870	0.751	0.740	0.811	0.958	0.716	0.729	0.822	0.690
$k_y/k_{y,FEM}$ Standard Deviation	0.273	0.223	0.227	0.229	0.316	0.213	0.257	0.231	0.206

Table 9.7 : Mean and standard deviation of SHS 60 x 60 x 5 column specimens (Austenitic,  $\psi = 1$ )

SHS 60 X 60 X 5, Ferritic, L = 1050 mm, $\psi = 1$									
	EN 1993-1-4	EN 1993-1-1 Method 2	EN 1993-1-1 Method 1	ENV 1993-1-1	Talja [17]	Lopes-Real [15]	Greiner-Kettler [13]	Modif. Aluminium 1	Modif. Aluminium 2
$k_y/k_{y,FEM}$ Mean (Average)	1.066	1.045	0.961	1.189	1.230	0.898	0.873	0.856	0.998
$k_y/k_{y,FEM}$ Standard Deviation	0.270	0.308	0.264	0.363	0.428	0.229	0.253	0.212	0.251
SHS 60 X 60 X 5, Ferritic, L = 1700 mm, $\psi = 1$									
	EN 1993-1-4	EN 1993-1-1 Method 2	EN 1993-1-1 Method 1	ENV 1993-1-1	Talja [17]	Lopes-Real [15]	Greiner-Kettler [13]	Modif. Aluminium 1	Modif. Aluminium 2
$k_y/k_{y,FEM}$ Mean (Average)	0.906	0.851	0.851	0.920	1.032	0.767	0.826	0.757	0.774
$k_y/k_{y,FEM}$ Standard Deviation	0.243	0.221	0.234	0.228	0.303	0.196	0.275	0.193	0.195
SHS 60 X 60 X 5, Ferritic, L = 2350 mm, $\psi = 1$									
	EN 1993-1-4	EN 1993-1-1 Method 2	EN 1993-1-1 Method 1	ENV 1993-1-1	Talja [17]	Lopes-Real [15]	Greiner-Kettler [13]	Modif. Aluminium 1	Modif. Aluminium 2
$k_y/k_{y,FEM}$ Mean (Average)	1.007	0.821	0.870	0.882	1.106	0.796	0.822	0.868	0.737
$k_y/k_{y,FEM}$ Standard Deviation	0.382	0.271	0.325	0.252	0.470	0.244	0.388	0.243	0.215

Table 9.8 : Mean and standard deviation of SHS 60 x 60 x 5 column specimens (Ferritic,  $\psi = 1$ )

SHS 60 X 60 X 5, Duplex, L = 1050 mm, $\psi = 1$									
	EN 1993-1-4	EN 1993-1-1 Method 2	EN 1993-1-1 Method 1	ENV 1993-1-1	Talja [17]	Lopes-Real [15]	Greiner-Kettler [13]	Modif. Aluminium 1	Modif. Aluminium 2
$k_y/k_{y,FEM}$ Mean (Average)	1.068	1.038	1.020	1.151	1.234	0.923	0.952	0.854	0.955
$k_y/k_{y,FEM}$ Standard Deviation	0.297	0.309	0.319	0.320	0.446	0.242	0.354	0.208	0.230
SHS 60 X 60 X 5, Duplex, L = 1700 mm, $\psi = 1$									
	EN 1993-1-4	EN 1993-1-1 Method 2	EN 1993-1-1 Method 1	ENV 1993-1-1	Talja [17]	Lopes-Real [15]	Greiner-Kettler [13]	Modif. Aluminium 1	Modif. Aluminium 2
$k_y/k_{y,FEM}$ Mean (Average)	0.967	0.819	0.883	0.898	1.055	0.792	0.784	0.824	0.753
$k_y/k_{y,FEM}$ Standard Deviation	0.228	0.188	0.211	0.215	0.266	0.184	0.207	0.192	0.186
SHS 60 X 60 X 5, Duplex, L = 2350 mm, $\psi = 1$									
	EN 1993-1-4	EN 1993-1-1 Method 2	EN 1993-1-1 Method 1	ENV 1993-1-1	Talja [17]	Lopes-Real [15]	Greiner-Kettler [13]	Modif. Aluminium 1	Modif. Aluminium 2
$k_y/k_{y,FEM}$ Mean (Average)	1.143	0.805	0.856	0.883	1.230	0.827	0.795	1.010	0.731
$k_y/k_{y,FEM}$ Standard Deviation	0.374	0.223	0.244	0.243	0.447	0.220	0.283	0.263	0.206

Table 9.9 : Mean and standard deviation of SHS 60 x 60 x 5 column specimens (Duplex,  $\psi = 1$ )



**9.2. RHS 150 X 100 X 3 ( $\psi = 1$ ) Comparison result**

Section	RHS 150 X 100 X 3	RHS 150 X 100 X 3	RHS 150 X 100 X 3	RHS 150 X 100 X 3	RHS 150 X 100 X 3	RHS 150 X 100 X 3	RHS 150 X 100 X 3	RHS 150 X 100 X 3	RHS 150 X 100 X 3
Steel material	Aust	Aust	Aust	Fert	Fert	Fert	Dupl	Dupl	Dupl
Steel Grade material	1.4301	1.4301	1.4301	1.4003	1.4003	1.4003	1.4462	1.4462	1.4462
Specimen length, L (mm)	2700	4350	6000	2700	4350	6000	2700	4350	6000
Section class	4	4	4	4	4	4	4	4	4
$N_{cr, FEM}$ (kN)	1195.7	467.53	246.83	1195.7	467.53	246.83	1195.7	467.53	246.83
$A_{eff}$ (mm <sup>2</sup> )	1309.35	1309.35	1309.35	1279.04	1279.04	1279.04	1210.63	1210.63	1210.63
$\lambda_{FEM}$	0.502	0.803	1.105	0.547	0.875	1.205	0.697	1.115	1.534
$X_{b,y}$ EN 1993-1-4	0.757	0.609	0.469	0.771	0.701	0.479	0.710	0.547	0.358

Table 9.10 : Parametric result of RHS 150 x 100 x 3 column specimens ( $\psi = 1$ )

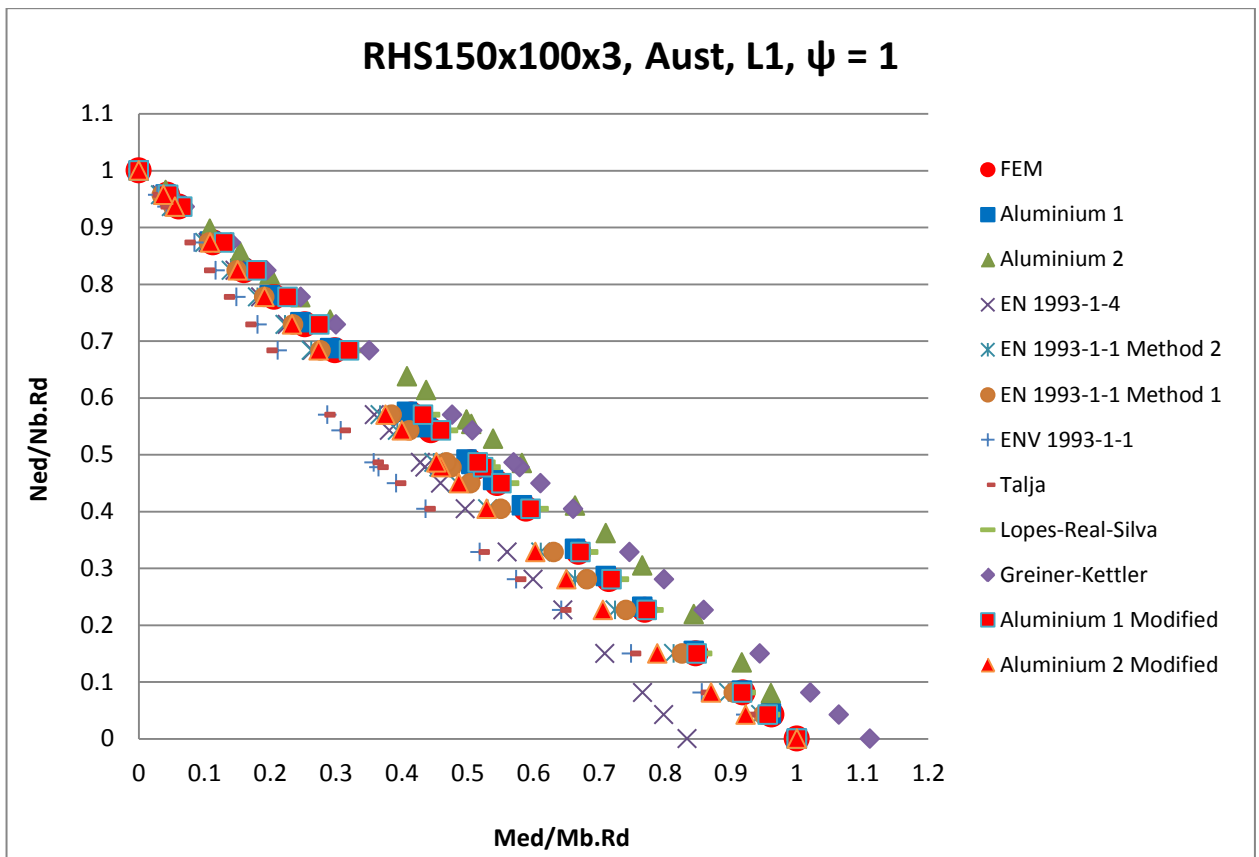


Figure 9-10 : RHS 150 x 100 x 3 Interaction axial force and bending moment diagram comparison, Austenitic, L=2700 mm,  $\psi = 1$

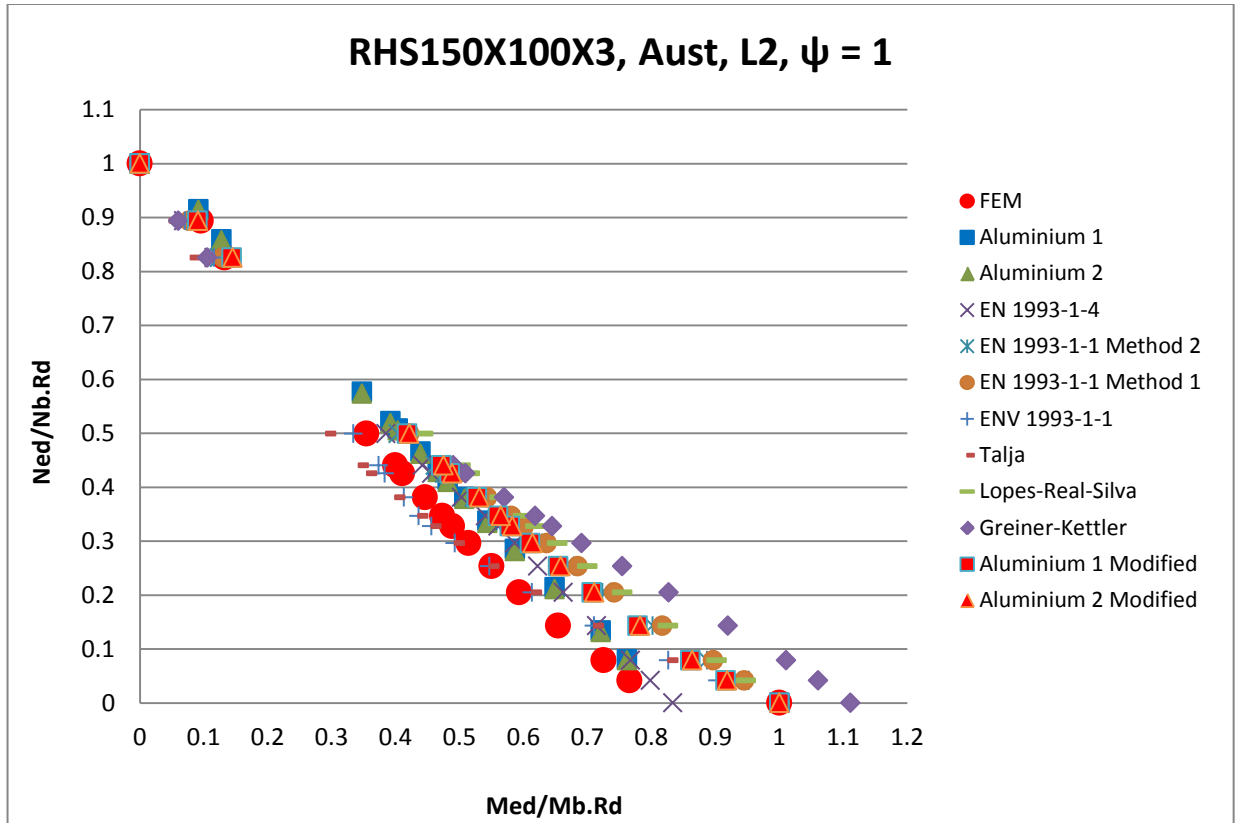


Figure 9-11 : RHS 150 x 100 x 3 Interaction axial force and bending moment diagram comparison, Austenitic, L=4350 mm,  $\psi = 1$

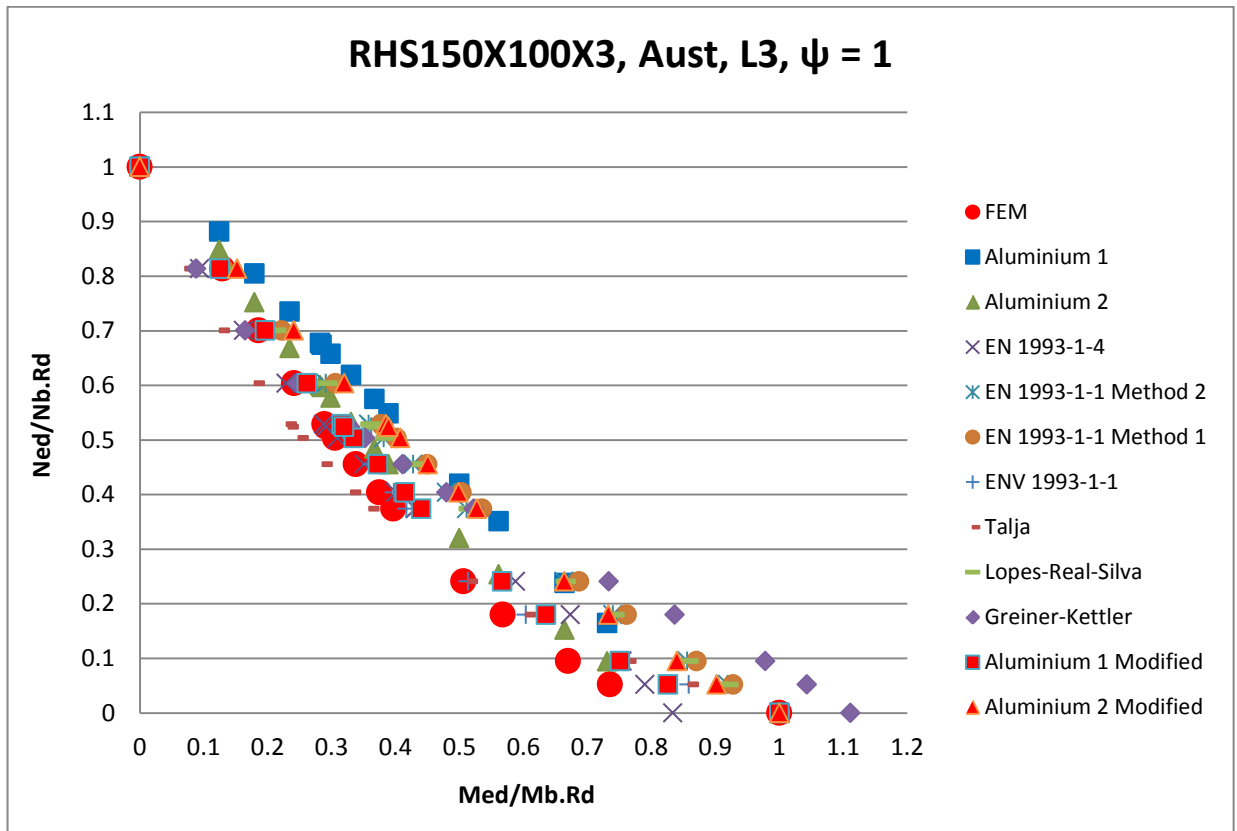


Figure 9-12 : RHS 150 x 100 x 3 Interaction axial force and bending moment diagram comparison, Austenitic, L=6000 mm,  $\psi = 1$

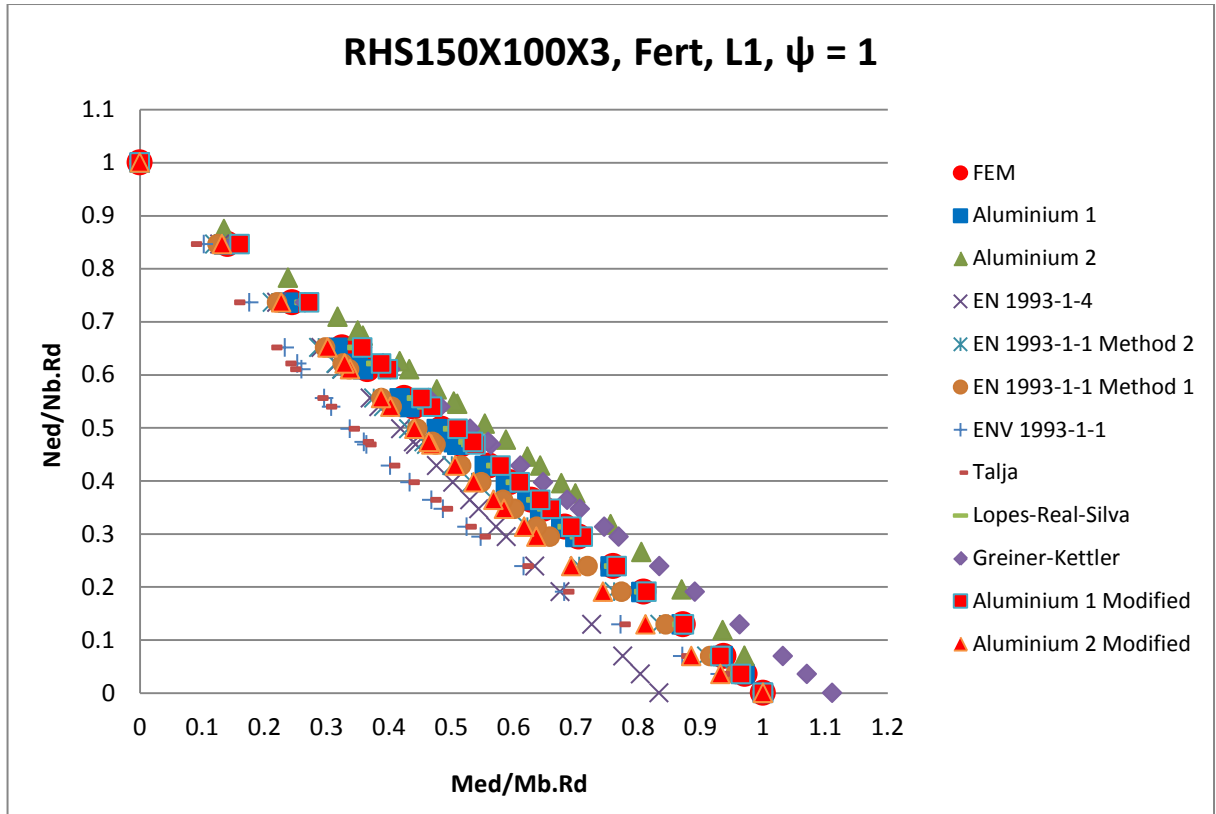


Figure 9-13 : RHS 150 x 100 x 3 Interaction axial force and bending moment diagram comparison, Ferritic, L=2700 mm,  $\psi = 1$

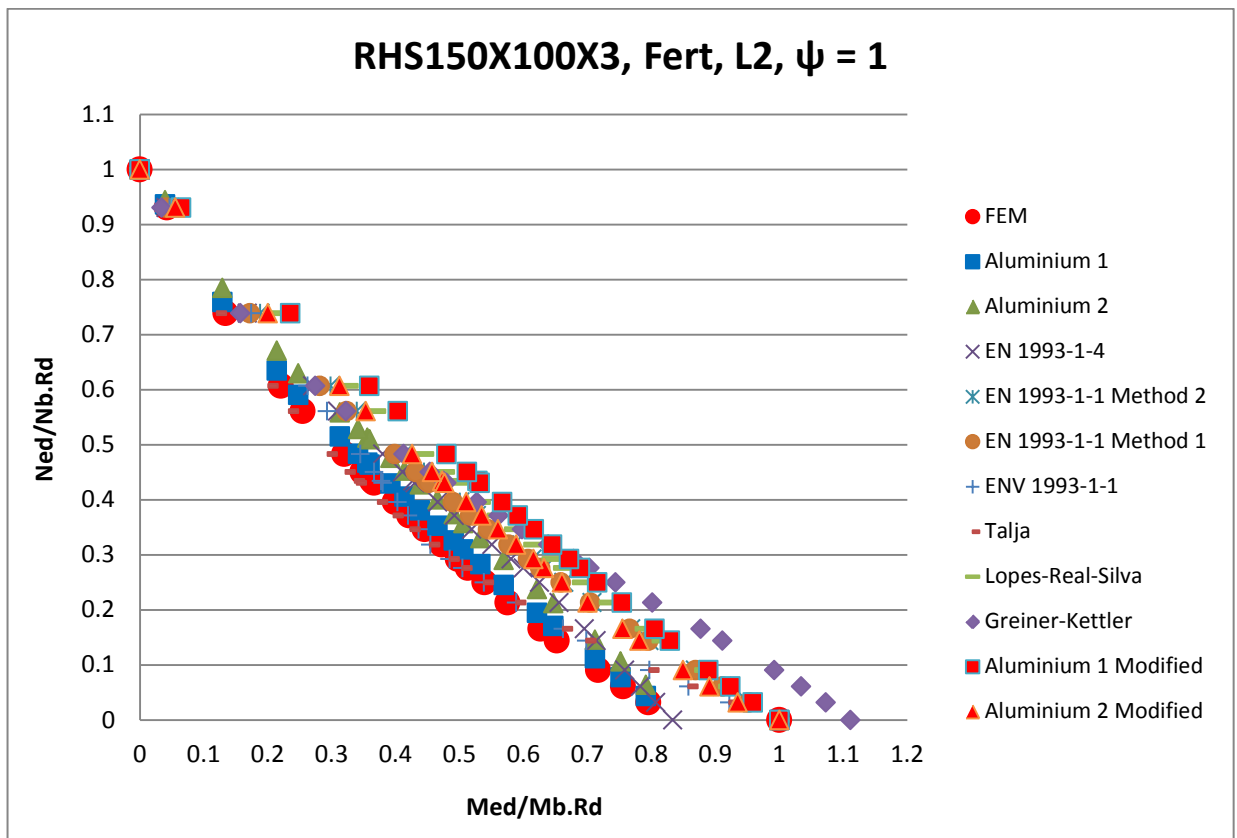


Figure 9-14 : RHS 150 x 100 x 3 Interaction axial force and bending moment diagram comparison, Ferritic, L=4350 mm,  $\psi = 1$

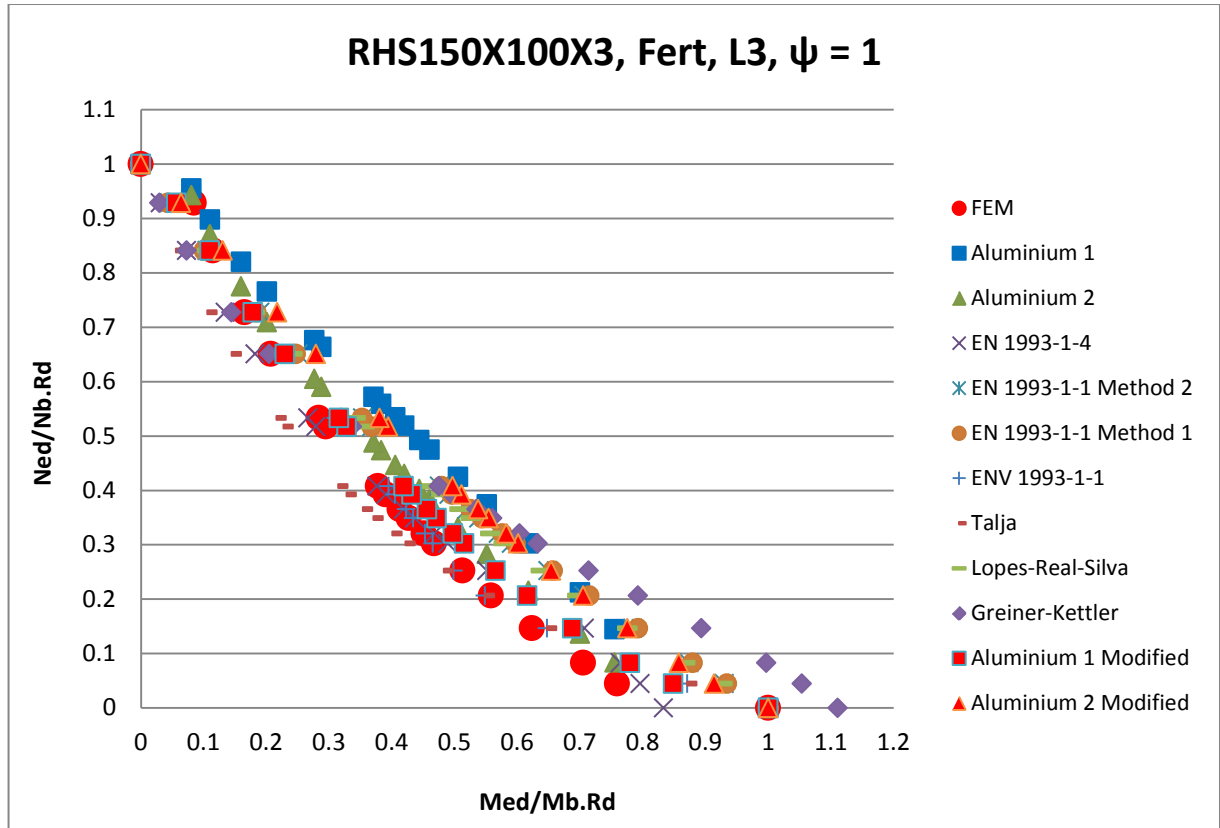


Figure 9-15 : RHS 150 x 100 x 3 Interaction axial force and bending moment diagram comparison, Ferritic, L=6000 mm,  $\psi = 1$

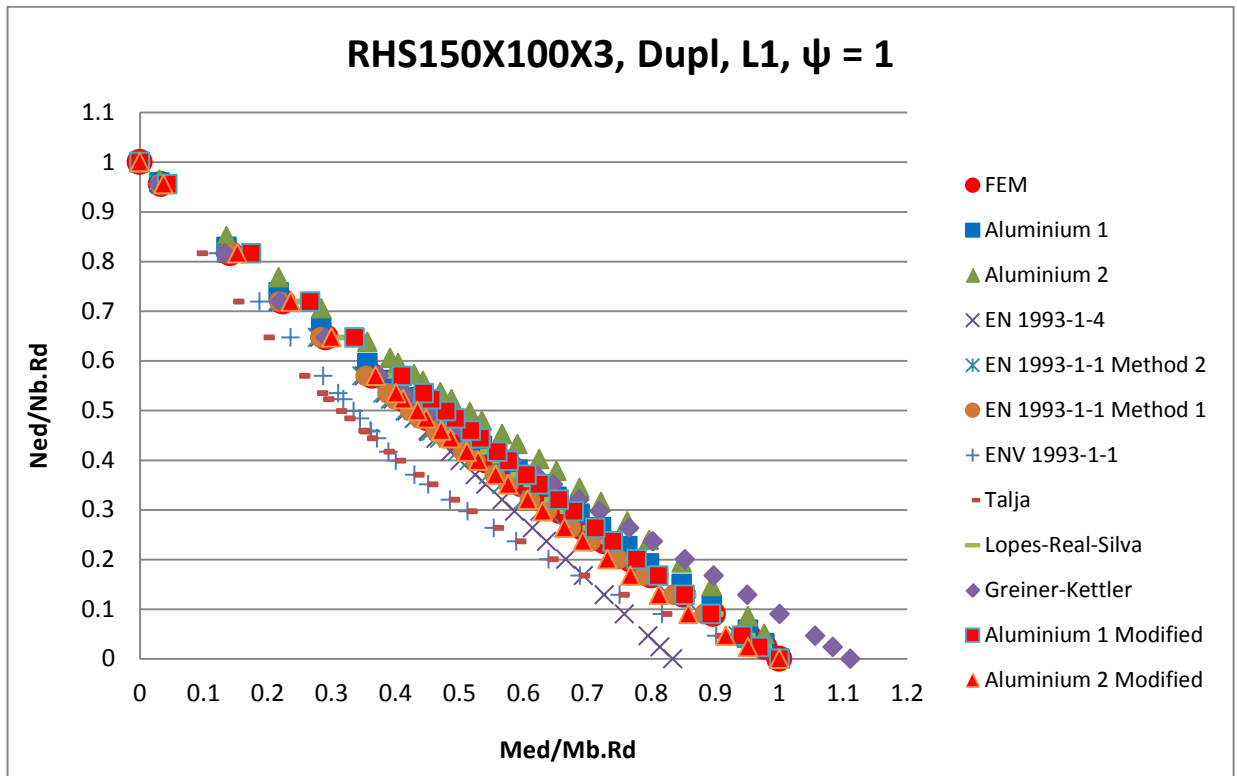


Figure 9-16 : RHS 150 x 100 x 3 Interaction axial force and bending moment diagram comparison, Duplex, L=2700 mm,  $\psi = 1$

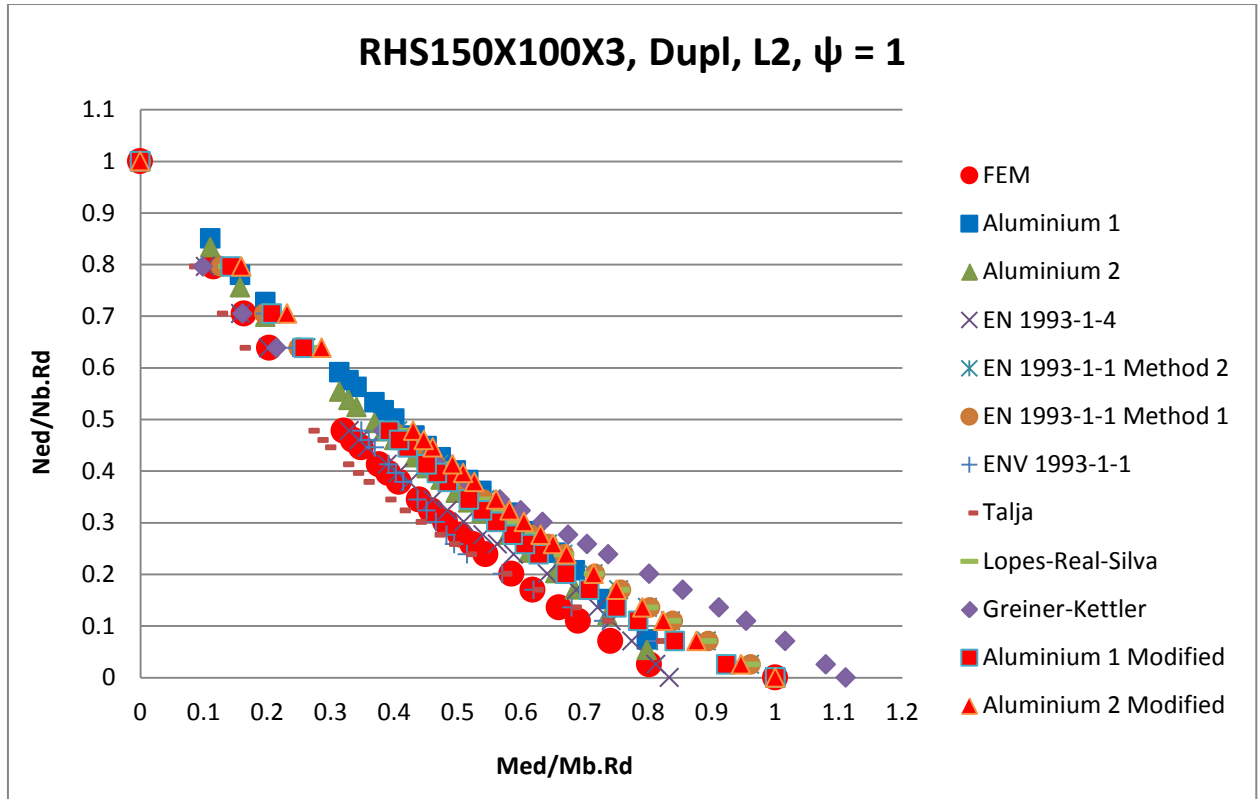


Figure 9-17 : RHS 150 x 100 x 3 Interaction axial force and bending moment diagram comparison, Duplex, L=4350 mm,  $\psi = 1$

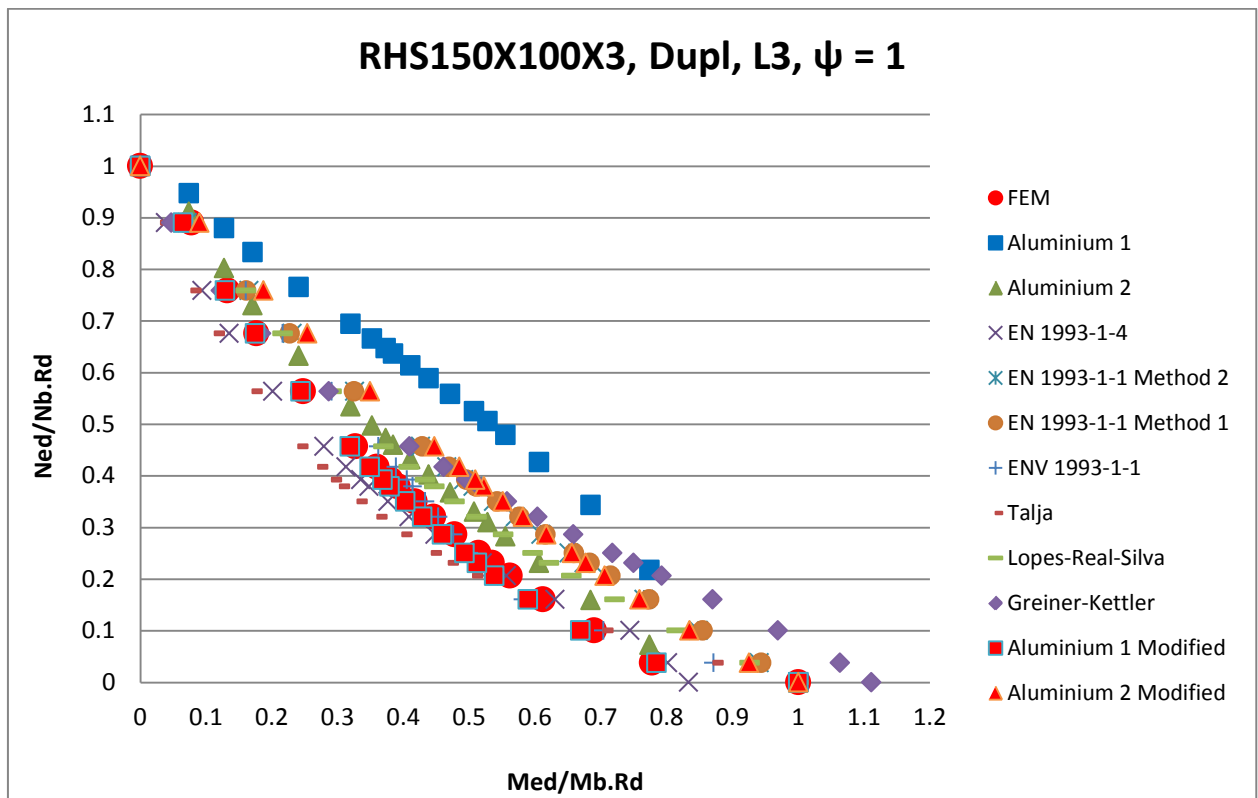


Figure 9-18 : RHS 150 x 100 x 3 Interaction axial force and bending moment diagram comparison, Duplex, L=6000 mm,  $\psi = 1$

The graph comparison for RHS 150 x 100 x 3, physically seen that all the approaches were tending to follow the FEM simulation graph result. And again that Greiner-Kettler formula tends to overestimate under low axial force and high bending moment. And also Aluminium 1 has out of the FEM result's trend graph on Duplex L = 6000 mm,  $\lambda = 1.53$ .

The mean and standard deviation of the ratio  $k_y$  of the proposed by standard codes or research journals and with  $k_y$  Finite Element (FEM) result ( $k_y/k_{y,FEM}$  summarize in table 9.11, table 9.12 and table 9.13.

RHS 150 X 100 X 3, Austenitic, L = 2700 mm, $\psi = 1$									
	EN 1993-1-4	EN 1993-1-1 Method 2	EN 1993-1-1 Method 1	ENV 1993-1-1	Talja [17]	Lopes-Real [15]	Greiner-Kettler [13]	Modif. Aluminium 1	Modif. Aluminium 2
$k_y/k_{y,FEM}$ Mean (Average)	1.111	1.061	1.020	1.253	1.331	0.903	0.835	0.918	1.036
$k_y/k_{y,FEM}$ Standard Deviation	0.258	0.253	0.239	0.322	0.383	0.211	0.194	0.214	0.240
RHS 150 X 100 X 3, Austenitic, L = 6000 mm, $\psi = 1$									
	EN 1993-1-4	EN 1993-1-1 Method 2	EN 1993-1-1 Method 1	ENV 1993-1-1	Talja [17]	Lopes-Real [15]	Greiner-Kettler [13]	Modif. Aluminium 1	Modif. Aluminium 2
$k_y/k_{y,FEM}$ Mean (Average)	0.911	0.839	0.815	0.975	1.076	0.786	0.804	0.819	0.814
$k_y/k_{y,FEM}$ Standard Deviation	0.284	0.257	0.249	0.285	0.422	0.230	0.320	0.228	0.227
RHS 150 X 100 X 3, Austenitic, L =6000 mm, $\psi = 1$									
	EN 1993-1-4	EN 1993-1-1 Method 2	EN 1993-1-1 Method 1	ENV 1993-1-1	Talja [17]	Lopes-Real [15]	Greiner-Kettler [13]	Modif. Aluminium 1	Modif. Aluminium 2
$k_y/k_{y,FEM}$ Mean (Average)	0.941	0.774	0.746	0.875	1.097	0.769	0.816	0.861	0.735
$k_y/k_{y,FEM}$ Standard Deviation	0.296	0.229	0.223	0.246	0.393	0.228	0.305	0.242	0.214

Table 9.11 : Mean and standard deviation of RHS 150 x 100 x 3 column specimens (Austenitic,  $\psi = 1$ )

RHS 150 X 100 X 3, Ferritic, L = 2700 mm, $\psi = 1$									
	EN 1993-1-4	EN 1993-1-1 Method 2	EN 1993-1-1 Method 1	ENV 1993-1-1	Talja [17]	Lopes-Real [15]	Greiner-Kettler [13]	Modif. Aluminium 1	Modif. Aluminium 2
$k_y/k_{y,FEM}$ Mean (Average)	1.117	1.052	1.026	1.253	1.293	0.930	0.874	0.919	1.038
$k_y/k_{y,FEM}$ Standard Deviation	0.246	0.233	0.226	0.304	0.333	0.205	0.191	0.204	0.228
RHS 150 X 100 X 3, Ferritic, L = 4350 mm, $\psi = 1$									
	EN 1993-1-4	EN 1993-1-1 Method 2	EN 1993-1-1 Method 1	ENV 1993-1-1	Talja [17]	Lopes-Real [15]	Greiner-Kettler [13]	Modif. Aluminium 1	Modif. Aluminium 2
$k_y/k_{y,FEM}$ Mean (Average)	0.855	0.775	0.796	0.904	0.996	0.736	0.748	0.700	0.763
$k_y/k_{y,FEM}$ Standard Deviation	0.206	0.178	0.184	0.209	0.250	0.174	0.197	0.176	0.178
RHS 150 X 100 X 3, Ferritic, L = 6000 mm, $\psi = 1$									
	EN 1993-1-4	EN 1993-1-1 Method 2	EN 1993-1-1 Method 1	ENV 1993-1-1	Talja [17]	Lopes-Real [15]	Greiner-Kettler [13]	Modif. Aluminium 1	Modif. Aluminium 2
$k_y/k_{y,FEM}$ Mean (Average)	1.078	0.841	0.850	0.956	1.262	0.852	0.917	0.901	0.781
$k_y/k_{y,FEM}$ Standard Deviation	0.494	0.319	0.346	0.302	0.677	0.305	0.555	0.258	0.232

Table 9.12 : Mean and standard deviation of RHS 150 x 100 x 3 column specimens (Ferritic,  $\psi = 1$ )

RHS 150 X 100 X 3, Duplex, L = 2700 mm, $\psi = 1$									
	EN 1993-1-4	EN 1993-1-1 Method 2	EN 1993-1-1 Method 1	ENV 1993-1-1	Talja [17]	Lopes-Real [15]	Greiner-Kettler [13]	Modif. Aluminium 1	Modif. Aluminium 2
$k_y/k_{y,FEM}$ Mean (Average)	1.057	1.003	0.990	1.187	1.271	0.919	0.910	0.901	0.975
$k_y/k_{y,FEM}$ Standard Deviation	0.216	0.197	0.194	0.254	0.296	0.185	0.187	0.187	0.195
RHS 150 X 100 X 3, Duplex, L = 4350 mm, $\psi = 1$									
	EN 1993-1-4	EN 1993-1-1 Method 2	EN 1993-1-1 Method 1	ENV 1993-1-1	Talja [17]	Lopes-Real [15]	Greiner-Kettler [13]	Modif. Aluminium 1	Modif. Aluminium 2
$k_y/k_{y,FEM}$ Mean (Average)	0.930	0.783	0.792	0.920	1.063	0.781	0.774	0.816	0.760
$k_y/k_{y,FEM}$ Standard Deviation	0.214	0.176	0.178	0.212	0.270	0.176	0.200	0.183	0.176
RHS 150 X 100 X 3, Duplex, L = 6000 mm, $\psi = 1$									
	EN 1993-1-4	EN 1993-1-1 Method 2	EN 1993-1-1 Method 1	ENV 1993-1-1	Talja [17]	Lopes-Real [15]	Greiner-Kettler [13]	Modif. Aluminium 1	Modif. Aluminium 2
$k_y/k_{y,FEM}$ Mean (Average)	1.103	0.771	0.772	0.909	1.236	0.832	0.792	0.983	0.741
$k_y/k_{y,FEM}$ Standard Deviation	0.358	0.205	0.210	0.233	0.455	0.210	0.292	0.242	0.192

Table 9.13 : Mean and standard deviation of RHS 150 x 100 x 3 column specimens (Duplex,  $\psi = 1$ )



### 9.3. I 160 X 80 ( $\psi = 1$ ) Comparison result

Section	I 160 X 80	I 160 X 80	I 160 X 80	I 160 X 80	I 160 X 80	I 160 X 80	I 160 X 80	I 160 X 80	I 160 X 80
Steel material	Aust	Aust	Aust	Fert	Fert	Fert	Dupl	Dupl	Dupl
Steel Grade material	1.4301	1.4301	1.4301	1.4003	1.4003	1.4003	1.4462	1.4462	1.4462
Specimen length, L (mm)	3000	6000	9500	3000	6000	9500	3000	6000	9500
Section class	1	1	1	1	1	1	2	2	2
$N_{cr, FEM}$ (kN)	2220.7	567.41	227.5	2220.7	567.41	227.5	2220.7	567.41	227.5
$A_{eff}$ (mm <sup>2</sup> )	2409.34	2409.34	2409.34	2409.34	2409.34	2409.34	2409.34	2409.34	2409.34
$\lambda_{FEM}$	0.500	0.988	1.561	0.551	1.090	1.722	0.722	1.428	2.255
$X_{b,y}$ EN 1993-1-4	0.804	0.517	0.306	0.800	0.528	0.284	0.760	0.399	0.181

Table 9.14 : Parametric result of I- 160 x 80 column specimens ( $\psi = 1$ )

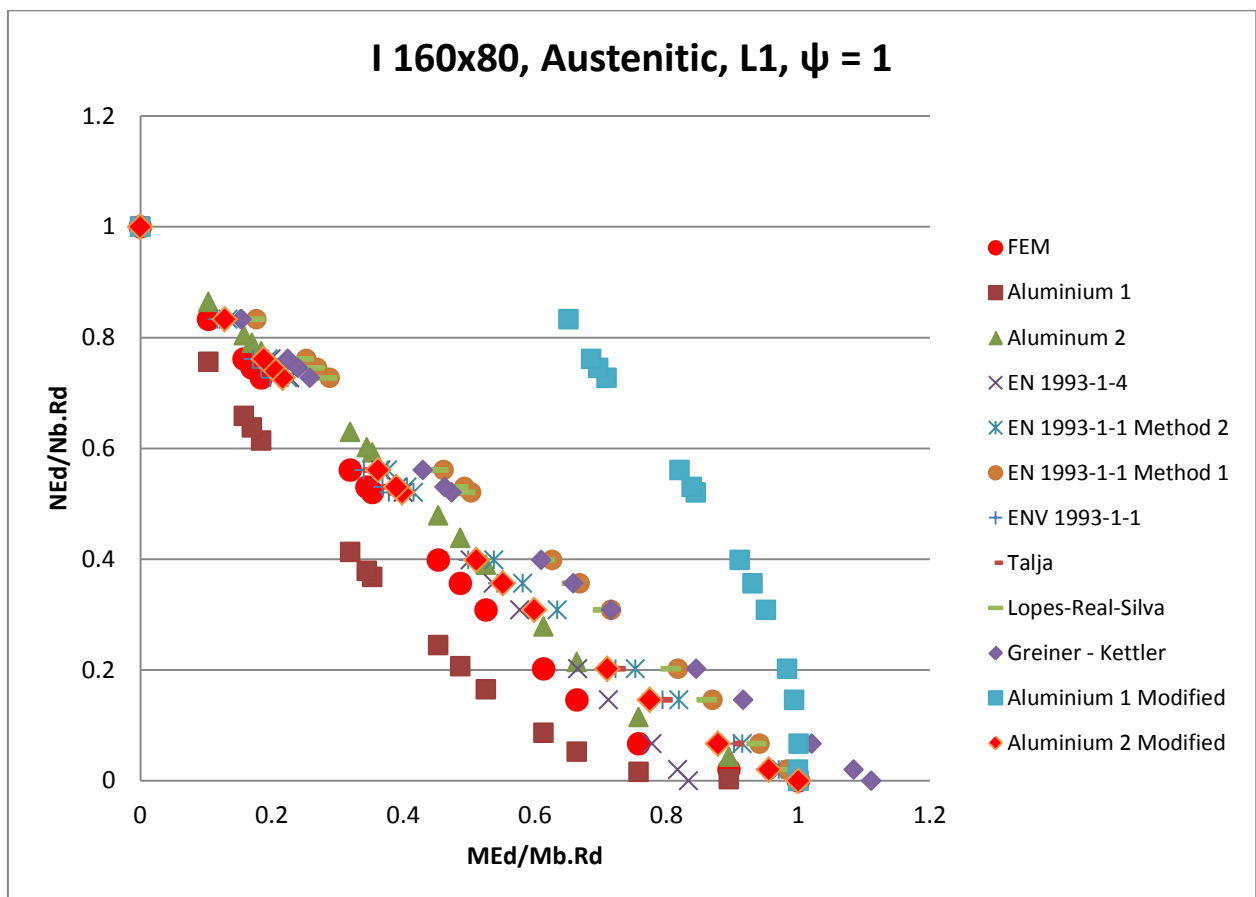


Figure 9-19 : I 160 x 80 Interaction axial force and bending moment diagram comparison, Austenitic, L=3000 mm,  $\psi = 1$

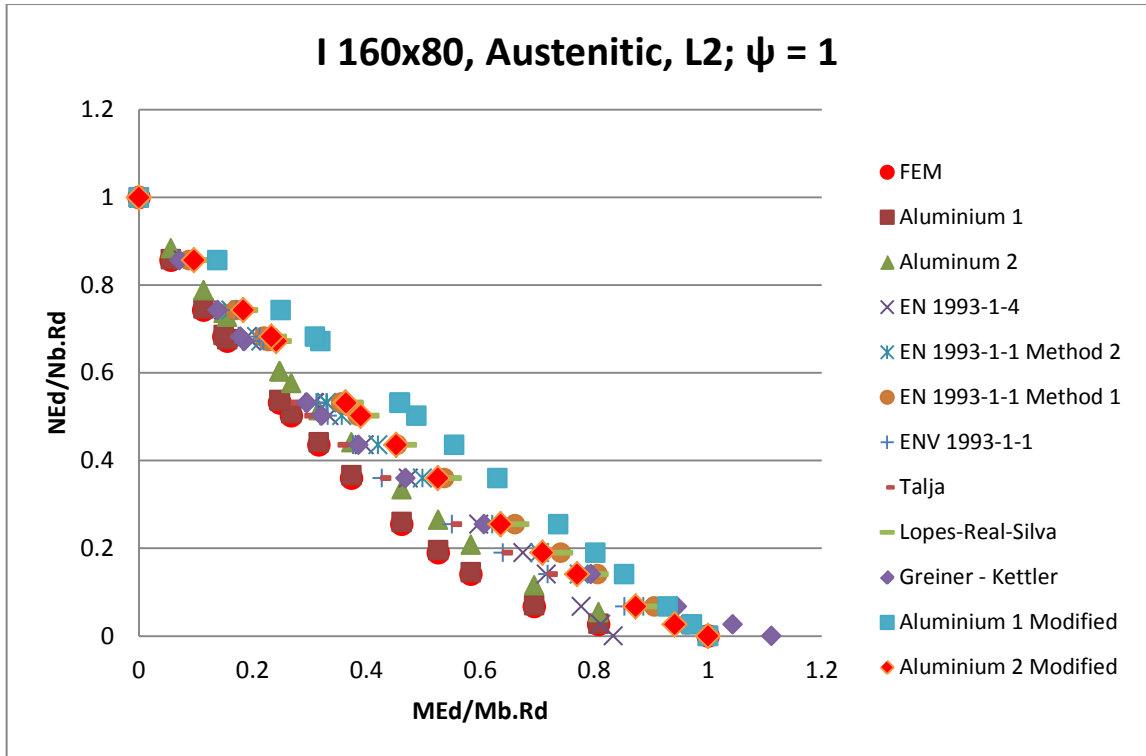


Figure 9-20 : I 160 x 80 Interaction axial force and bending moment diagram comparison, Austenitic, L=6000 mm,  $\psi = 1$

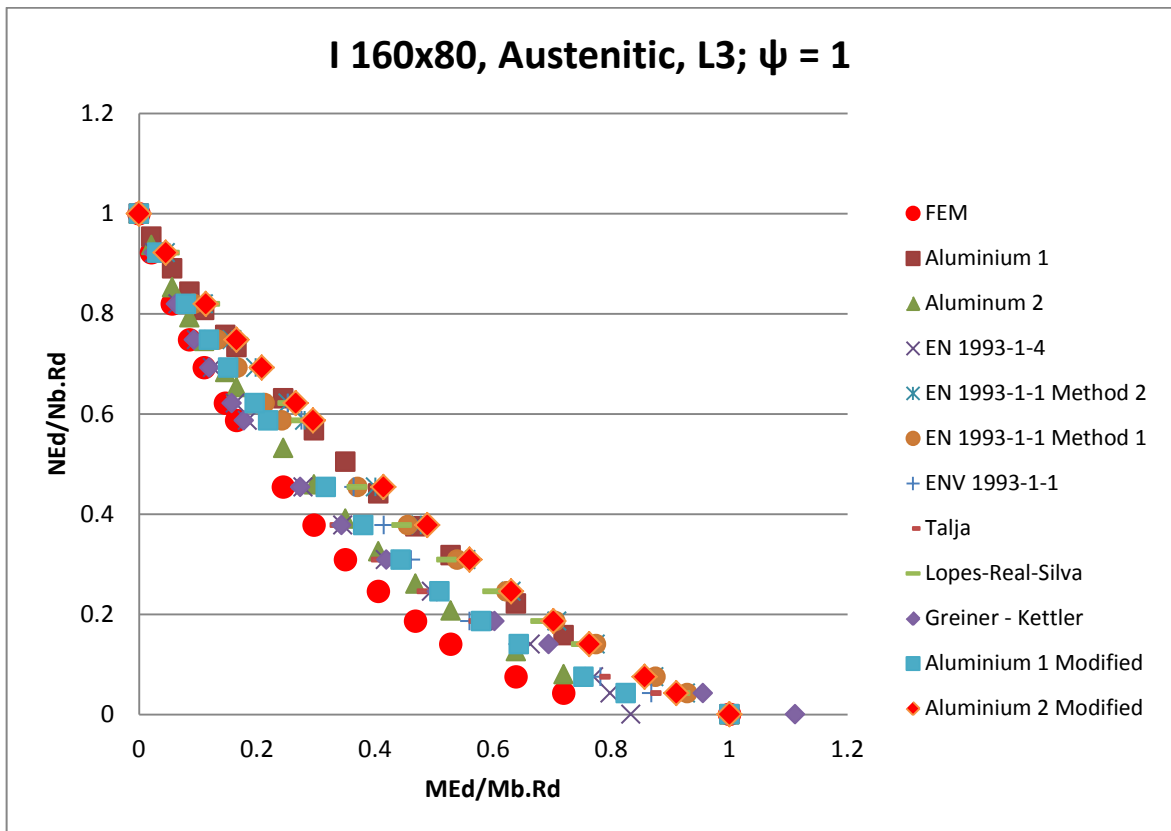


Figure 9-21 : I 160 x 80 Interaction axial force and bending moment diagram comparison, Austenitic, L=9500 mm,  $\psi = 1$

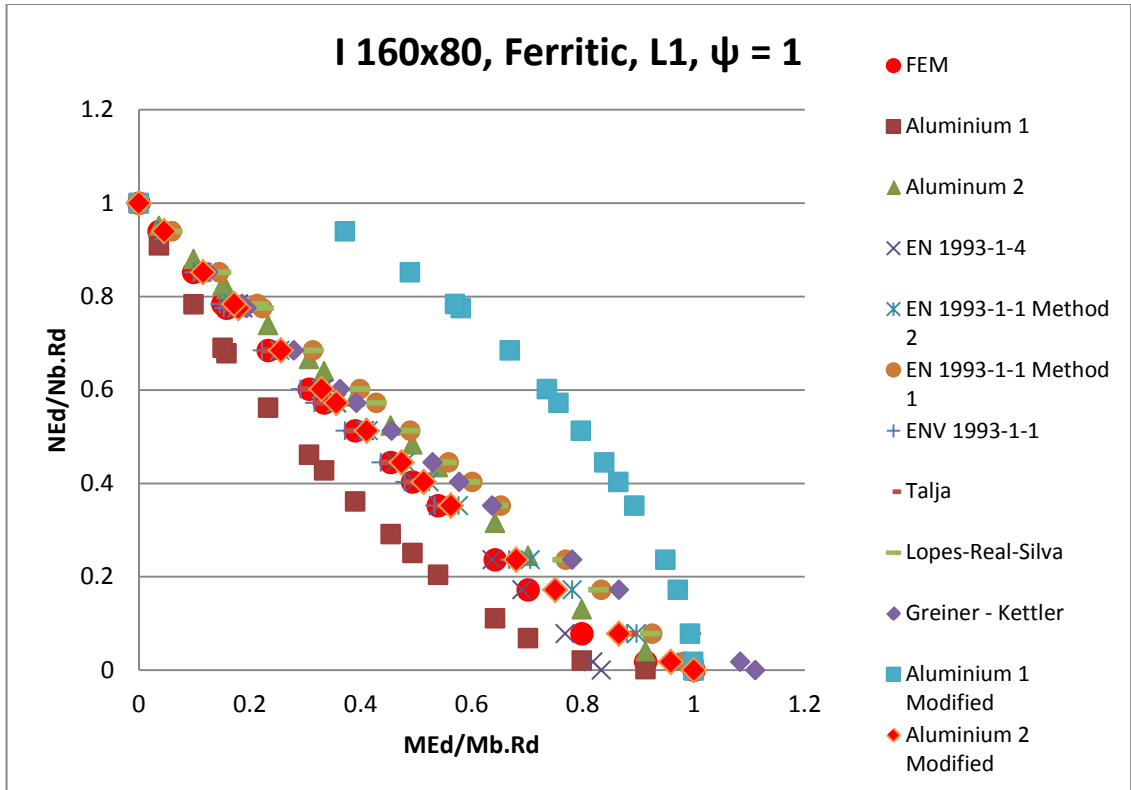


Figure 9-22 : I 160 x 80 Interaction axial force and bending moment diagram comparison, Ferritic, L=3000 mm,  $\psi = 1$

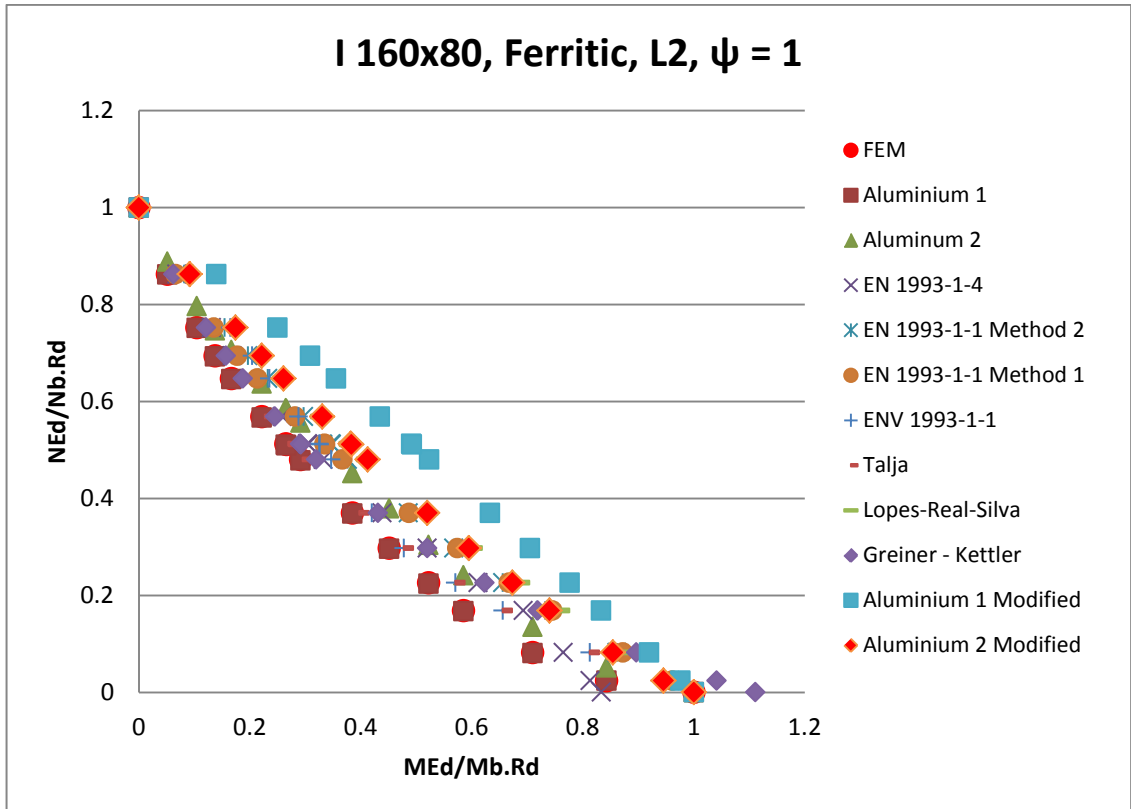


Figure 9-23 : I 160 x 80 Interaction axial force and bending moment diagram comparison, Ferritic, L=6000 mm,  $\psi = 1$

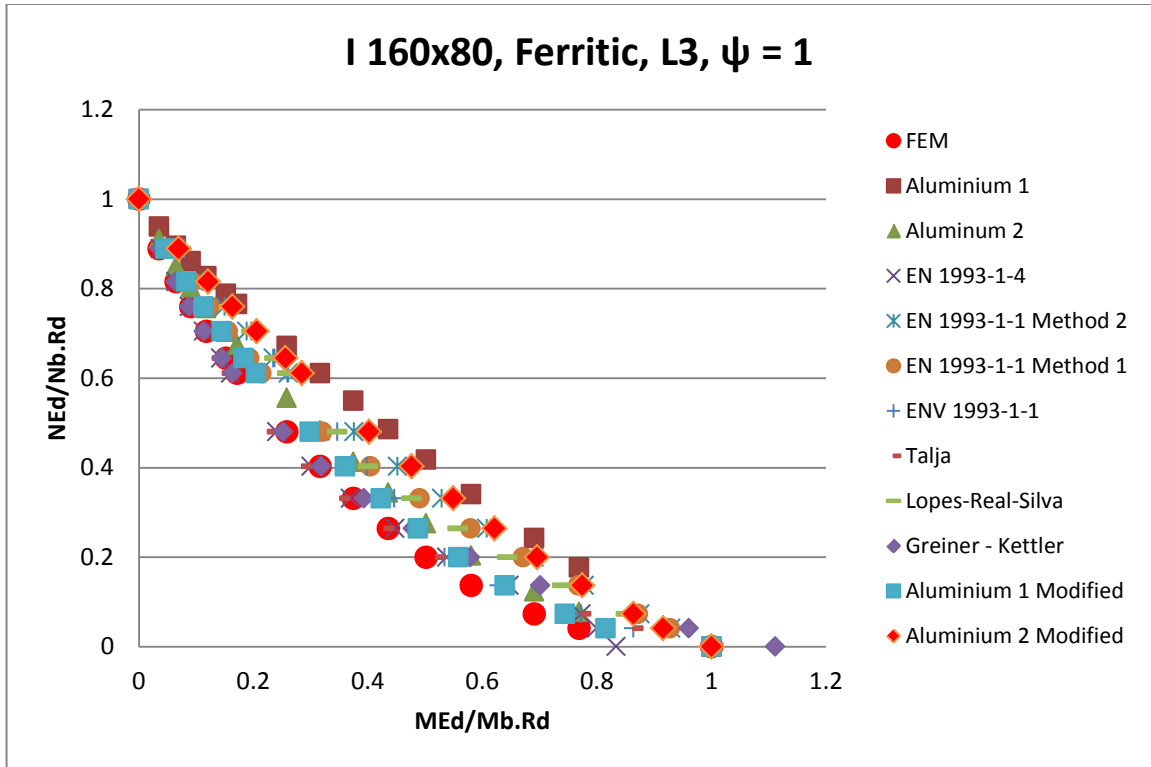


Figure 9-24 : I 160 x 80 Interaction axial force and bending moment diagram comparison, Ferritic, L=9500 mm,  $\psi = 1$

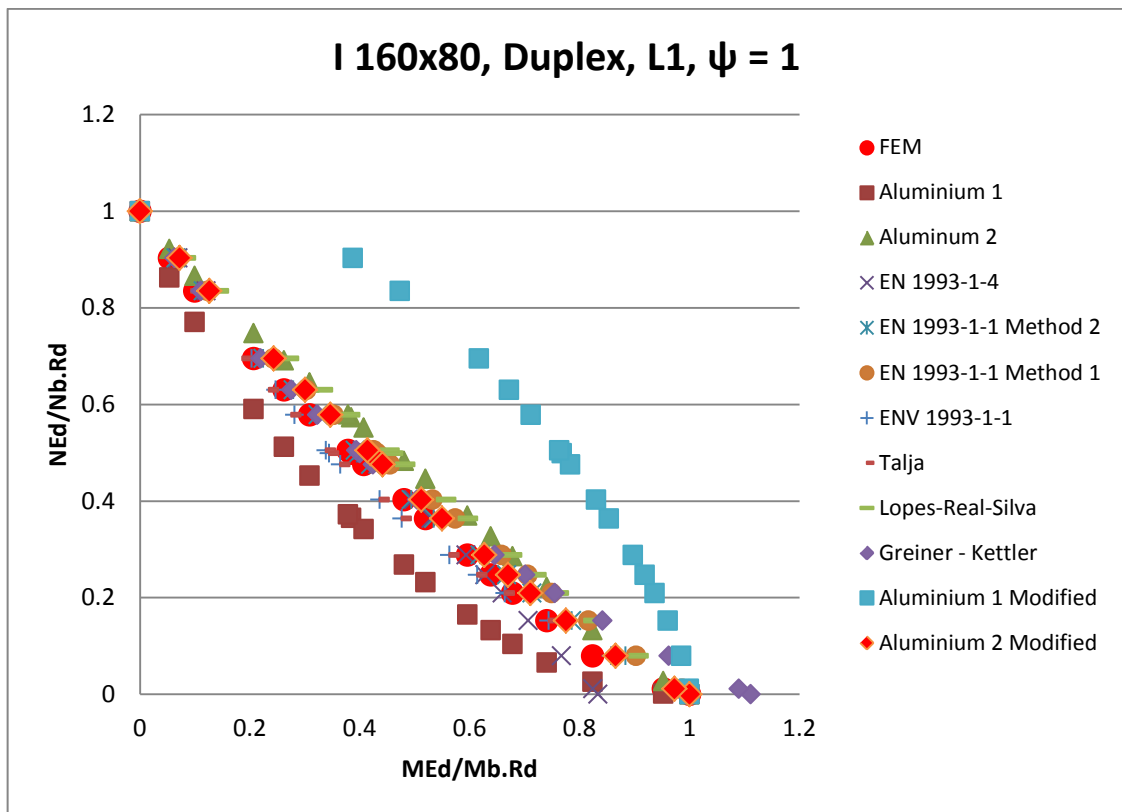


Figure 9-25 : I 160 x 80 Interaction axial force and bending moment diagram comparison, Duplex, L=3000 mm,  $\psi = 1$

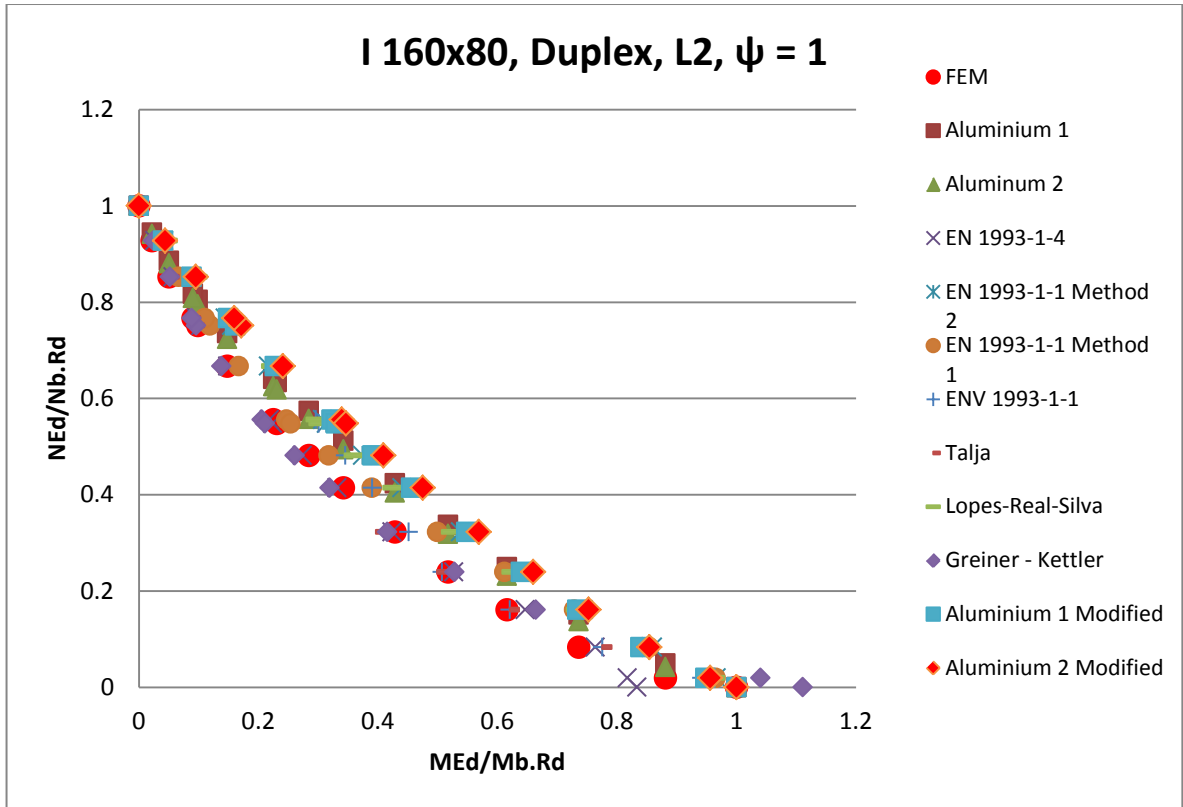


Figure 9-26 : I 160 x 80 Interaction axial force and bending moment diagram comparison, Duplex, L=6000 mm,  $\psi = 1$

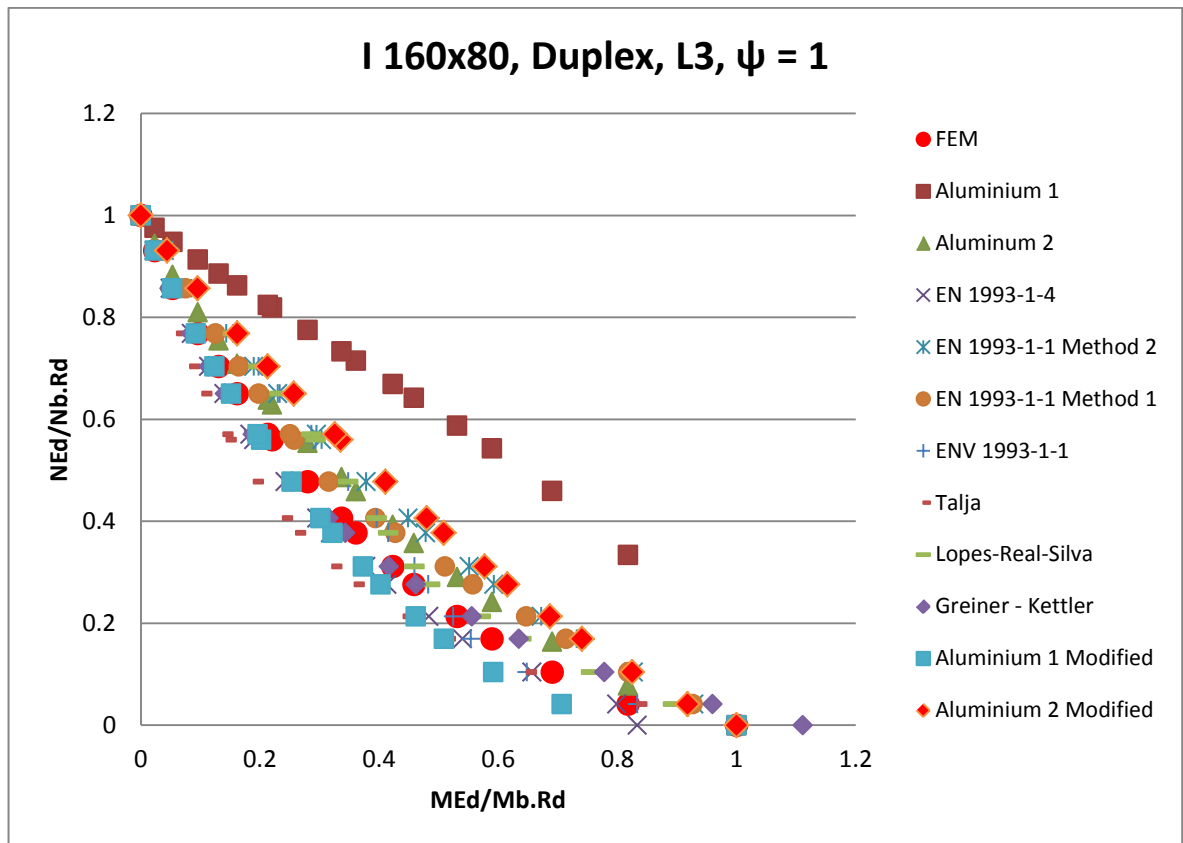


Figure 9-27 : I 160 x 80 Interaction axial force and bending moment diagram comparison, Duplex, L=9500 mm,  $\psi = 1$

The graph comparison for I - 160 x 80, physically seen that all the approaches were tending to follow the FEM simulation graph result.

Only Aluminium 1 modified approach is far out of the FEM result interaction on L = 3000 mm for all Austenitic, Ferritic, and Duplex materials.

And again that Greiner-Kettler formula tends to overestimate under low axial force and high bending moment. And also Aluminium 1 has out of the FEM result's trend graph on Duplex L = 9500 mm,  $\lambda = 2.255$ .

The mean and standard deviation of the ratio  $k_y$  of the proposed by standard codes or research journals and with  $k_y$  Finite Element (FEM) result ( $k_y/k_{y,FEM}$  summarize in table 9.15, table 9.16 and table 9.17.

I-Section 160 X 80, Austenitic, L = 3000 mm, $\psi = 1$									
	EN 1993-1-4	EN 1993-1-1 Method 2	EN 1993-1-1 Method 1	ENV 1993-1-1	Talja [17]	Lopes-Real [15]	Greiner-Kettler [13]	Modif. Aluminium 1	Modif. Aluminium 2
$k_y/k_{y,FEM}$ Mean (Average)	0.851	0.790	0.687	0.850	0.850	0.695	0.698	0.477	0.822
$k_y/k_{y,FEM}$ Standard Deviation	0.253	0.217	0.211	0.230	0.230	0.212	0.193	0.271	0.224
I-Section 160 X 80, Austenitic, L = 6000 mm, $\psi = 1$									
	EN 1993-1-4	EN 1993-1-1 Method 2	EN 1993-1-1 Method 1	ENV 1993-1-1	Talja [17]	Lopes-Real [15]	Greiner-Kettler [13]	Modif. Aluminium 1	Modif. Aluminium 2
$k_y/k_{y,FEM}$ Mean (Average)	0.781	0.714	0.680	0.745	0.830	0.651	0.754	0.573	0.676
$k_y/k_{y,FEM}$ Standard Deviation	0.238	0.205	0.201	0.220	0.227	0.204	0.206	0.214	0.207
I-Section 160 X 80, Austenitic, L =9500 mm, $\psi = 1$									
	EN 1993-1-4	EN 1993-1-1 Method 2	EN 1993-1-1 Method 1	ENV 1993-1-1	Talja [17]	Lopes-Real [15]	Greiner-Kettler [13]	Modif. Aluminium 1	Modif. Aluminium 2
$k_y/k_{y,FEM}$ Mean (Average)	0.821	0.601	0.643	0.647	0.848	0.606	0.799	0.739	0.592
$k_y/k_{y,FEM}$ Standard Deviation	0.238	0.202	0.197	0.237	0.234	0.213	0.223	0.211	0.206

Table 9.15 : Mean and standard deviation of I- 160 x 80 column specimens (Austenitic,  $\psi = 1$ )

I-Section 160 X 80, Ferritic, L = 3000 mm, $\psi = 1$									
	EN 1993-1-4	EN 1993-1-1 Method 2	EN 1993-1-1 Method 1	ENV 1993-1-1	Talja [17]	Lopes-Real [15]	Greiner-Kettler [13]	Modif. Aluminium 1	Modif. Aluminium 2
$k_y/k_{y,FEM}$ Mean (Average)	0.897	0.860	0.749	0.941	0.944	0.748	0.780	0.492	0.868
$k_y/k_{y,FEM}$ Standard Deviation	0.259	0.226	0.214	0.248	0.248	0.216	0.204	0.280	0.229
I-Section 160 X 80, Ferritic, L = 6000 mm, $\psi = 1$									
	EN 1993-1-4	EN 1993-1-1 Method 2	EN 1993-1-1 Method 1	ENV 1993-1-1	Talja [17]	Lopes-Real [15]	Greiner-Kettler [13]	Modif. Aluminium 1	Modif. Aluminium 2
$k_y/k_{y,FEM}$ Mean (Average)	0.830	0.729	0.757	0.766	0.883	0.682	0.813	0.569	0.686
$k_y/k_{y,FEM}$ Standard Deviation	0.245	0.212	0.210	0.238	0.239	0.212	0.221	0.226	0.214
I-Section 160 X 80, Ferritic, L = 9500 mm, $\psi = 1$									
	EN 1993-1-4	EN 1993-1-1 Method 2	EN 1993-1-1 Method 1	ENV 1993-1-1	Talja [17]	Lopes-Real [15]	Greiner-Kettler [13]	Modif. Aluminium 1	Modif. Aluminium 2
$k_y/k_{y,FEM}$ Mean (Average)	0.946	0.660	0.730	0.712	0.994	0.675	0.890	0.815	0.636
$k_y/k_{y,FEM}$ Standard Deviation	0.264	0.206	0.207	0.250	0.284	0.224	0.253	0.226	0.212

Table 9.16 : Mean and standard deviation of I- 160 x 80 column specimens (Ferritic,  $\psi = 1$ )

I-Section 160 X 80, Duplex, L = 3000 mm, $\psi = 1$									
	EN 1993-1-4	EN 1993-1-1 Method 2	EN 1993-1-1 Method 1	ENV 1993-1-1	Talja [17]	Lopes-Real [15]	Greiner-Kettler [13]	Modif. Aluminium 1	Modif. Aluminium 2
$k_y/k_{y,FEM}$ Mean (Average)	0.922	0.892	0.842	0.972	1.001	0.797	0.868	0.548	0.862
$k_y/k_{y,FEM}$ Standard Deviation	0.253	0.227	0.216	0.255	0.256	0.217	0.220	0.270	0.225
I-Section 160 X 80, Duplex, L = 6000 mm, $\psi = 1$									
	EN 1993-1-4	EN 1993-1-1 Method 2	EN 1993-1-1 Method 1	ENV 1993-1-1	Talja [17]	Lopes-Real [15]	Greiner-Kettler [13]	Modif. Aluminium 1	Modif. Aluminium 2
$k_y/k_{y,FEM}$ Mean (Average)	0.693	0.667	0.932	0.703	0.807	0.743	0.973	0.700	0.932
$k_y/k_{y,FEM}$ Standard Deviation	0.226	0.227	0.262	0.224	0.225	0.270	0.269	0.238	0.262
I-Section 160 X 80, Duplex, L = 9500 mm, $\psi = 1$									
	EN 1993-1-4	EN 1993-1-1 Method 2	EN 1993-1-1 Method 1	ENV 1993-1-1	Talja [17]	Lopes-Real [15]	Greiner-Kettler [13]	Modif. Aluminium 1	Modif. Aluminium 2
$k_y/k_{y,FEM}$ Mean (Average)	1.055	0.712	0.782	0.780	1.283	0.755	0.978	1.033	0.672
$k_y/k_{y,FEM}$ Standard Deviation	0.268	0.201	0.208	0.260	0.379	0.238	0.262	0.264	0.205

Table 9.17 : Mean and standard deviation of I- 160 x 80 column specimens (Duplex,  $\psi = 1$ )



**9.4. SHS 60 X 60 X 5 ( $\psi = 0$  and  $\psi = -1$ ) Comparison result**

Section	SHS 60 X 60 X 5	SHS 60 X 60 X 5	SHS 60 X 60 X 5	SHS 60 X 60 X 5	SHS 60 X 60 X 5	SHS 60 X 60 X 5
Steel material	Austenitic	Austenitic	Austenitic	Austenitic	Austenitic	Austenitic
Steel Grade material	1.4301	1.4301	1.4301	1.4301	1.4301	1.4301
Specimen length, L (mm)	1050	2130	3410	1050	2130	3410
Load variation, $\psi$	0	0	0	-1	-1	-1
Section class	1	1	1	1	1	1
$N_{cr, FEM}$ (kN)	864.19	214.28	83.935	864.19	214.28	83.935
$A_{eff}$ (mm <sup>2</sup> )	1010.776	1010.776	1010.776	1010.776	1010.776	1010.776
$\lambda_{FEM}$	0.518665	1.041599	1.664255	0.518665	1.041599	1.664255
$X_{b,y}$ EN 1993-1-4	0.789539	0.501517	0.28881	0.789539	0.501517	0.28881

Table 9.18 : Parametric result of SHS 60 x 60 x 5 column specimens ( $\psi = 0$  and  $\psi = -1$ )

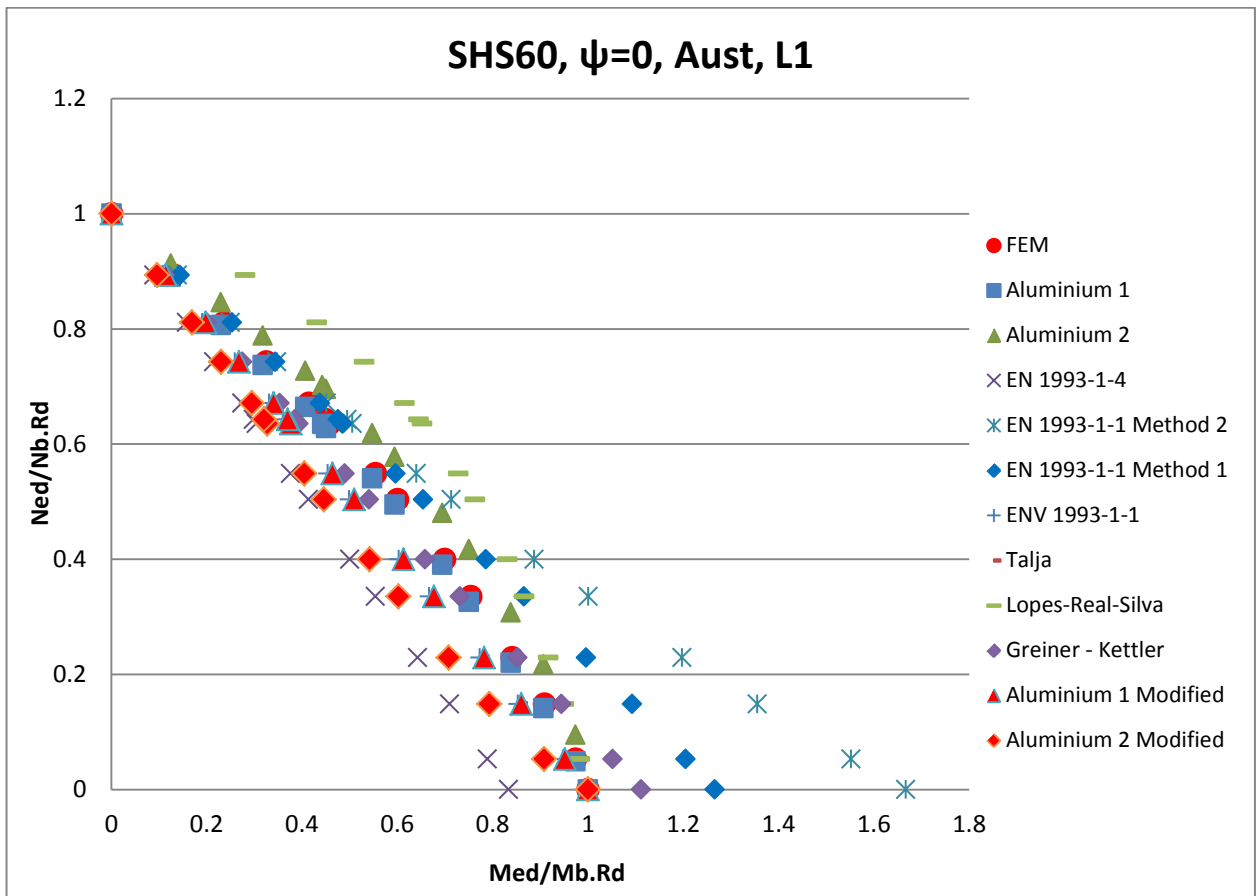


Figure 9-28 : SHS 60 x 60 x 5 Interaction axial force and bending moment diagram comparison, Austenitic, L=1050 mm,  $\psi = 0$

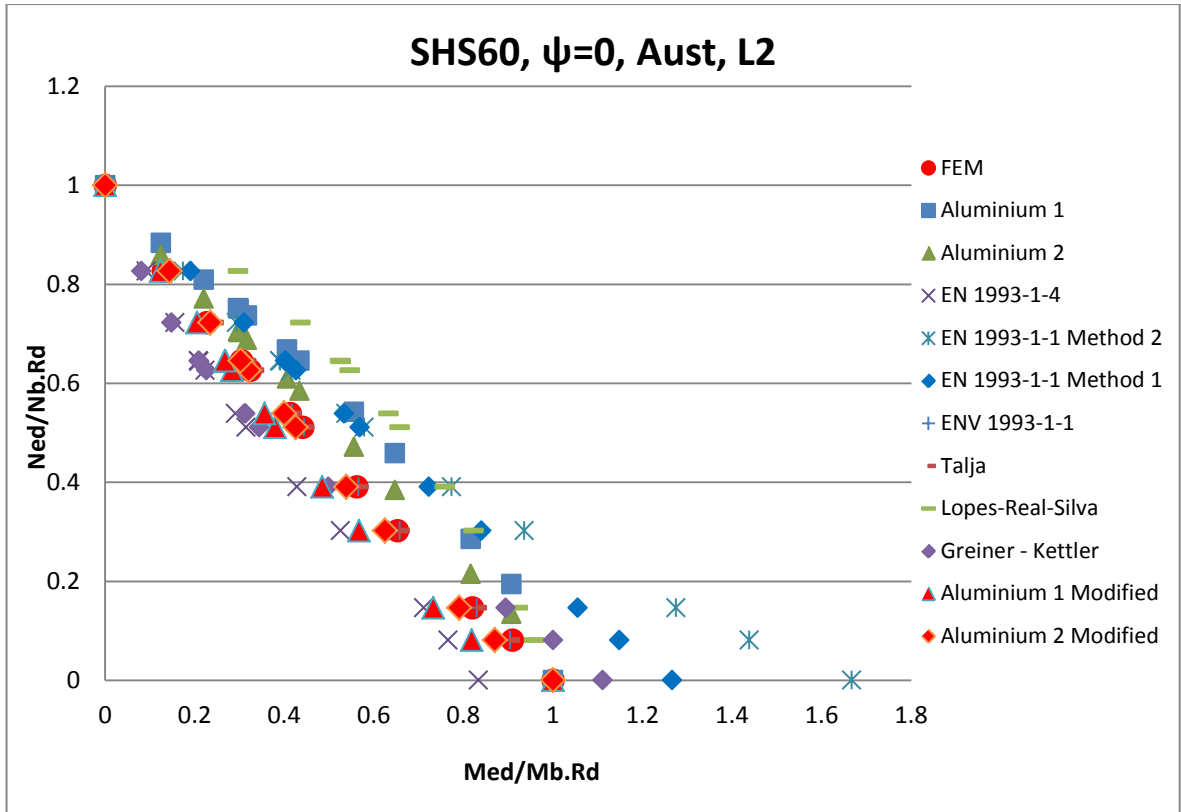


Figure 9-29 : SHS 60 x 60 x 5 Interaction axial force and bending moment diagram comparison, Austenitic, L=1700 mm,  $\psi = 0$

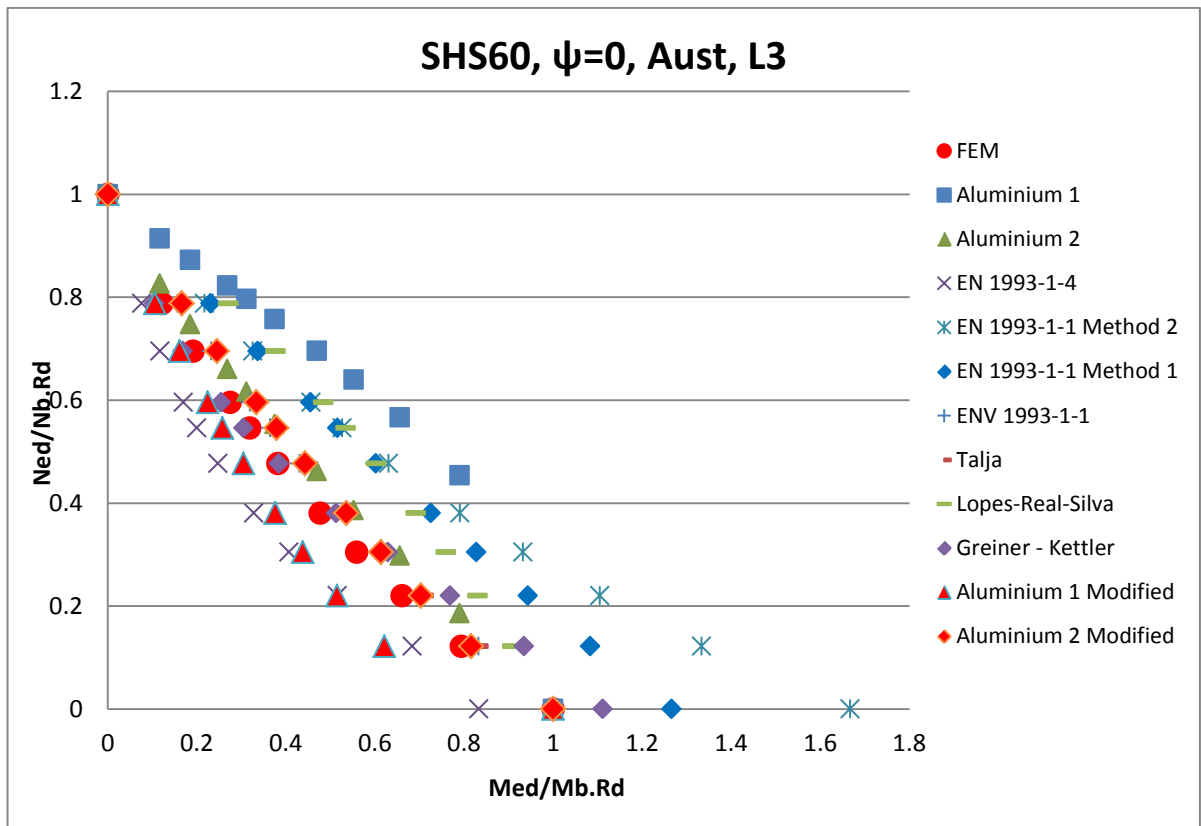


Figure 9-30 : SHS 60 x 60 x 5 Interaction axial force and bending moment diagram comparison, Austenitic, L=2350 mm,  $\psi = 0$

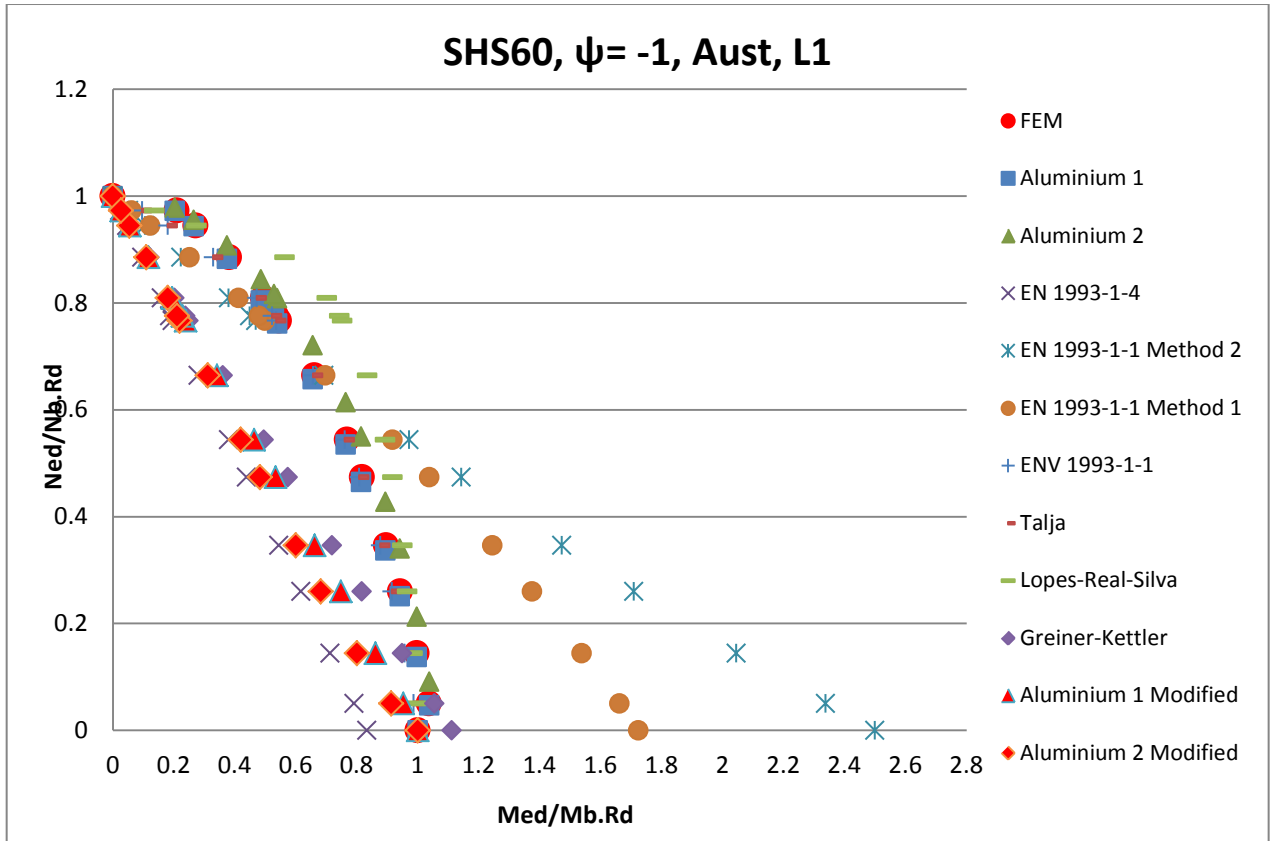


Figure 9-31 : SHS 60 x 60 x 5 Interaction axial force and bending moment diagram comparison, Austenitic, L=1050 mm,  $\psi = -1$

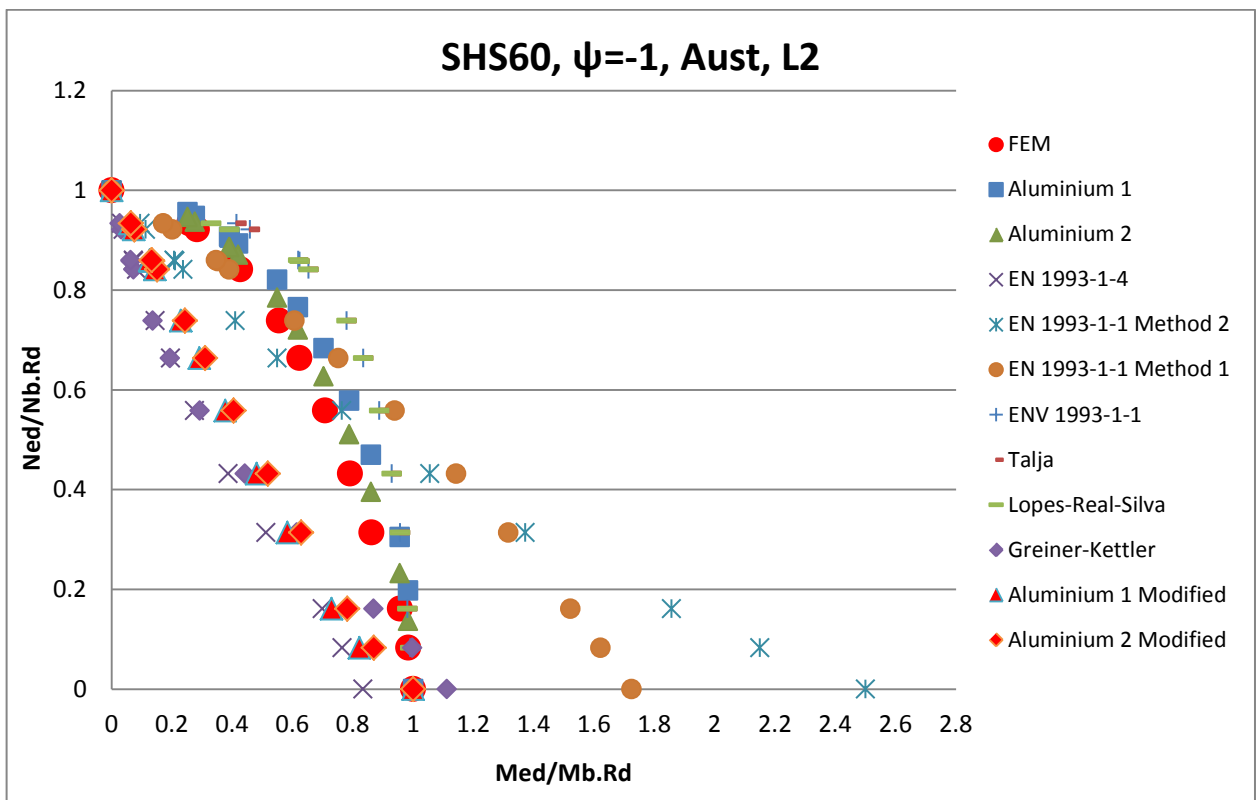


Figure 9-32 : SHS 60 x 60 x 5 Interaction axial force and bending moment diagram comparison, Austenitic, L=1700 mm,  $\psi = -1$

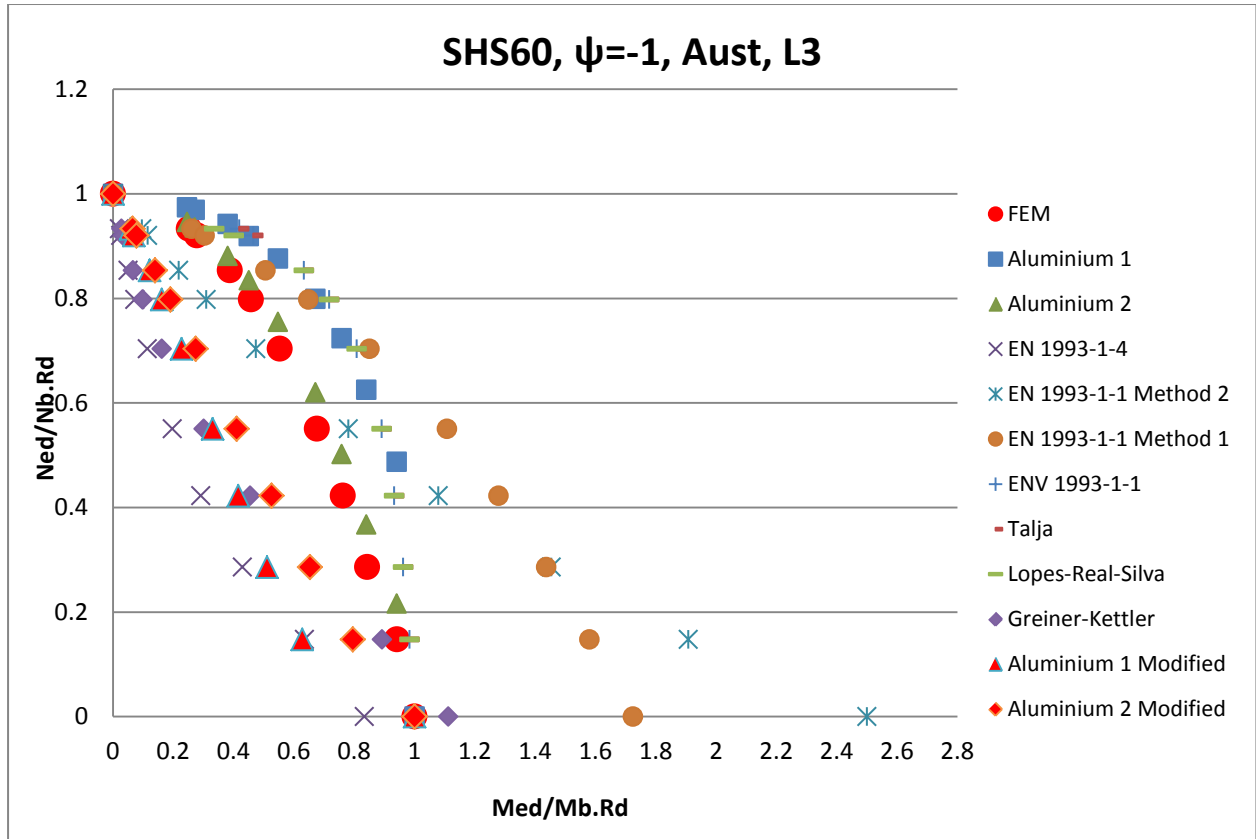


Figure 9-33 : SHS 60 x 60 x 5 Interaction axial force and bending moment diagram comparison, Austenitic, L=2350 mm,  $\psi = -1$

The graphs presented above based on  $\omega_x$  factor due to unequal end moments ( $\psi = 0$ , and  $\psi = -1$ ) for Aluminium formulation considered as one ( $\omega_x = 1$ ), due to the calculated  $\omega_x$  result, based on equation (3.43), shows unreliable interaction graphs. As conclusion, the  $\omega_x$  factor in Aluminium formula has not influenced the interaction calculation for stainless steel materials.

The graph comparison for SHS 60x60x5 ( $\psi = 0$ , and  $\psi = -1$ ), physically seen that :

- EN 1993-1-1 (both method 1 and method 2), and Greiner-Kettler formula tends to overestimate under low axial force and high bending moment.
- EN 1993-1-4 tends to underestimate under low axial force and high bending moment for all length slenderness tested.
- Aluminium 1 and Aluminium 2 formulas show better results as they have the same tendency to FEM result graph. However, Aluminium 2 shows out of trends' FEM shape on both Austenitic  $\psi = 0$ , and  $\psi = -1$ , at L = 3410 mm, and  $\lambda = 1.664$
- Lopes-Real-Silva approach has tendency to follow the trend of finite element result, but need to improve for better typical shape of the graph as FEM simulation result.

The mean and standard deviation of the ratio  $k_y$  of the proposed by standard codes or research journals and with  $k_y$  Finite Element (FEM) result ( $k_y/k_{y,FEM}$  summarize in table 9.19.

SHS 60 X 60 X 5, Austenitic, L = 1050 mm, $\psi = 0$									
	EN 1993-1-4	EN 1993-1-1 Method 2	EN 1993-1-1 Method 1	ENV 1993-1-1	Talja [17]	Lopes-Real [15]	Greiner-Kettler [13]	Modif. Aluminium 1	Modif. Aluminium 2
$k_y/k_{y,FEM}$ Mean (Average)	1.314	0.760	0.834	1.090	1.090	0.721	1.010	0.999	1.203
$k_y/k_{y,FEM}$ Standard Deviation	0.379	0.241	0.237	0.313	0.313	0.256	0.296	0.410	0.358
SHS 60 X 60 X 5, Austenitic, L = 2130 mm, $\psi = 0$									
	EN 1993-1-4	EN 1993-1-1 Method 2	EN 1993-1-1 Method 1	ENV 1993-1-1	Talja [17]	Lopes-Real [15]	Greiner-Kettler [13]	Modif. Aluminium 1	Modif. Aluminium 2
$k_y/k_{y,FEM}$ Mean (Average)	1.243	0.669	0.704	0.899	0.899	0.647	1.152	1.034	0.934
$k_y/k_{y,FEM}$ Standard Deviation	0.391	0.211	0.213	0.272	0.272	0.258	0.426	0.314	0.283
SHS 60 X 60 X 5, Austenitic, L = 3410 mm, $\psi = 0$									
	EN 1993-1-4	EN 1993-1-1 Method 2	EN 1993-1-1 Method 1	ENV 1993-1-1	Talja [17]	Lopes-Real [15]	Greiner-Kettler [13]	Modif. Aluminium 1	Modif. Aluminium 2
$k_y/k_{y,FEM}$ Mean (Average)	1.313	0.541	0.591	0.811	0.811	0.622	0.896	1.105	0.795
$k_y/k_{y,FEM}$ Standard Deviation	0.468	0.180	0.210	0.276	0.276	0.262	0.317	0.376	0.276

Table 9.19 : Mean and standard deviation of SHS 60 x 60 x 5 column specimens (Austenitic,  $\psi = 0$ )

SHS 60 X 60 X 5, Austenitic, L = 1050 mm, $\psi = -1$									
	EN 1993-1-4	EN 1993-1-1 Method 2	EN 1993-1-1 Method 1	ENV 1993-1-1	Talja [17]	Lopes-Real [15]	Greiner-Kettler [13]	Modif. Aluminium 1	Modif. Aluminium 2
$k_y/k_{y,FEM}$ Mean (Average)	2.754	1.129	1.093	1.074	1.074	0.859	2.159	2.241	2.388
$k_y/k_{y,FEM}$ Standard Deviation	2.273	1.020	0.813	0.433	0.433	0.319	1.837	1.824	1.878
SHS 60 X 60 X 5, Austenitic, L = 2130 mm, $\psi = -1$									
	EN 1993-1-4	EN 1993-1-1 Method 2	EN 1993-1-1 Method 1	ENV 1993-1-1	Talja [17]	Lopes-Real [15]	Greiner-Kettler [13]	Modif. Aluminium 1	Modif. Aluminium 2
$k_y/k_{y,FEM}$ Mean (Average)	3.454	1.217	0.854	0.725	0.725	0.744	3.766	2.163	2.056
$k_y/k_{y,FEM}$ Standard Deviation	2.434	0.841	0.388	0.253	0.253	0.249	3.100	1.173	1.131
SHS 60 X 60 X 5, Austenitic, L = 3410 mm, $\psi = -1$									
	EN 1993-1-4	EN 1993-1-1 Method 2	EN 1993-1-1 Method 1	ENV 1993-1-1	Talja [17]	Lopes-Real [15]	Greiner-Kettler [13]	Modif. Aluminium 1	Modif. Aluminium 2
$k_y/k_{y,FEM}$ Mean (Average)	4.694	1.137	0.634	0.686	0.686	0.709	3.513	2.250	1.928
$k_y/k_{y,FEM}$ Standard Deviation	3.878	0.848	0.250	0.269	0.269	0.266	3.123	1.271	1.150

Table 9.20 : Mean and standard deviation of SHS 60 x 60 x 5 column specimens (Austenitic,  $\psi = -1$ )

### 9.5. Ratio of $k_y/k_{y,FEM}$ comparison distribution data (Overall group data result)

Individual comparisons (material, section, and bending moment variation) have been presented in previous chapter (Chapter 9.1 to chapter 9.4) and obtained  $k_y/k_{y,FEM}$  for all standard codes and researcher approaches.

Hence, the ratio of  $k_y/k_{y,FEM}$  can be compared and observed for distribution data in relation with slenderness ( $\lambda$ ), ratio of axial force ( $NEd/Nb.Rd$ ), and the end bending moments variation ( $\psi$ ).

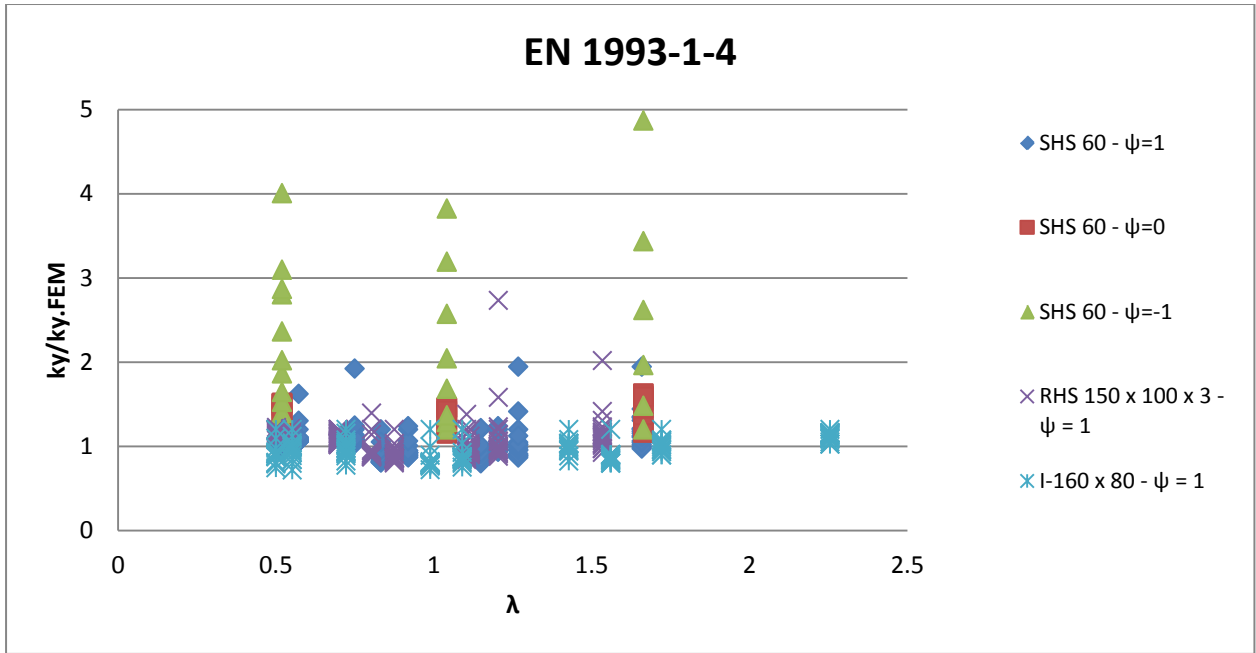


Figure 9-34 : distribution data result for ratio of  $k_y/k_{y.FEM}$  with  $\lambda$  (EN 1993-1-4)

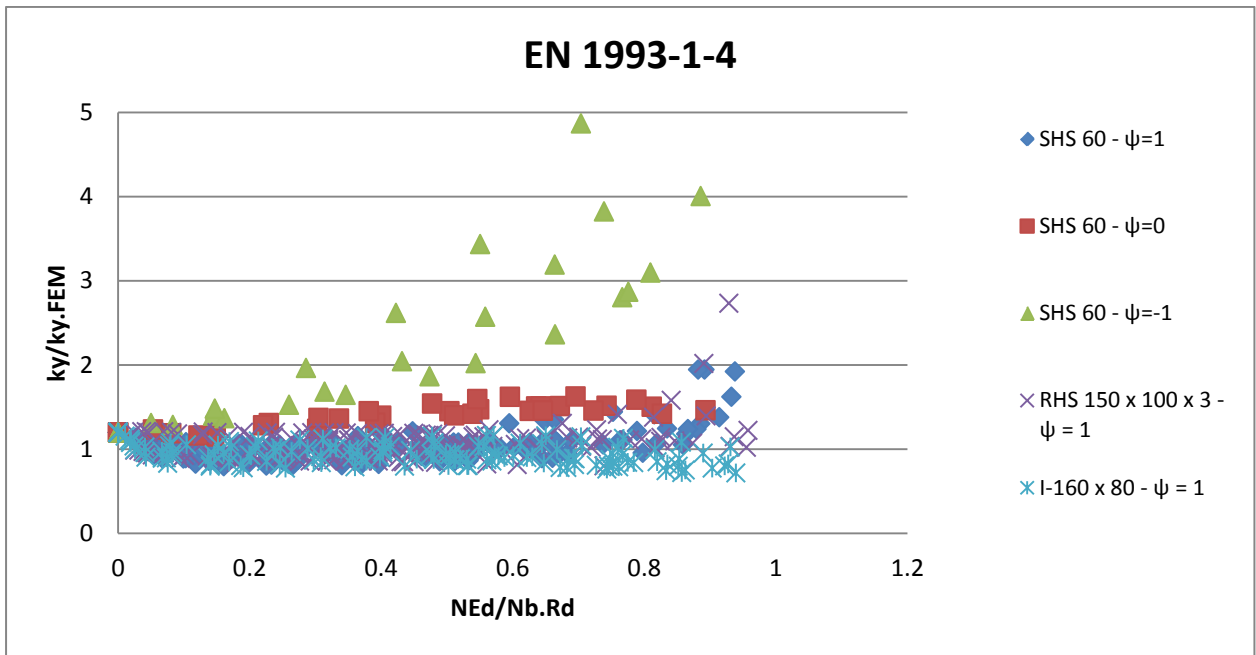


Figure 9-35 : distribution data result for ratio of  $k_y/k_{y.FEM}$  with  $N_{Ed}/N_{b.Rd}$  (EN 1993-1-4)

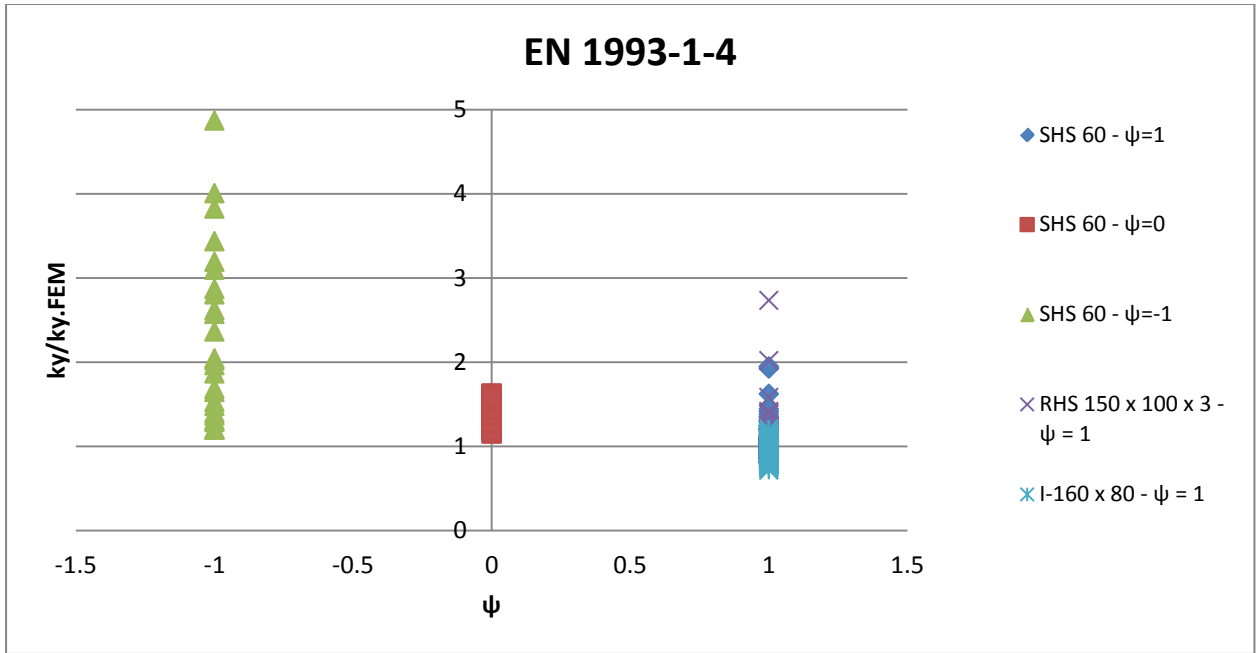


Figure 9-36 : distribution data result for ratio of  $k_y/k_{y.FEM}$  with  $\psi$  (EN 1993-1-4)

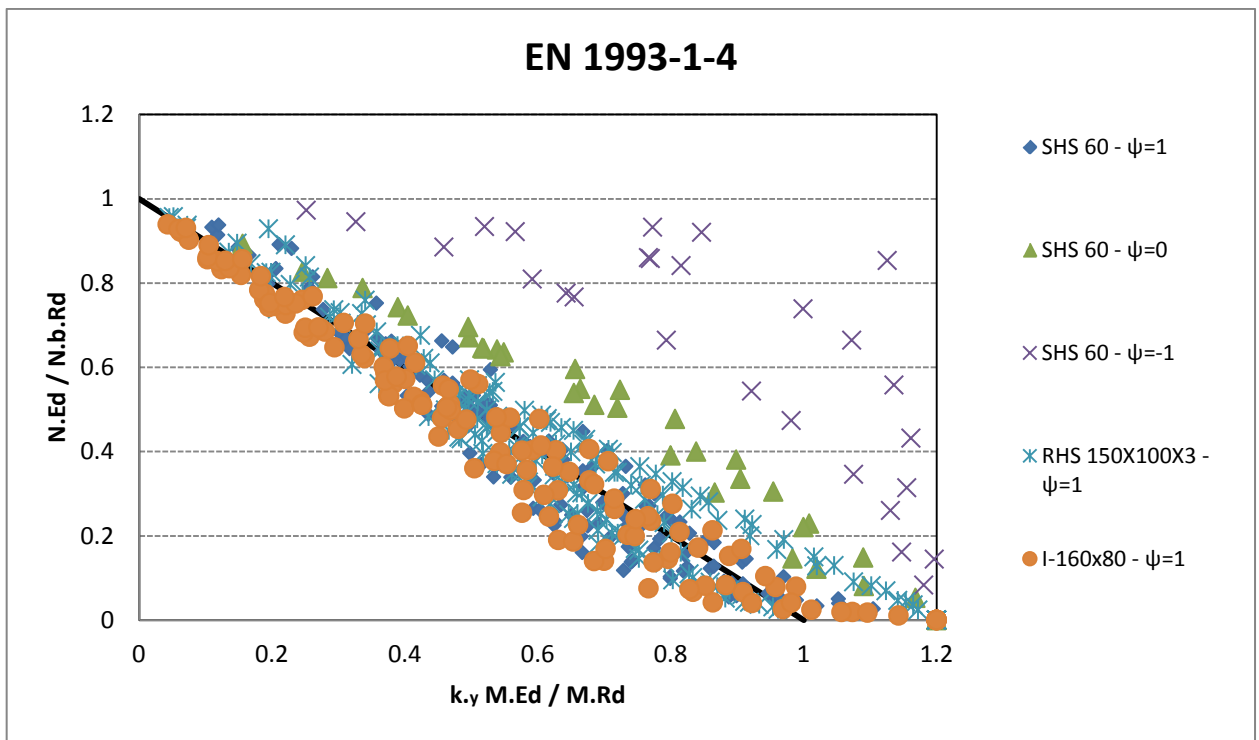


Figure 9-37 : distribution data result for ratio of  $N_{Ed}/N_{b.Rd}$  with  $k_y * M_{Ed}/M_{Rd}$  (EN 1993-1-4)



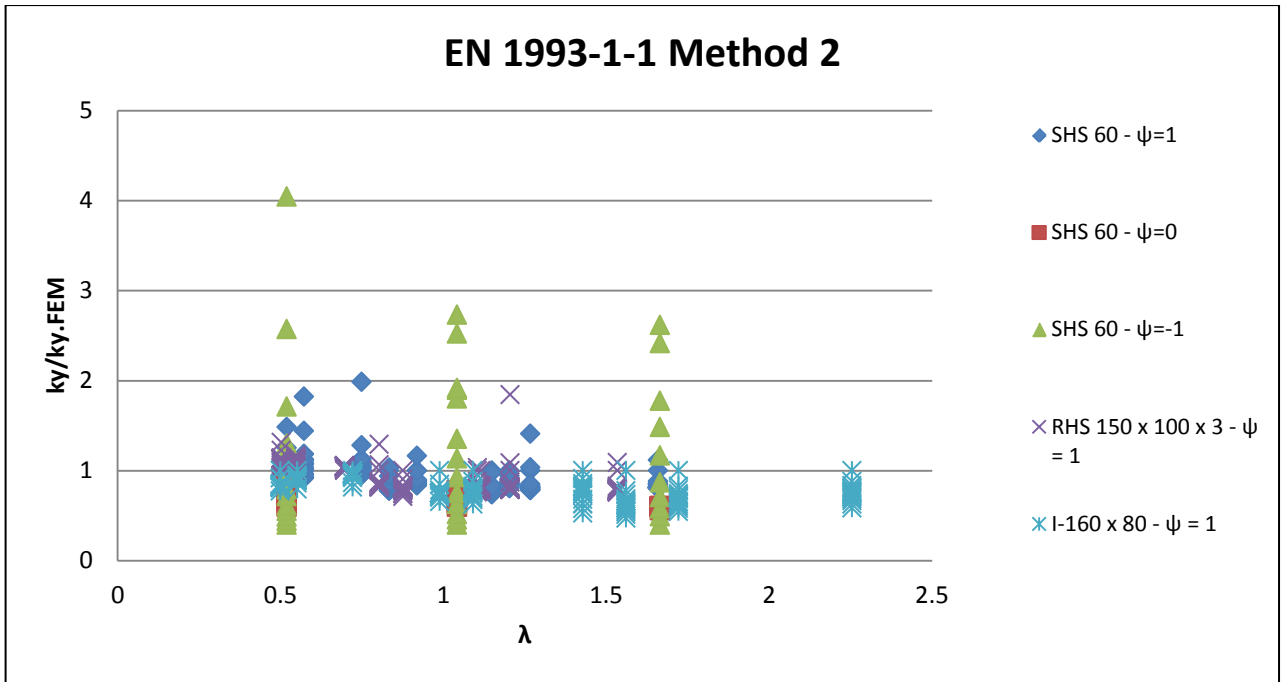


Figure 9-38 : distribution data result for ratio of  $k_y/k_{y.FEM}$  with  $\lambda$  (EN 1993-1-1 Method 2)

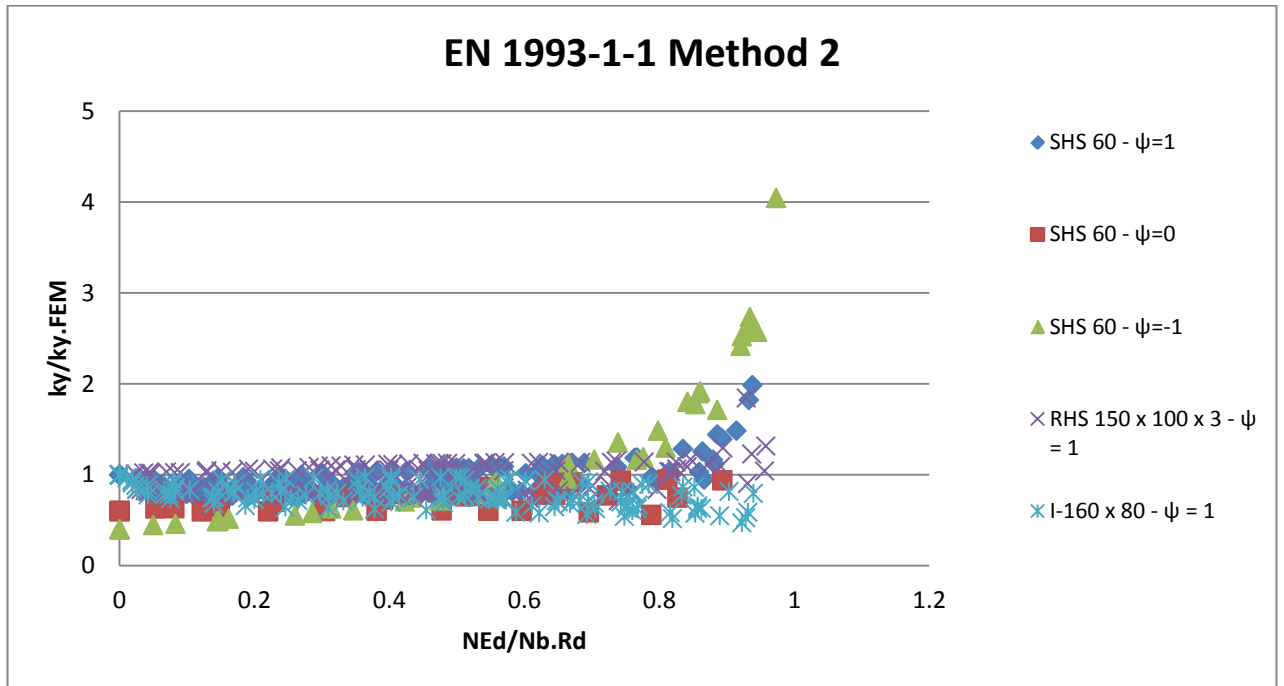


Figure 9-39 : distribution data result for ratio of  $k_y/k_{y.FEM}$  with  $N_{Ed}/N_{b.Rd}$  (EN 1993-1-1 Method 2)

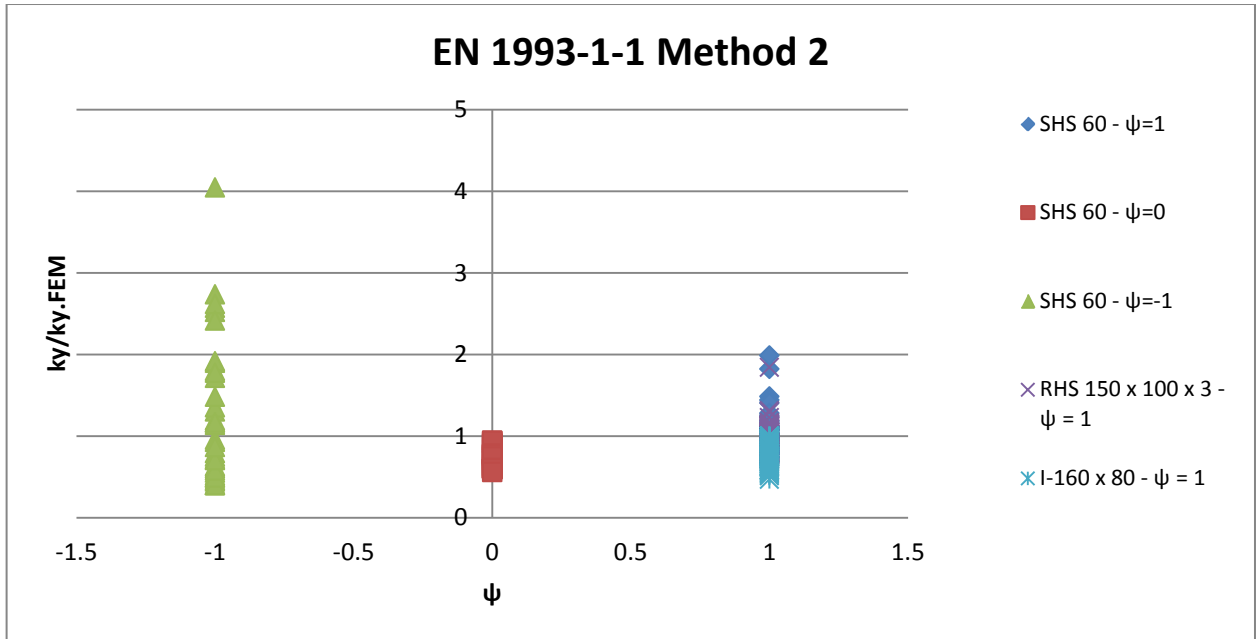


Figure 9-40 : distribution data result for ratio of  $k_y/k_{y.FEM}$  with  $\psi$  (EN 1993-1-1 Method 2)

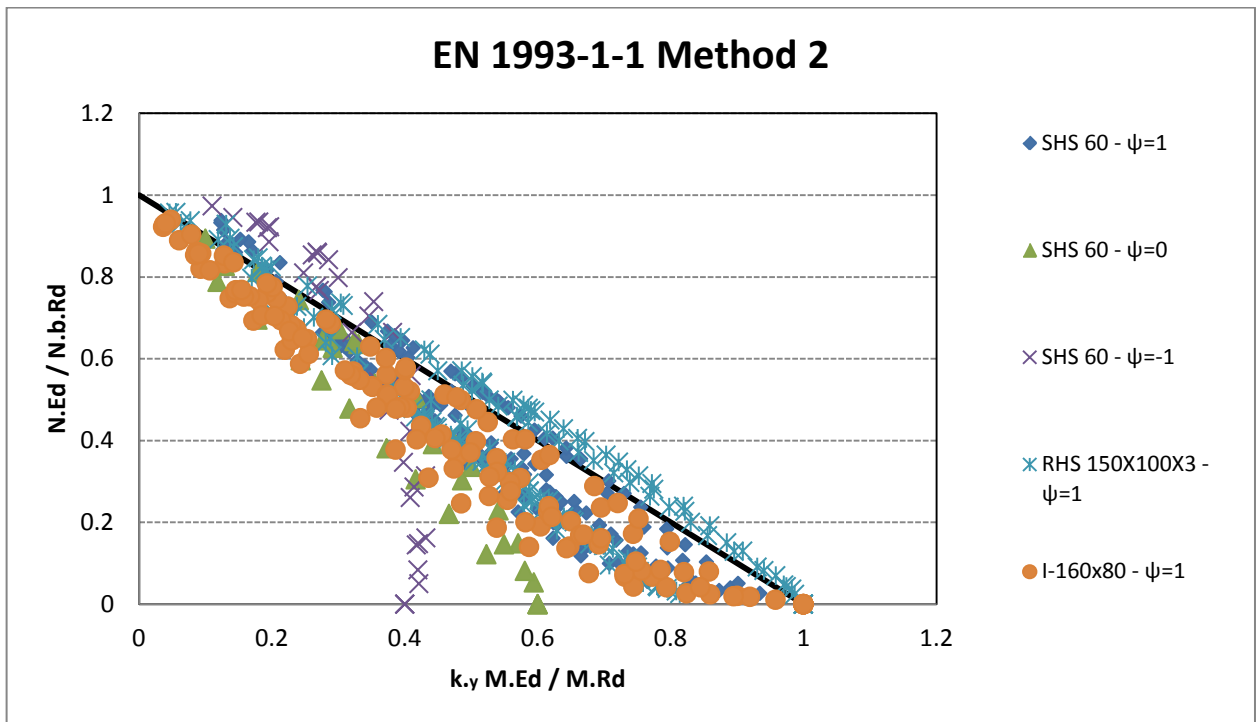


Figure 9-41 : distribution data result for ratio of  $N_{Ed}/N_{b.Rd}$  with  $k_y * M_{Ed}/M_{Rd}$  (EN 1993-1-1 Method 2)

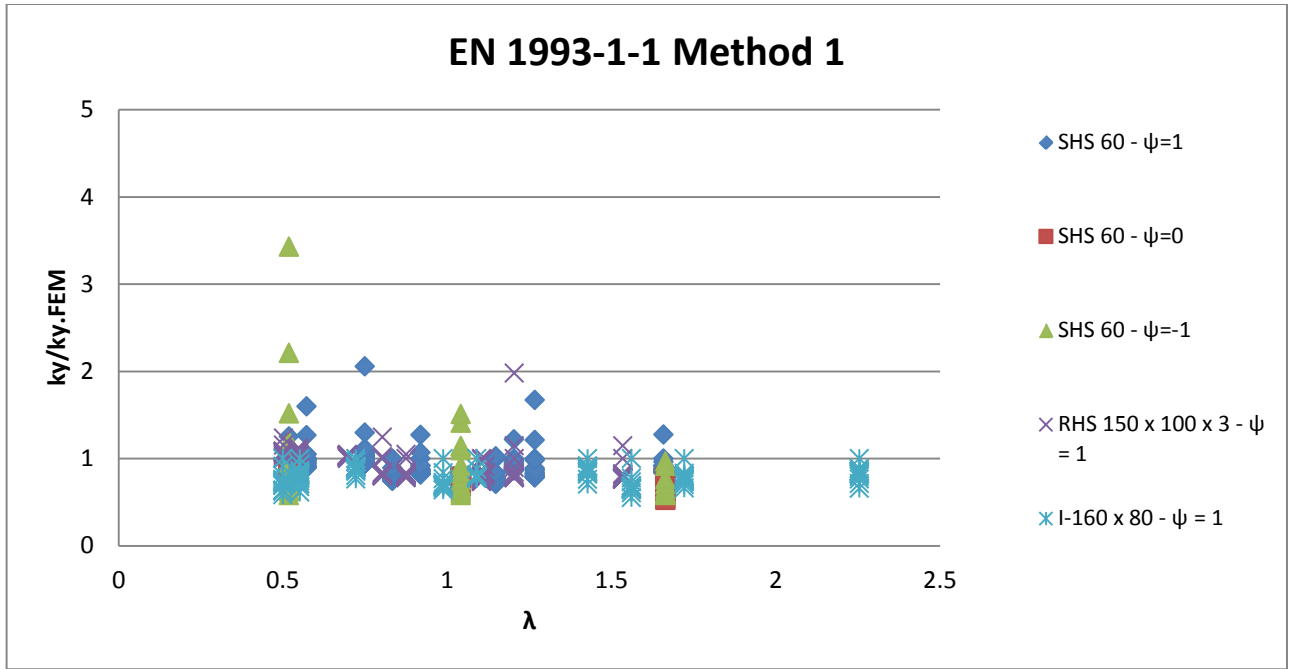


Figure 9-42 : distribution data result for ratio of  $k_y/k_{y,FEM}$  with  $\lambda$  (EN 1993-1-1 Method 1)

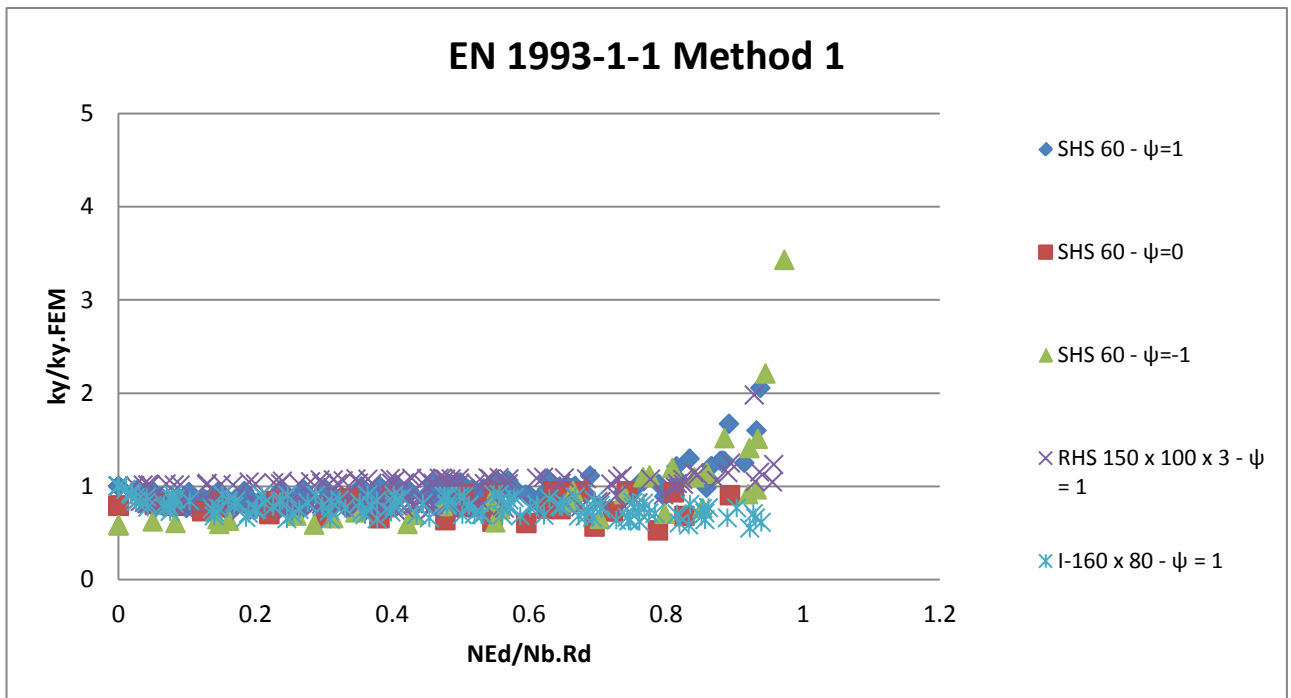


Figure 9-43 : distribution data result for ratio of  $k_y/k_{y,FEM}$  with  $N_{Ed}/N_{b,Rd}$  (EN 1993-1-1 Method 1)

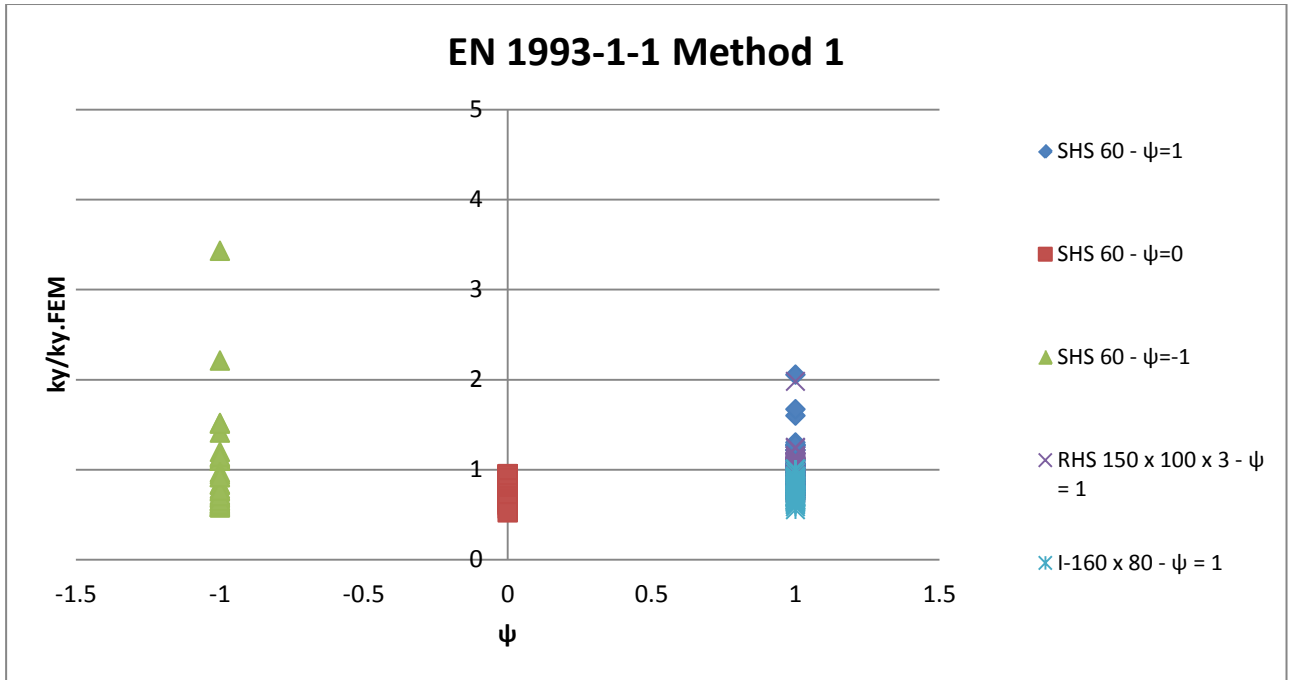


Figure 9-44 : distribution data result for ratio of  $k_y/k_{y.FEM}$  with  $\psi$  (EN 1993-1-1 Method 1)

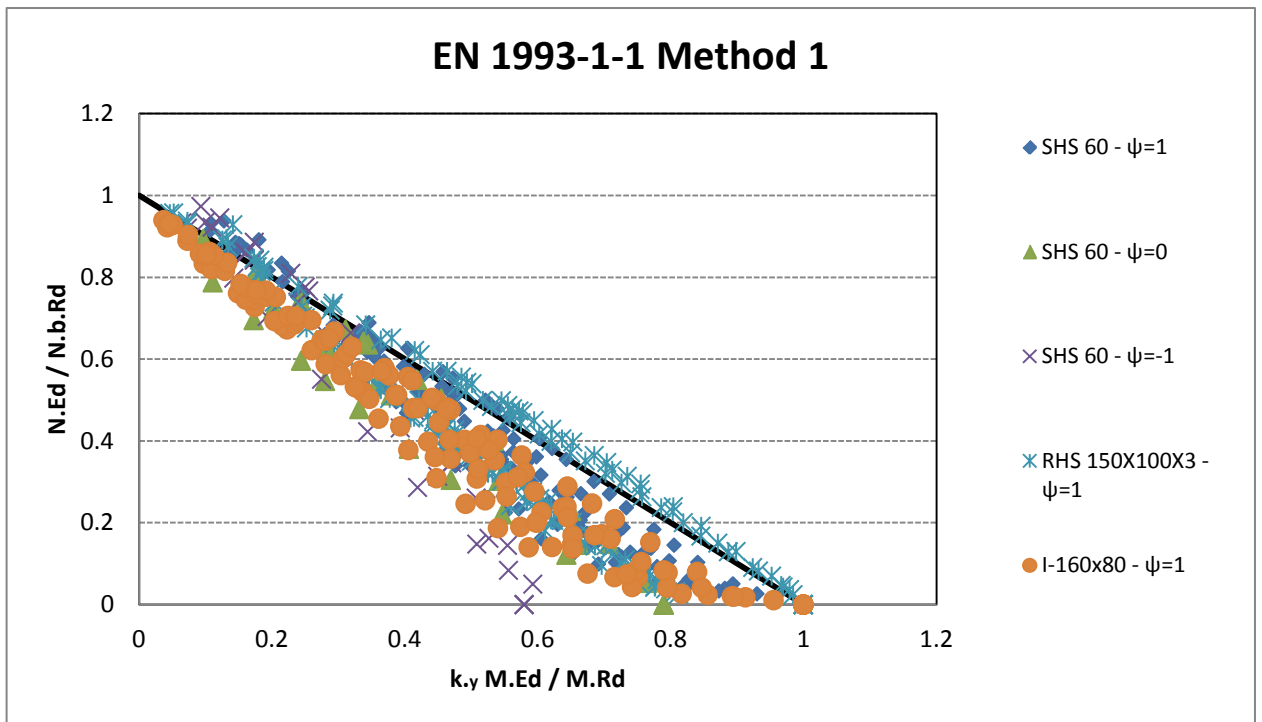


Figure 9-45 : distribution data result for ratio of  $N_{Ed}/N_{b.Rd}$  with  $k_y * M_{Ed}/M_{Rd}$  (EN 1993-1-1 Method 1)

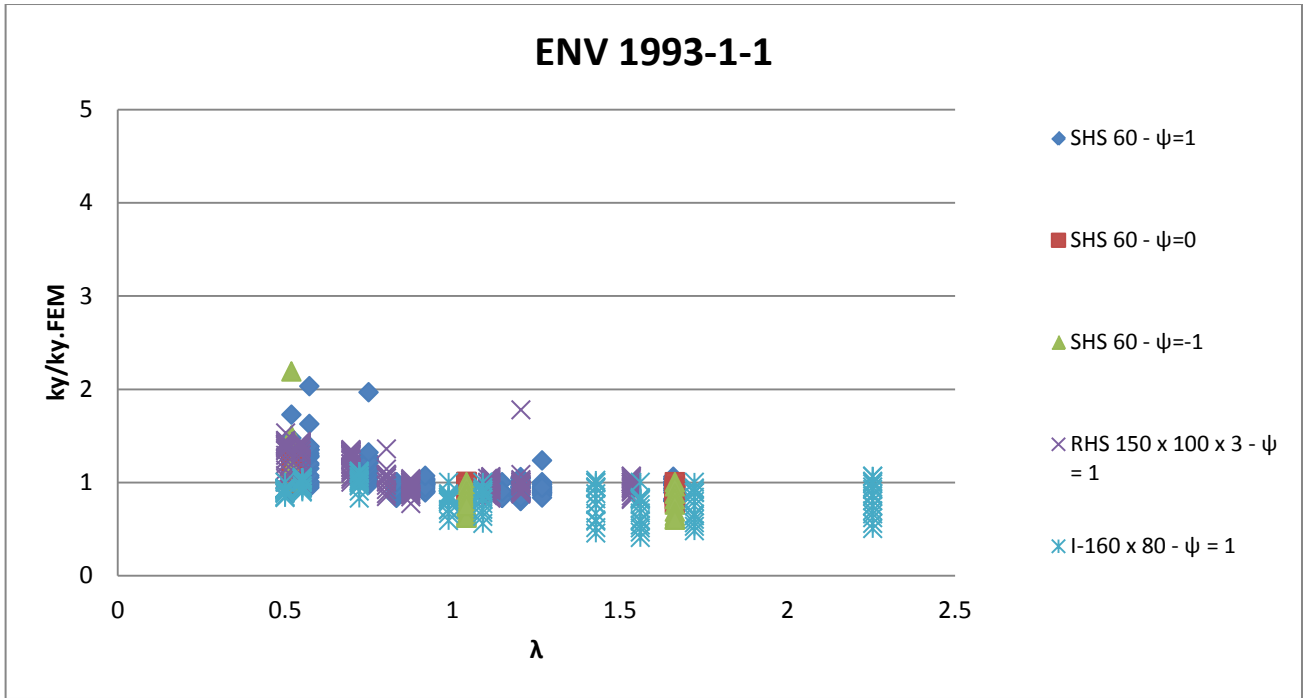


Figure 9-46 : distribution data result for ratio of  $k_y/k_{y.FEM}$  with  $\lambda$  (ENV 1993-1-1)

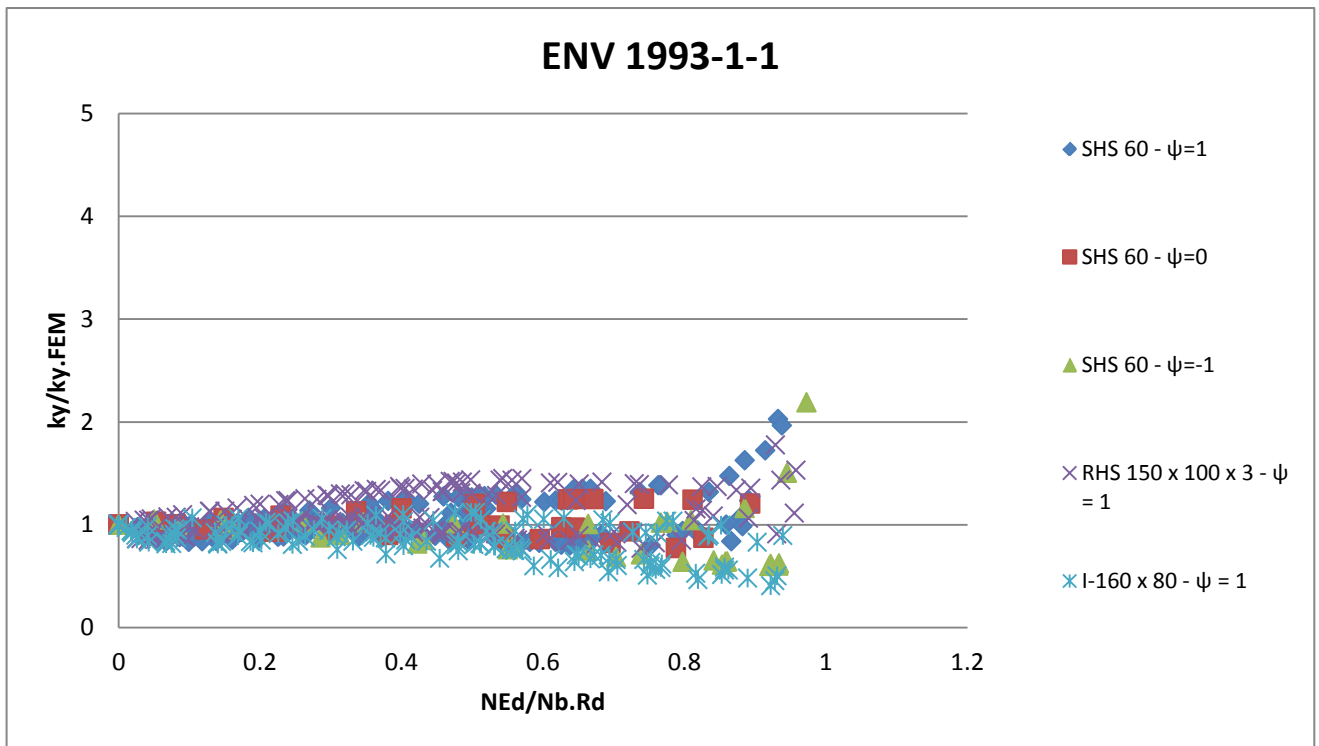


Figure 9-47 : distribution data result for ratio of  $k_y/k_{y.FEM}$  with  $N_{Ed}/N_{b.Rd}$  (ENV 1993-1-1)

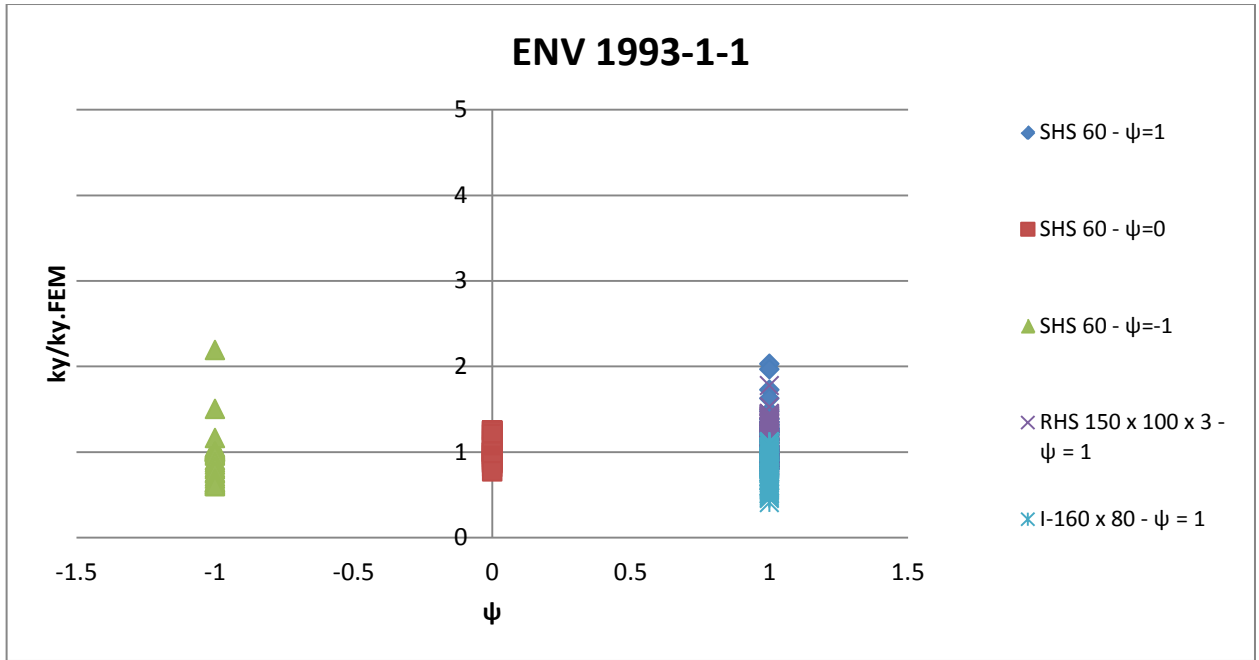


Figure 9-48 : distribution data result for ratio of  $k_y/k_{y.FEM}$  with  $\psi$  (ENV 1993-1-1)

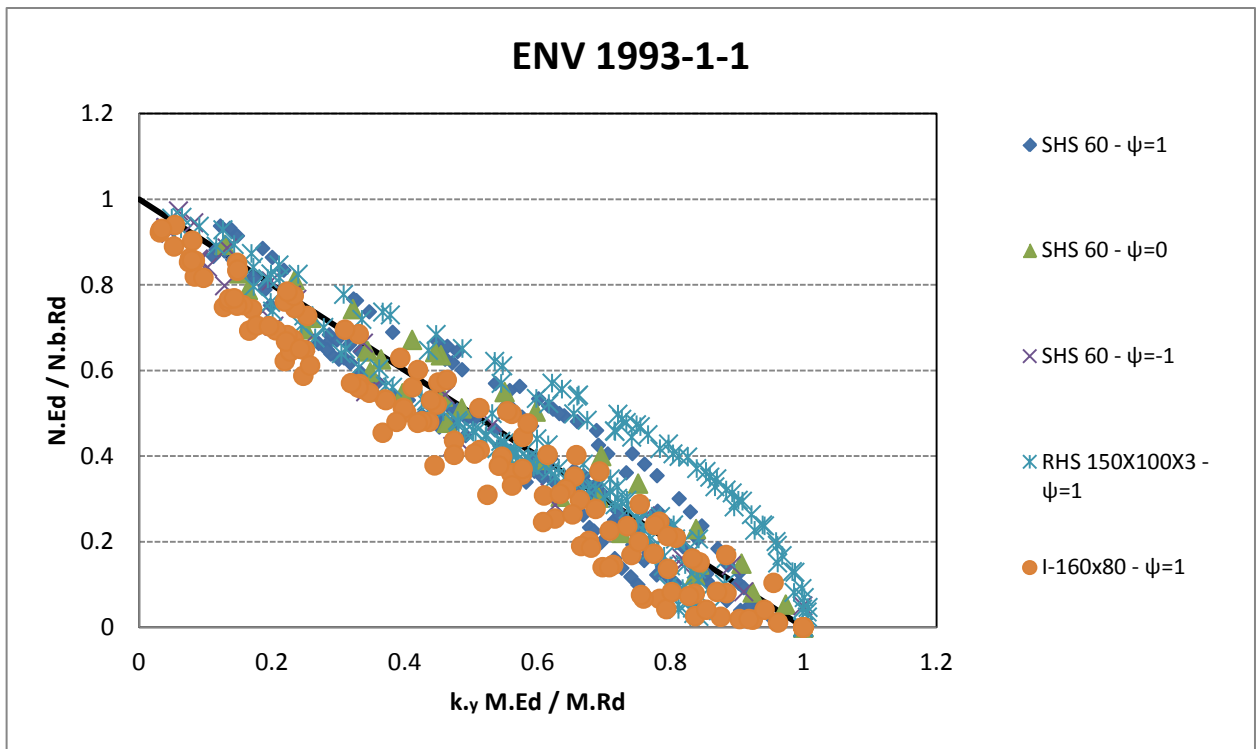


Figure 9-49 : distribution data result for ratio of  $N_{Ed}/N_{b.Rd}$  with  $k_y * M_{Ed}/M_{Rd}$  (ENV 1993-1-1)

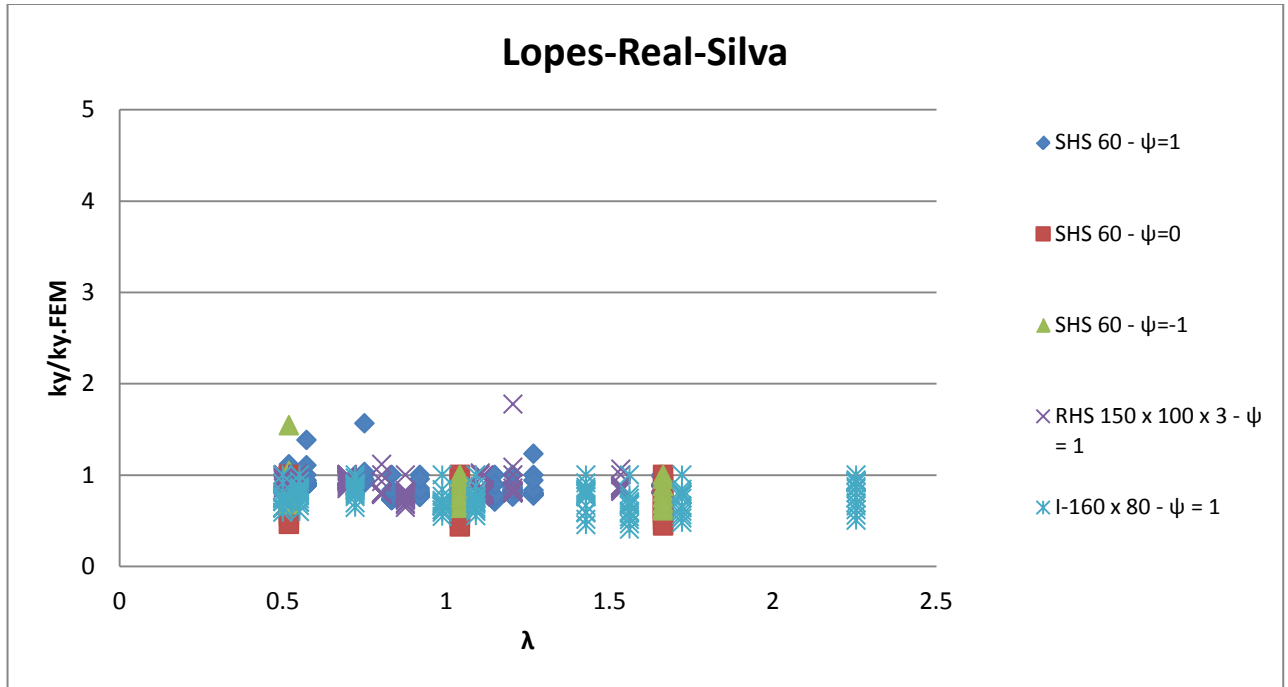


Figure 9-50 : distribution data result for ratio of  $k_y/k_{y,FEM}$  with  $\lambda$  (Lopes-Real-Silva)

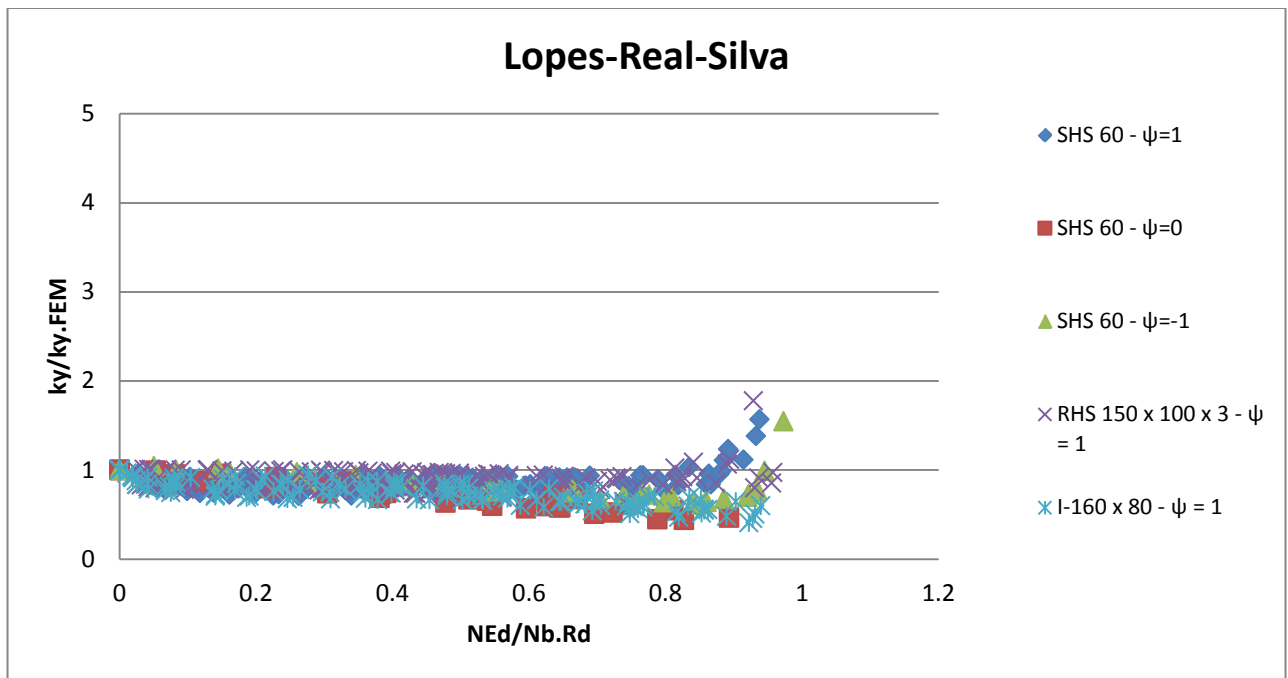


Figure 9-51 : distribution data result for ratio of  $k_y/k_{y,FEM}$  with  $N_{Ed}/N_{b,Rd}$  (Lopes-Real-Silva)

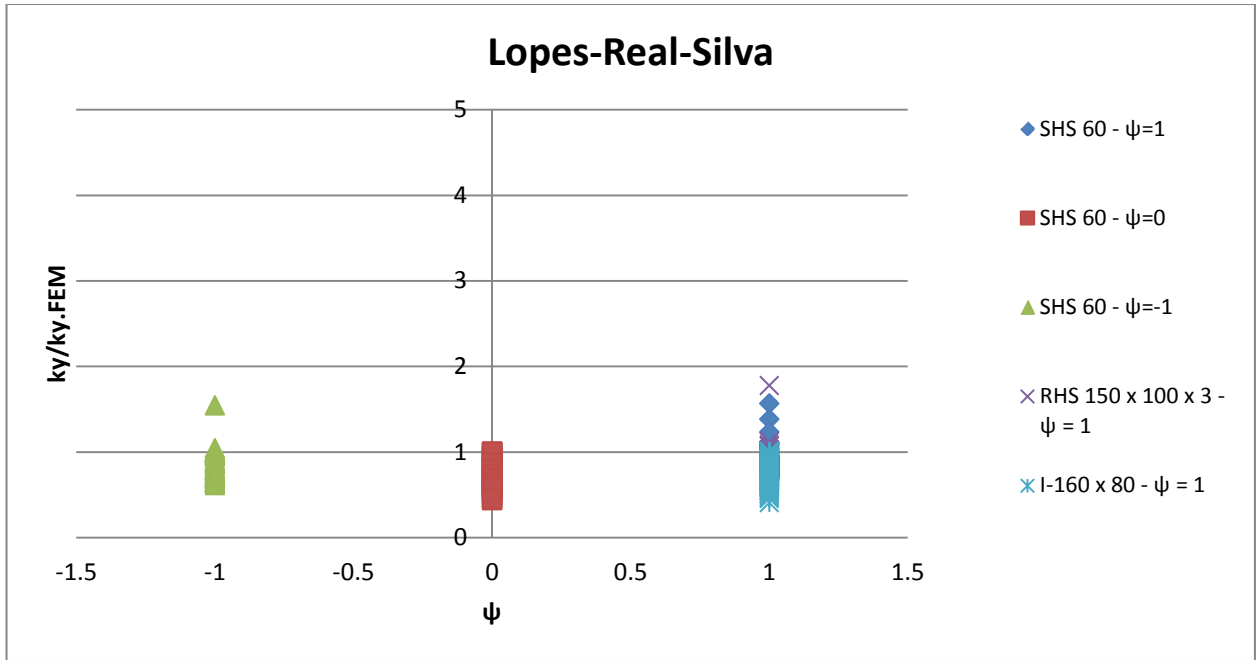


Figure 9-52 : distribution data result for ratio of  $k_y/k_{y.FEM}$  with  $\psi$  (Lopes-Real-Silva)

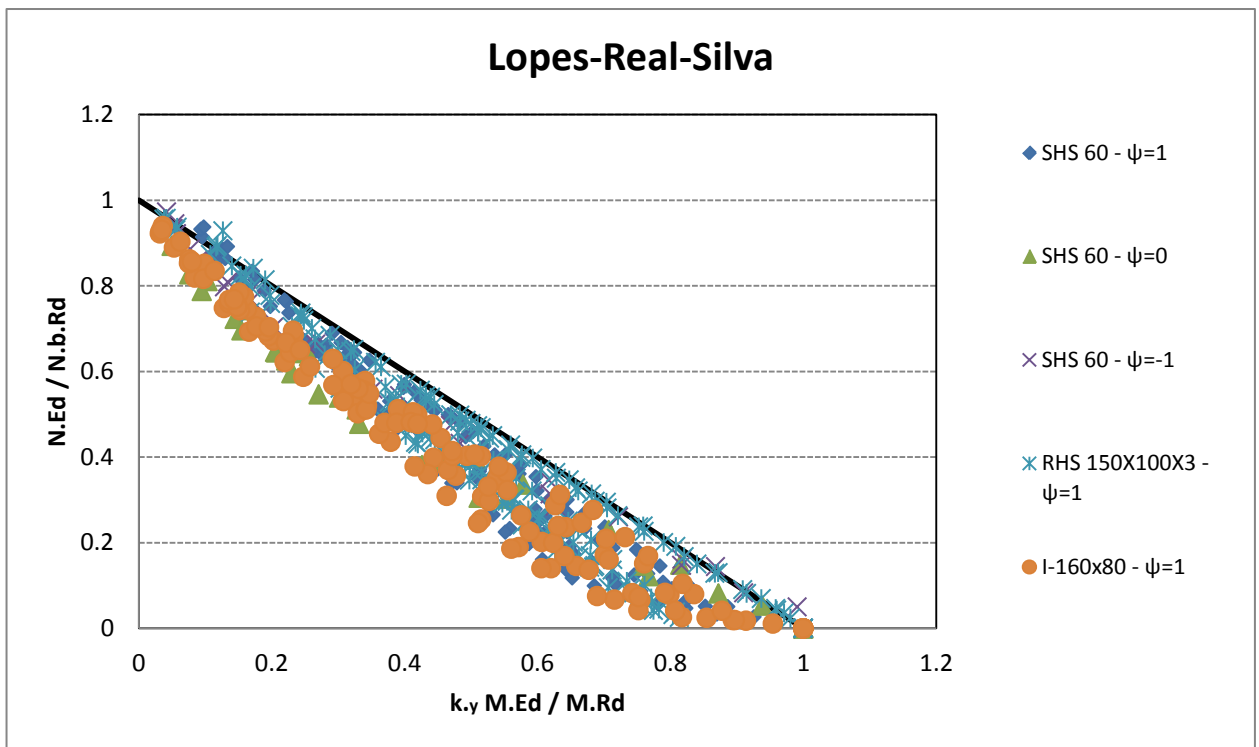


Figure 9-53 : distribution data result for ratio of  $N_{Ed}/N_{b.Rd}$  with  $k_y * M_{Ed}/M_{Rd}$  (Lopes-Real-Silva)



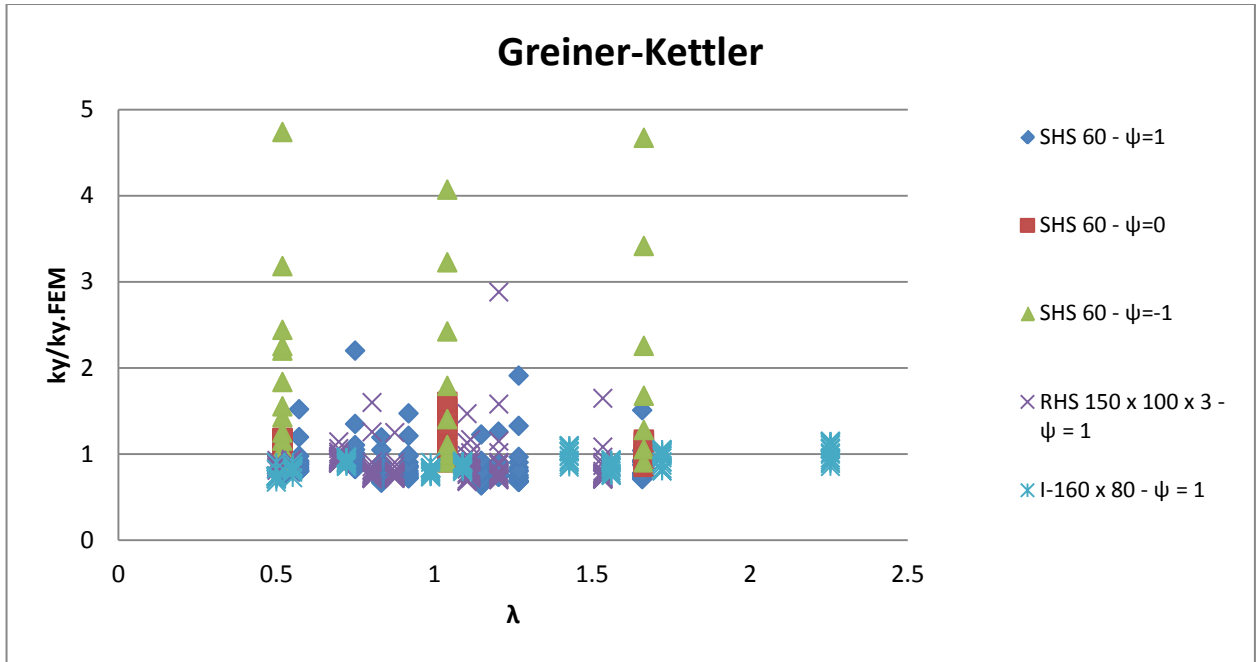


Figure 9-54 : distribution data result for ratio of  $k_y/k_{y.FEM}$  with  $\lambda$  (Greiner-Kettler)

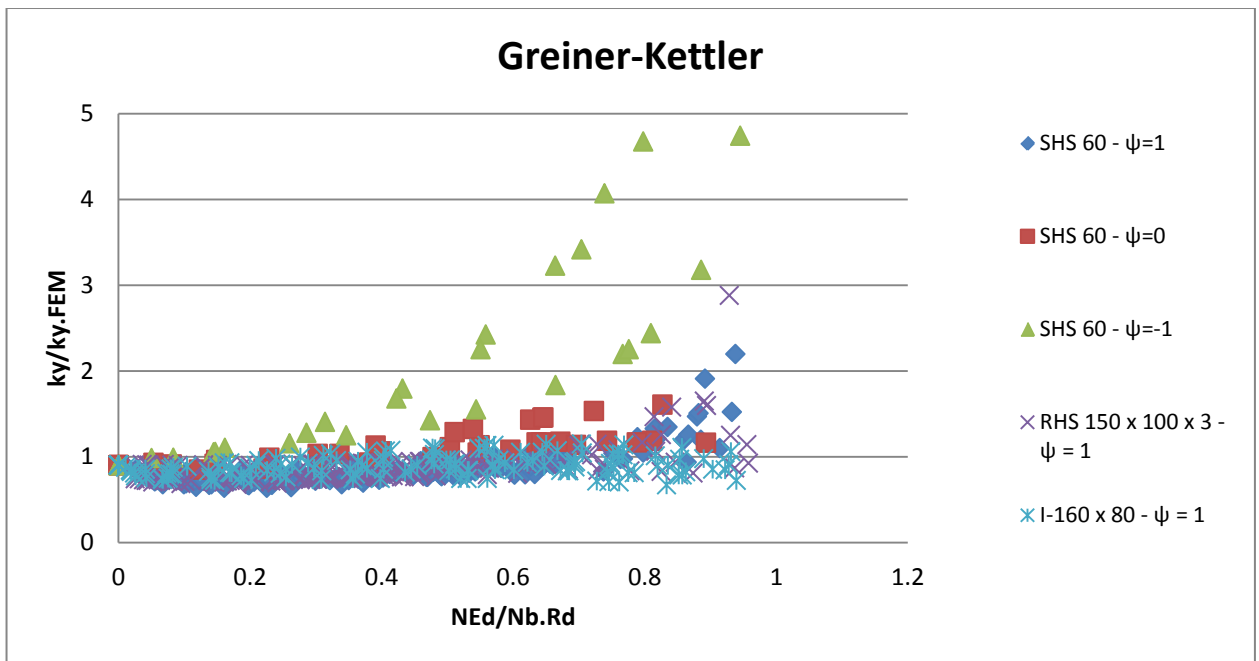


Figure 9-55 : distribution data result for ratio of  $k_y/k_{y.FEM}$  with  $N_{Ed}/N_{b.Rd}$  (Greiner-Kettler)

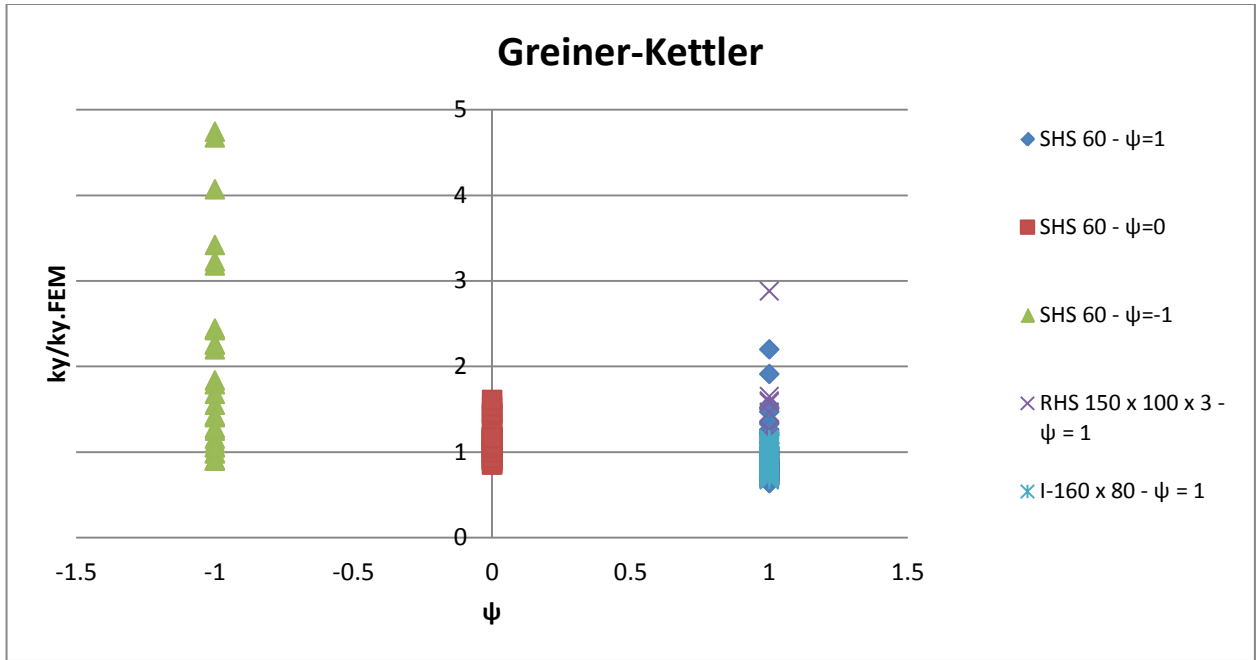


Figure 9-56 : distribution data result for ratio of  $k_y/k_{y.FEM}$  with  $\psi$  (Greiner-Kettler)

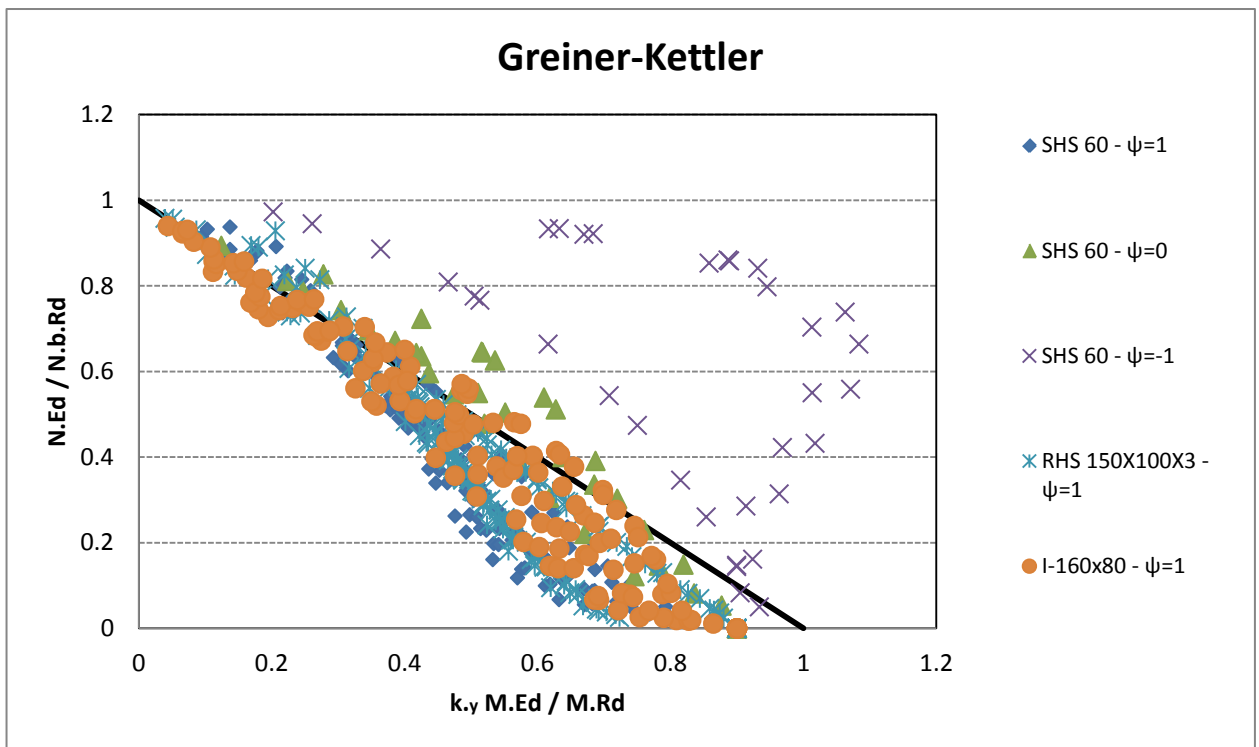


Figure 9-57 : distribution data result for ratio of  $N_{Ed}/N_{b.Rd}$  with  $k_y \cdot M_{Ed}/M_{Rd}$  (Greiner-Kettler)

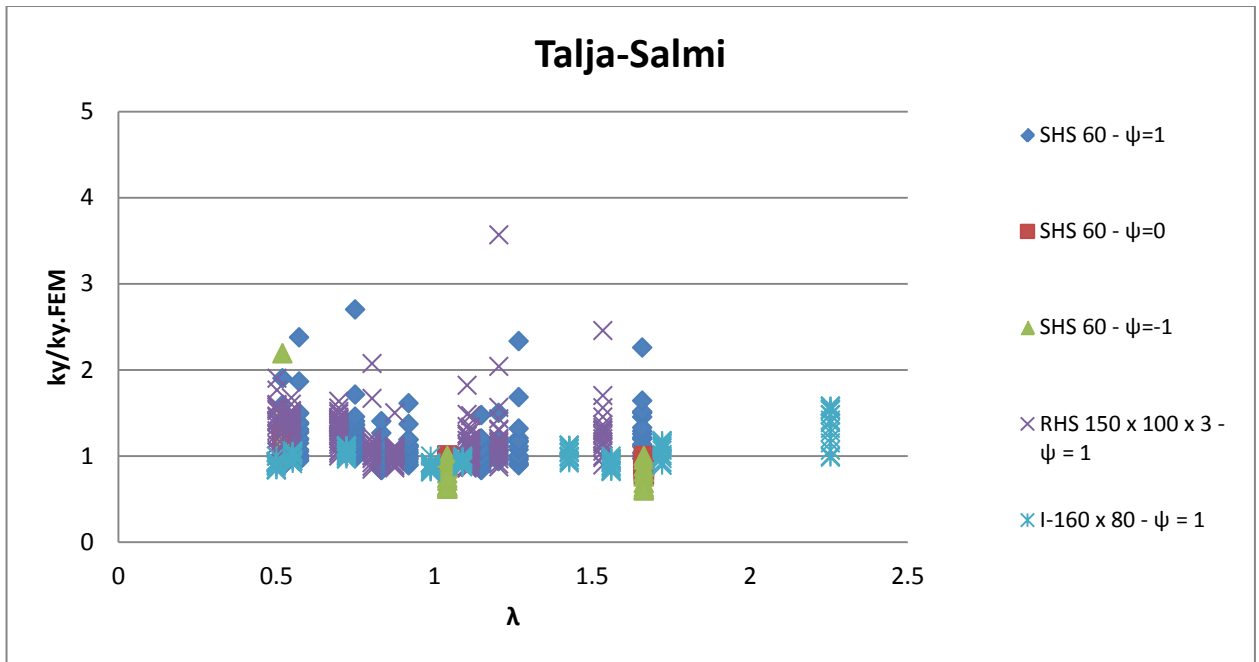


Figure 9-58 : distribution data result for ratio of  $k_y/k_{y,FEM}$  with  $\lambda$  (Talja-Salmi)

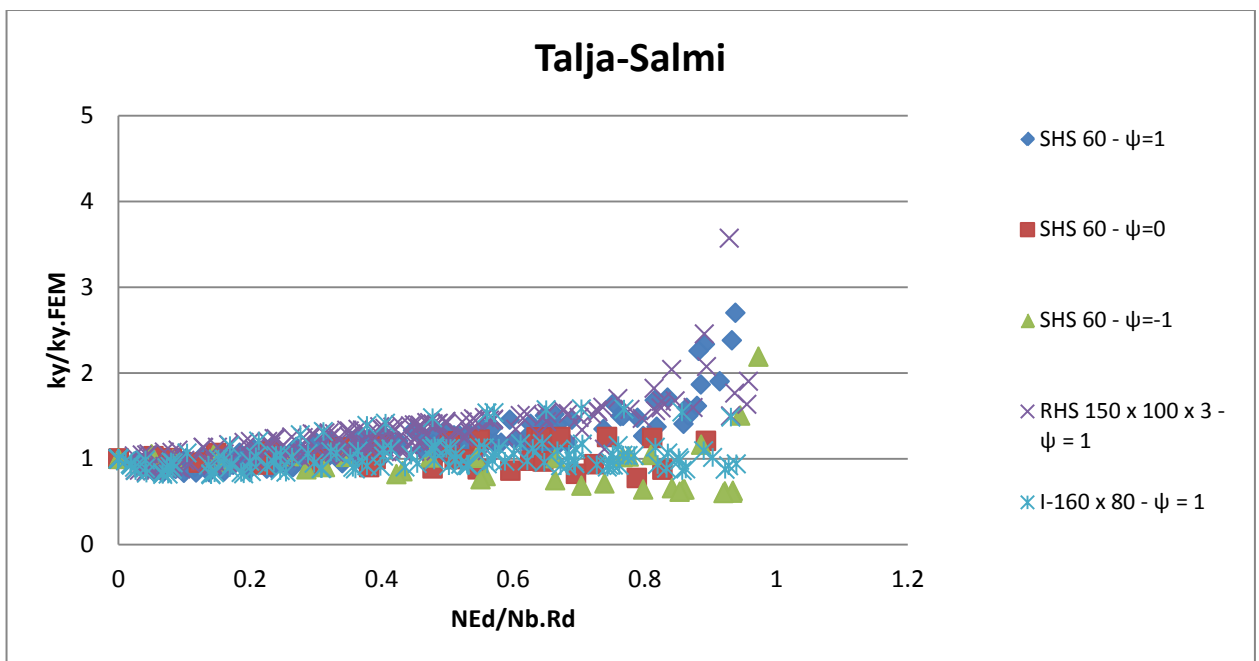


Figure 9-59 : distribution data result for ratio of  $k_y/k_{y,FEM}$  with  $N_{Ed}/N_{b,Rd}$  (Talja-Salmi)

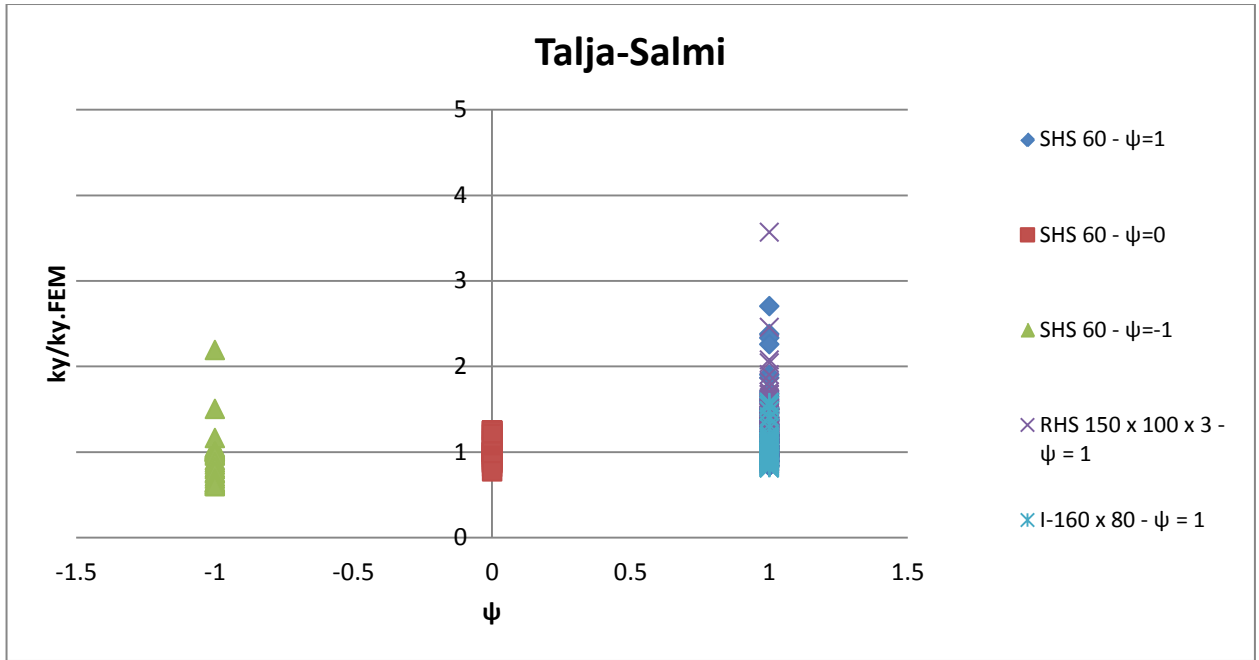


Figure 9-60 : distribution data result for ratio of  $k_y/k_{y.FEM}$  with  $\psi$  (Talja-Salmi)

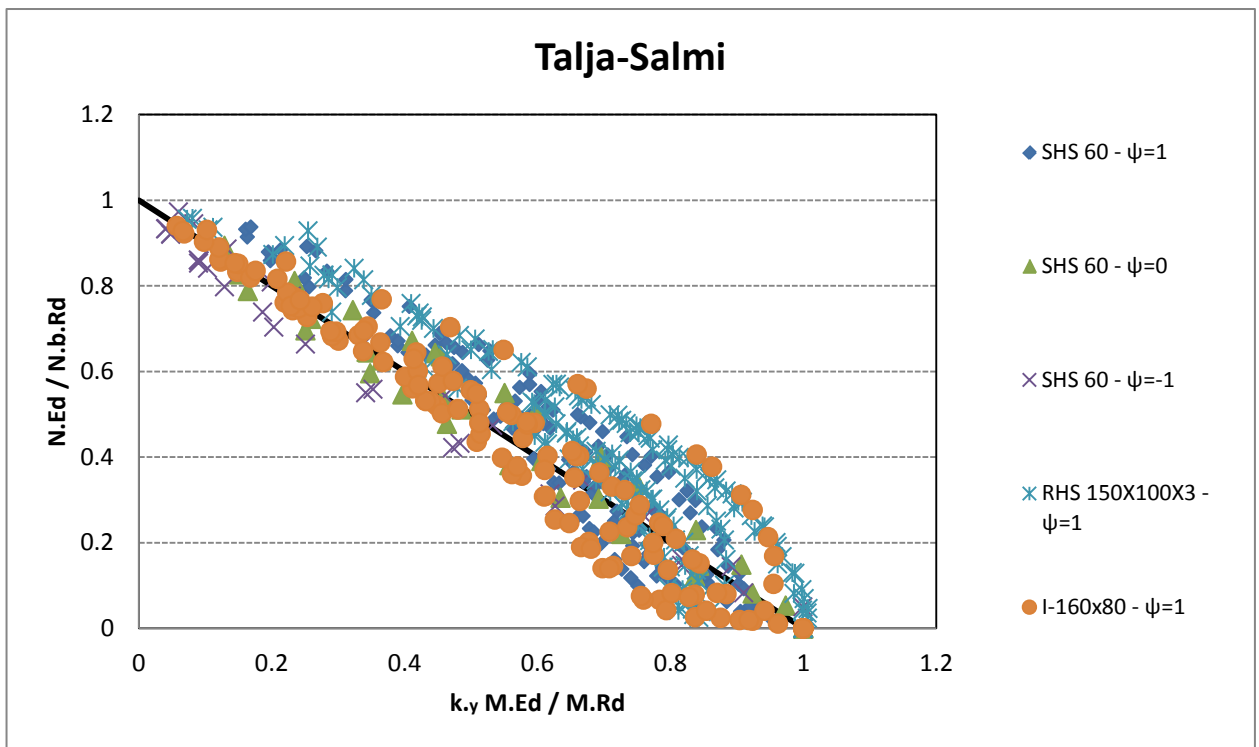


Figure 9-61 : distribution data result for ratio of  $N_{Ed}/N_{b.Rd}$  with  $k_y * M_{Ed}/M_{Rd}$  (Talja-Salmi)

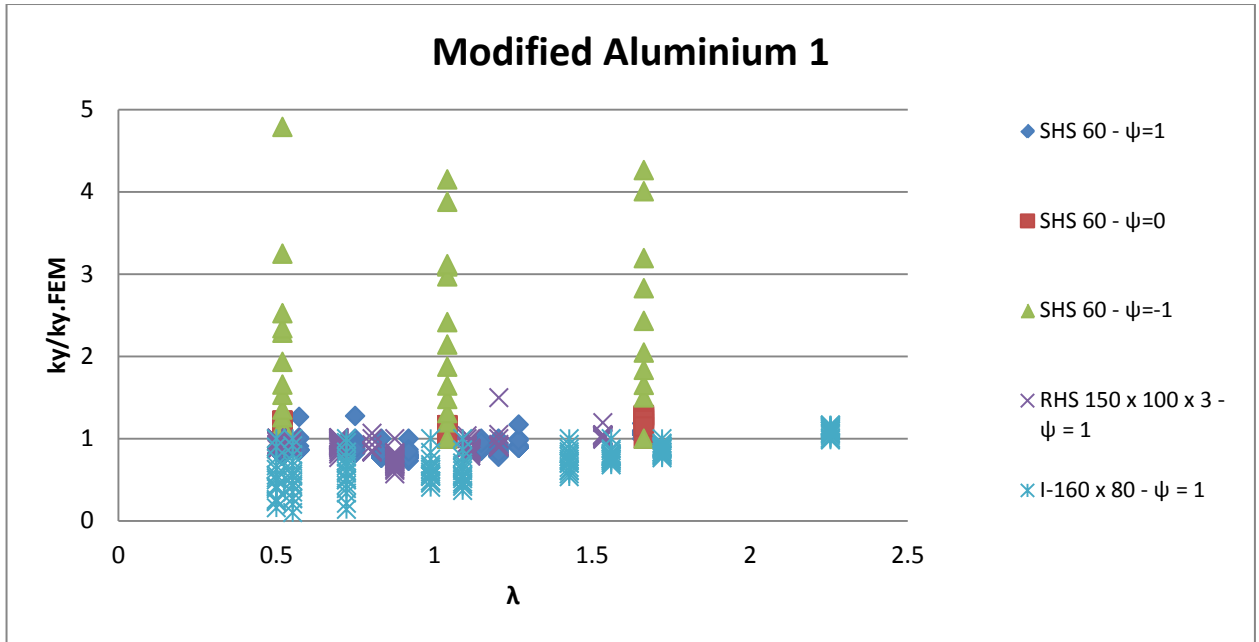


Figure 9-62 : distribution data result for ratio of  $k_y/k_{y.FEM}$  with  $\lambda$  (Modified Aluminium 1)

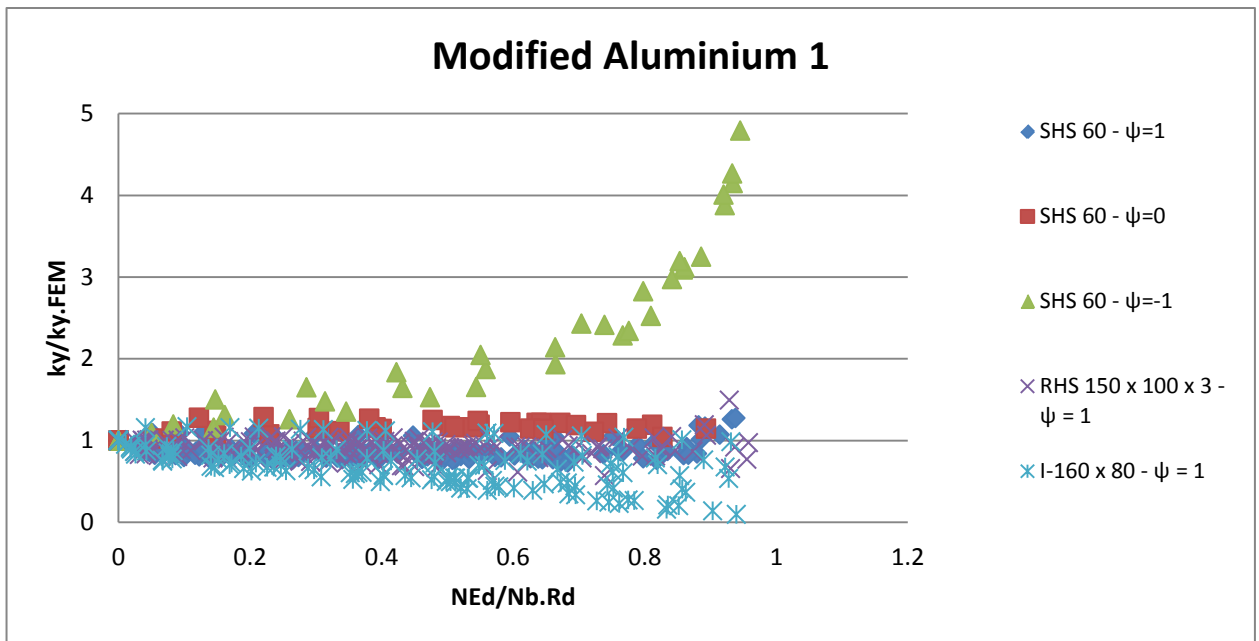


Figure 9-63 : distribution data result for ratio of  $k_y/k_{y.FEM}$  with  $N_{Ed}/N_{b.Rd}$  (Modified Aluminium 1)

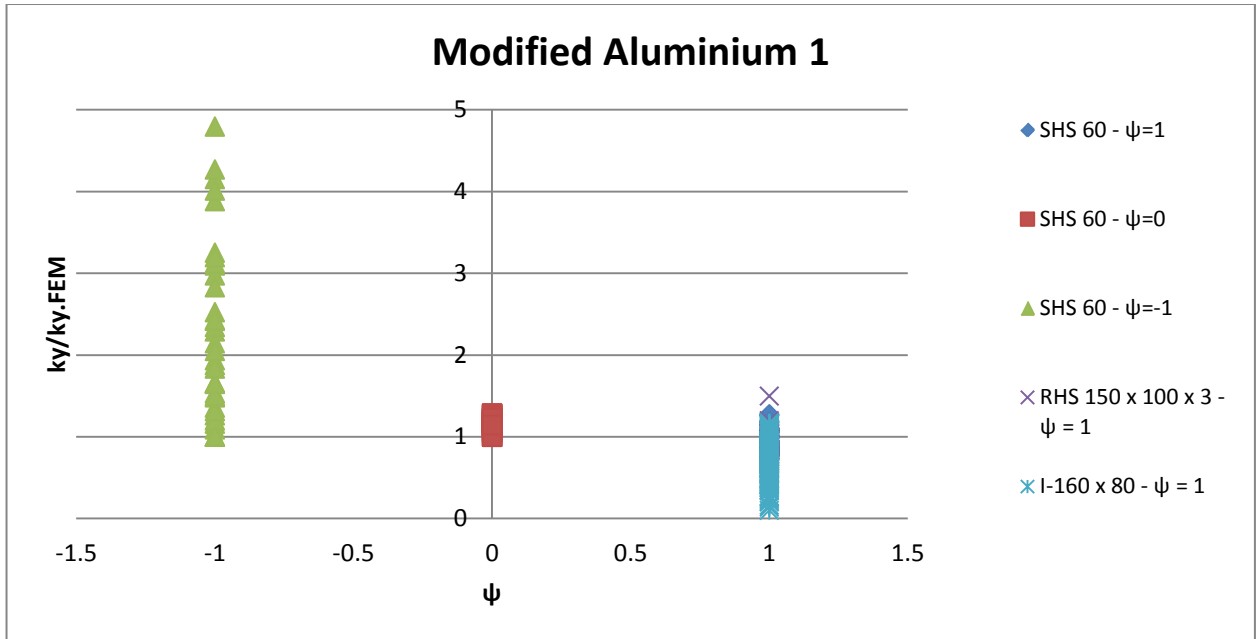


Figure 9-64 : distribution data result for ratio of  $k_y/k_{y,FEM}$  with  $\psi$  (Modified Aluminium 1)

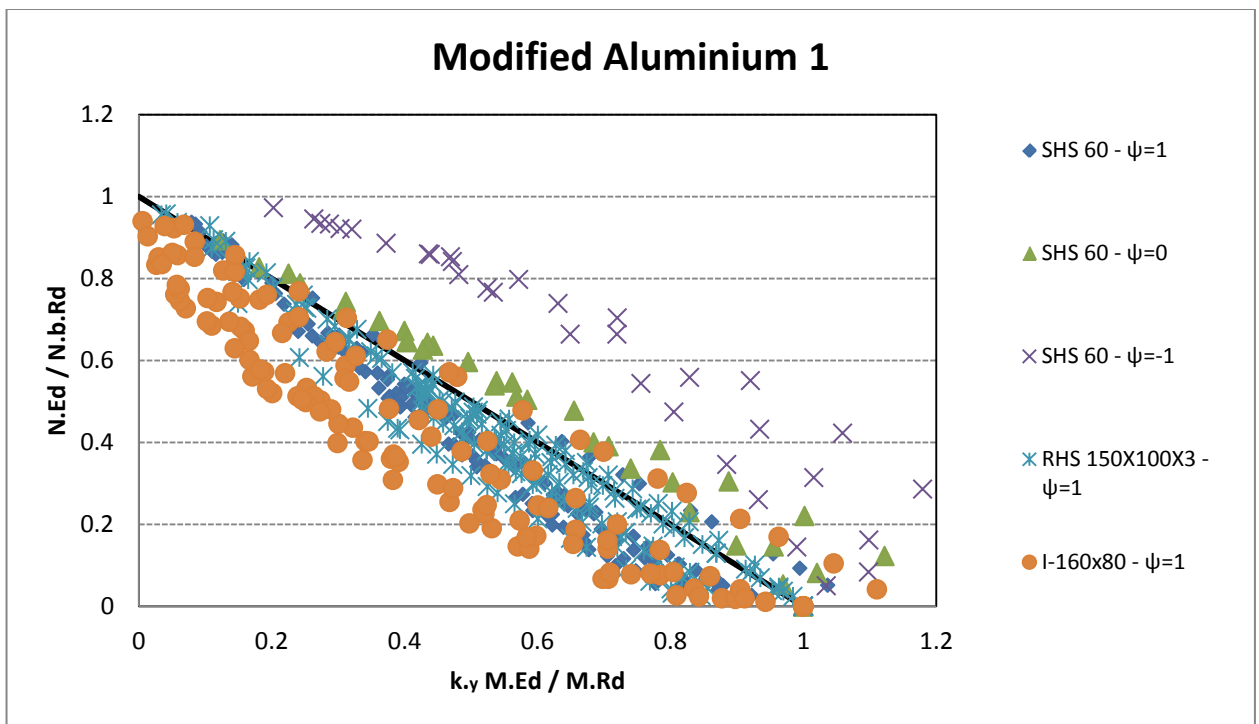


Figure 9-65 : distribution data result for ratio of  $N_{Ed}/N_{b,Rd}$  with  $k_y * M_{Ed}/M_{Rd}$  (Modified Aluminium 1)

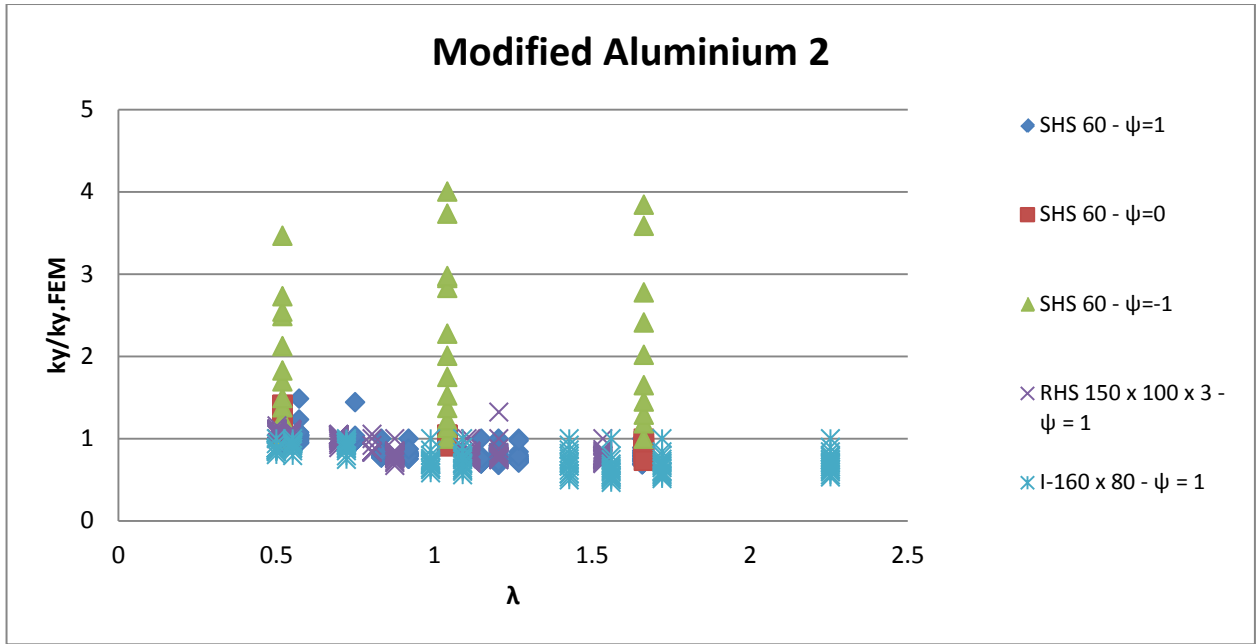


Figure 9-66 : distribution data result for ratio of  $k_y/k_{y.FEM}$  with  $\lambda$  (Modified Aluminium 2)

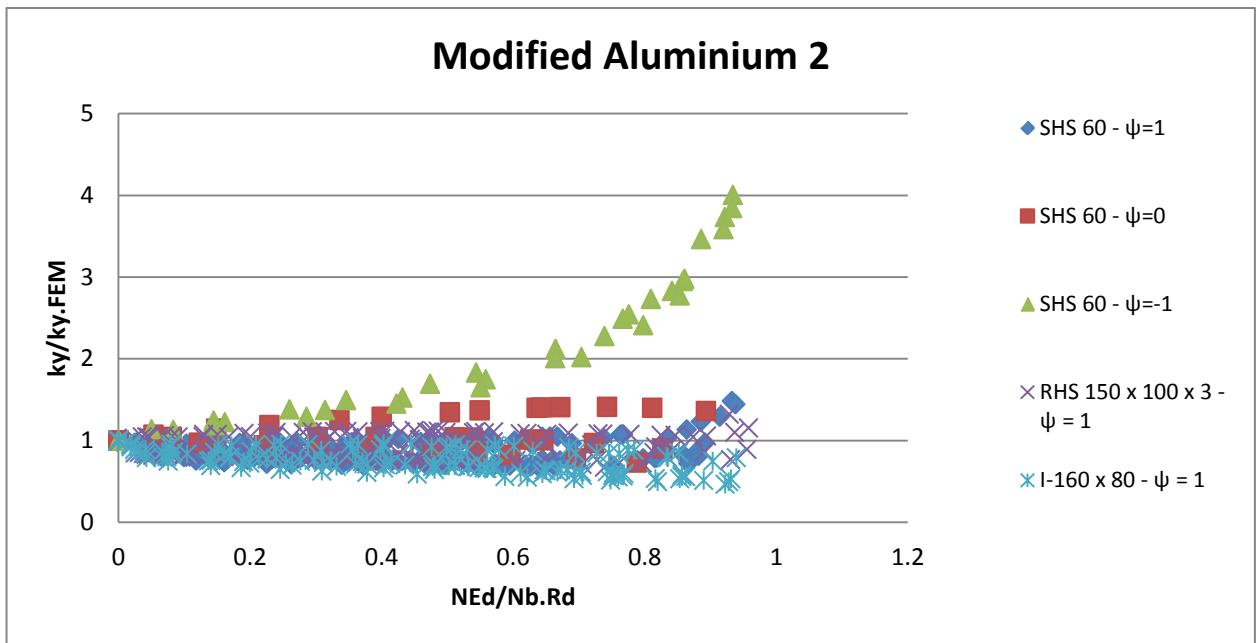


Figure 9-67 : distribution data result for ratio of  $k_y/k_{y.FEM}$  with  $N_{Ed}/N_{b.Rd}$  (Modified Aluminium 2)

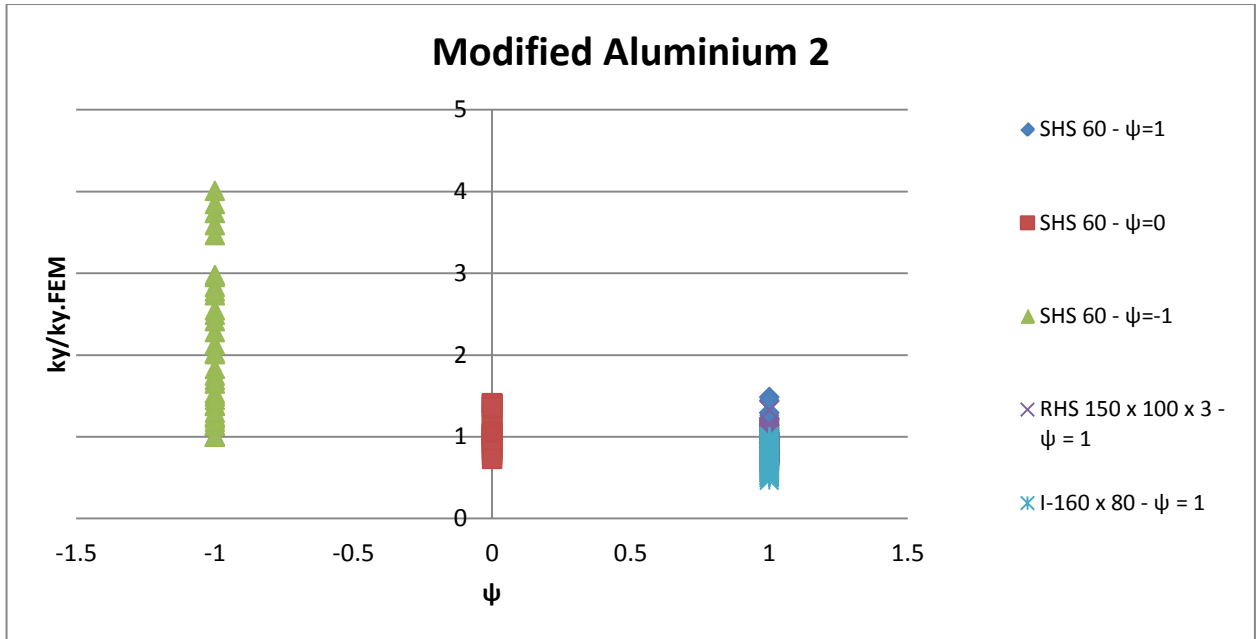


Figure 9-68 : distribution data result for ratio of  $k_y/k_{y,FEM}$  with  $\psi$  (Modified Aluminium 2)

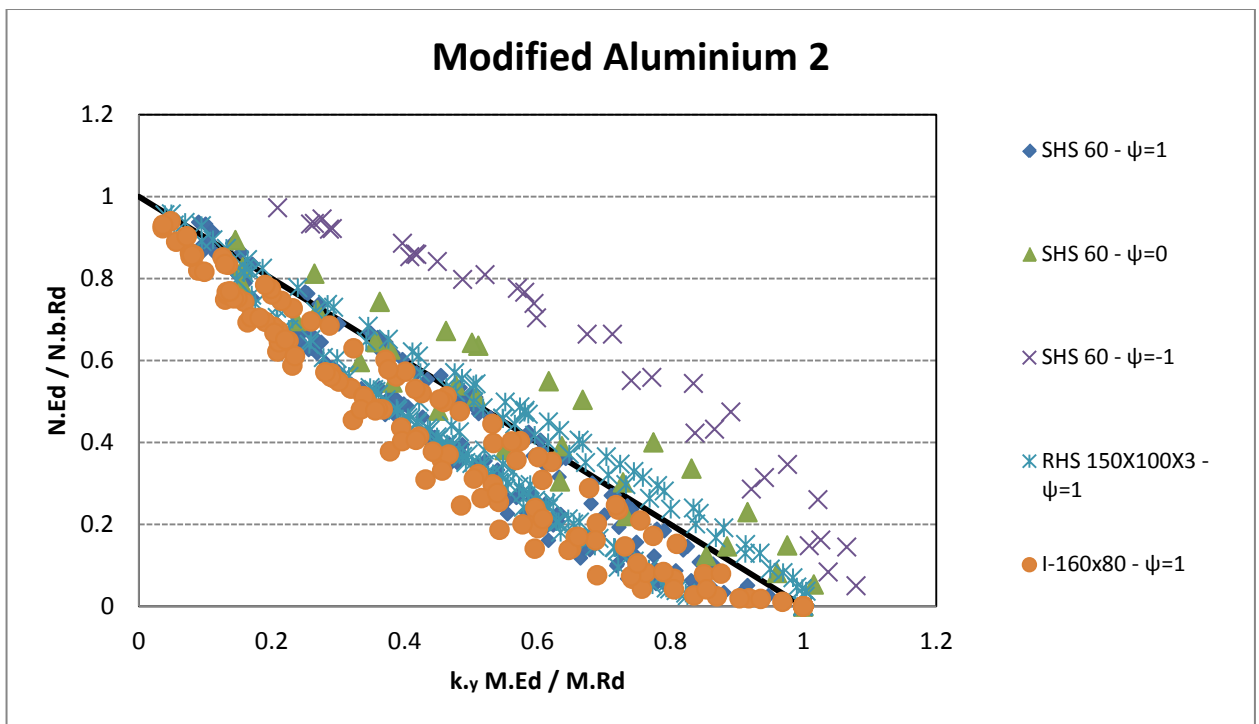


Figure 9-69 : distribution data result for ratio of  $N_{Ed}/N_{b,Rd}$  with  $k_y * M_{Ed}/M_{Rd}$  (Modified Aluminium 2)



Summary finite element data result comparison									
	EN 1993-1-4	EN 1993-1-1 Method 2	EN 1993-1-1 Method 1	ENV 1993-1-1	Talja [17]	Lopes-Real [15]	Greiner-Kettler [13]	Modified Aluminium 1	Modified Aluminium 2
$k_y/k_{y,FEM}$ Mean (Average)	1.235	0.905	0.883	0.997	1.129	0.828	1.053	0.965	0.966
$k_y/k_{y,FEM}$ Standard Deviation	1.012	0.290	0.206	0.215	0.282	0.140	0.937	0.546	0.524

Table 9.21 : Summary Mean and standard deviation of finite element data result column specimens

### 9.6. Analysis variance test of the simulation result

The comparison and judgment for choosing which methods or formulas that has tendency to have the same result to Finite Element results required statistic comparison method as supporting of previous calculation result such as average value (mean) and standard deviation value.

This thesis observes and analysis the variance between FEM result and the standard codes and other research approaches. The summary mean, variance of ratio  $k_y/k_{y,FEM}$  tabulated in table 9.22.

Groups	Count	Sum	Average	Variance
FEM	557	557	1	0
EN1993-1-4	557	687.6746364	1.234604374	1.023376
EN 1993-1-1 Method 2	557	504.1958843	0.905199074	0.083828
EN 1993-1-1 Method 1	557	491.6256973	0.882631414	0.042238
ENV 1993-1-1	557	555.2216613	0.996807291	0.046284
Lopes - Real - Silva	557	461.1629015	0.827940577	0.019682
Greiner, Kettler	557	586.6860689	1.053296354	0.87836
Talja, Salmi	557	628.7301163	1.128779383	0.079572
Aluminium 1	557	537.3434275	0.964709924	0.298138
Aluminium 2	557	537.7912767	0.965513962	0.275001

Table 9.22 : Summary Mean and variance of finite element data result column specimens

The comparison will using statistic **t-test method assuming unequal variances**, where the ratio of  $k_y/k_{y,FEM}$  and the  $k_y$  of FEM itself, in this case equal to one (1).

The t-test conditions and hypothesis:

- Significance level  $\alpha = 0.01$
- Null hypothesis  $H_0 = \mu_1 = \mu_2$  (Mean value is equal between two comparison variables)
- Alternate hypothesis  $H_a \neq \mu_1 \neq \mu_2$

And t-test result summarize in table 9.23 to table 9.31.

	<i>FEM</i>	<i>EN1993-1-4</i>
Mean	1	1.234604374
Variance	0	1.023375692
Observations	557	557
Hypothesized Mean Difference	0	
df	556	
t Stat	-5.473260947	
P(T<=t) one-tail	3.347E-08	
t Critical one-tail	2.333073384	
P(T<=t) two-tail	6.69399E-08	
t Critical two-tail	2.584700665	

Table 9.23 : t-Test: Two-Sample Assuming Unequal Variances (FEM Vs EN 1993-1-4)

	<i>FEM</i>	<i>EN 1993-1-1 Method 2</i>
Mean	1	0.905199074
Variance	0	0.083827778
Observations	557	557
Hypothesized Mean Difference	0	
df	556	
t Stat	7.727627836	
P(T<=t) one-tail	2.57536E-14	
t Critical one-tail	2.333073384	
P(T<=t) two-tail	5.15072E-14	
t Critical two-tail	2.584700665	

Table 9.24 : t-Test: Two-Sample Assuming Unequal Variances (FEM Vs EN 1993-1-1 Method 2)

	<i>FEM</i>	<i>EN 1993-1-1 Method 1</i>
Mean	1	0.882631414
Variance	0	0.042238452
Observations	557	557
Hypothesized Mean Difference	0	
df	556	
t Stat	13.47800065	
P(T<=t) one-tail	2.49724E-36	
t Critical one-tail	2.333073384	
P(T<=t) two-tail	4.99448E-36	
t Critical two-tail	2.584700665	

Table 9.25 : t-Test: Two-Sample Assuming Unequal Variances (FEM Vs EN 1993-1-1 Method 1)

	<i>FEM</i>	<i>ENV 1993-1-1</i>
Mean	1	0.996807291
Variance	0	0.046283767
Observations	557	557
Hypothesized Mean Difference	0	
df	556	
t Stat	0.350245478	
P(T<=t) one-tail	0.363143561	
t Critical one-tail	2.333073384	
P(T<=t) two-tail	0.726287122	
t Critical two-tail	2.584700665	

Table 9.26 : t-Test: Two-Sample Assuming Unequal Variances (FEM Vs ENV 1993-1-1)

	<i>FEM</i>	<i>Lopes - Real - Silva</i>
Mean	1	0.827940577
Variance	0	0.019682291
Observations	557	557
Hypothesized Mean Difference	0	
df	556	
t Stat	28.94464569	
P(T<=t) one-tail	2.4094E-113	
t Critical one-tail	2.333073384	
P(T<=t) two-tail	4.8188E-113	
t Critical two-tail	2.584700665	

Table 9.27 : t-Test: Two-Sample Assuming Unequal Variances (FEM Vs Lopes-Real-Silva)

	<i>FEM</i>	<i>Greiner, Kettler</i>
Mean	1	1.053296354
Variance	0	0.878360328
Observations	557	557
Hypothesized Mean Difference	0	
df	556	
t Stat	-1.342111932	
P(T<=t) one-tail	0.090053744	
t Critical one-tail	2.333073384	
P(T<=t) two-tail	0.180107489	
t Critical two-tail	2.584700665	

Table 9.28 : t-Test: Two-Sample Assuming Unequal Variances (FEM Vs Greiner-Kettler)

	<i>FEM</i>	<i>Talja, Salmi</i>
Mean	1	1.128779383
Variance	0	0.07957241
Observations	557	557
Hypothesized Mean Difference	0	
df	556	
t Stat	-10.77438972	
P(T<=t) one-tail	5.15544E-25	
t Critical one-tail	2.333073384	
P(T<=t) two-tail	1.03109E-24	
t Critical two-tail	2.584700665	

Table 9.29 : t-Test: Two-Sample Assuming Unequal Variances (FEM Vs Talja, Salmi)

	<i>FEM</i>	<i>Aluminium 1</i>
Mean	1	0.964709924
Variance	0	0.298137639
Observations	557	557
Hypothesized Mean Difference	0	
df	556	
t Stat	1.525358027	
P(T<=t) one-tail	0.063869212	
t Critical one-tail	2.333073384	
P(T<=t) two-tail	0.127738424	
t Critical two-tail	2.584700665	

Table 9.30 : t-Test: Two-Sample Assuming Unequal Variances (FEM Vs Aluminium 1)

	<i>FEM</i>	<i>Aluminium 2</i>
Mean	1	0.965513962
Variance	0	0.275001336
Observations	557	557
Hypothesized Mean Difference	0	
df	556	
t Stat	1.552042116	
P(T<=t) one-tail	0.060610573	
t Critical one-tail	2.333073384	
P(T<=t) two-tail	0.121221146	
t Critical two-tail	2.584700665	

Table 9.31 : t-Test: Two-Sample Assuming Unequal Variances (FEM Vs Aluminium 2)

The t-value (statistic) is related to the size of the difference between the means of the two comparing samples. The larger t-value is, compared to t-critical, the larger the difference. However, t-value is not the most useful result to compare between two data, which is why there are p-values for supporting hypothesis.

The p-value is the probability of obtaining a test statistic at least as extreme as the one that was actually observed, assuming that the null hypothesis is true. If the p-value turns out to be less than a certain significance level ( $\alpha$ ), in this thesis  $\alpha$  is 0.01, the null hypothesis is fail which means there is significant difference between two samples of comparison.

The t-test two tails method was taken since the alternate hypothesis did not clearly mention the differences; either the variance difference is higher or lower than observed data.

From this result, the methods which more likely to have the same result as finite element result, based on p-value and  $\alpha=0.01$  as its limitation, are **ENV 1993-1-1**, **Greiner & Kettler**, and both **modified Aluminium 1** and **modified Aluminium 2** methods, since all of those methods have p-value  $> \alpha$  (0.01), which means that the mean value of the ratio  $k_y/k_{y,FEM}$  has **no significance difference** compared to finite element result. Therefore, it fails to reject the null hypothesis ( $H_0$ ).

## 10. Result and conclusion

This manuscript has provided the summary of stainless steel nonlinearity behavior as explained in chapter 4 has illustrated the wide range variety of mechanical properties for each stainless steel materials grade of various section types observed (Rectangular Hollow Section and I-Section). Hence, the comparison observation and parametric study took the material properties value based on particular experimental test value which associates to particular investigation.

As one of the objectives of this paper to compare and validate the experimental compression test, the full length three dimension finite element models of various section members (various section members' type, section dimensions, lengths, and material grades) were modeled and applied various load cases as in the real laboratory test. The comparison result, with some simulation and experimental assumptions as describe in chapter 8, show that **there are no significant differences** between finite element result and experimental test report. The comparison result also shows that initial imperfections;

- Global initial imperfection :  $L/1000$
- Local initial imperfection (web) :  $c/200$

Have delivered reliable comparison result than other initial imperfection factors proposed in the experimental report. Hence, these initial imperfections are applicable for all models for parametric study as these imperfections factors were also applied in EN 1993-1-5.

The main objective of this thesis to study relevant interaction of axial force and bending moment formula proposed by existing standard code (EN 1993 Part 1-1, ENV 1993-1-1), some proposed formulas by researchers in their published journals (Talja, Lopes, and Greiner), and also the interaction formula for Aluminium (EN 1999 Part 1-1), as comparison to current interaction formula proposed by stainless steel

standard code (EN 1993-1-4) has been investigated and revealed. The parametric and numerical study was carried out for several stainless steel grades (austenitics, ferritic and duplex grades) considering different section type (hollow and open section) and various of slenderness as detailed explain in Chapter 9.

Based on individual interaction graphs comparison, distribution test data and t-test method, this study indicates that the **modified Aluminium 2** approach more likely to have the same result as finite element result but need some improvements. Though, **Modified Aluminium 2** formula gives conservative result for  $\psi = 0$  and  $\psi = -1$ , but still safe for design.

Hence, considered the parametric and numerical study result, it was suggested to modify and make some improvements on **modified Aluminium 2** approach for development of general interaction formula for stainless steel.

Suggestions for future work are as follows:

- a. The full length finite element models and parametric study for supporting the result
  - Section members with slenderness less than 0.5 with various material grades
  - Various section members with various material grades and various slenderness
  - Various section members with load variation  $\psi = 0$  and  $\psi = -1$
- b. Improved and develop **modified Aluminium 2** for new general interaction formula and interaction factor for stainless steel.

## 11. References

1. Design Manual for structural stainless steel, 3<sup>rd</sup> Edition, Euro Inox and The Steel Construction Institute, 2006
2. Design Manual For Structural Stainless Steel – Commentary, 3<sup>rd</sup> Edition, Euro Inox and The Steel Construction Institute, 2007
3. Rules for member stability in EN 1993-1-1, Background documentation and design guidelines, ECCS Technical Committee 8 – Stability No. 119, N. Boissonnade - R. Greiner - J.P. Jaspart - J. Lindner, ECCS, 2006
4. Journal : A comparison of structural stainless steel design standards, N.R. Baddoo, The Steel Construction Institute, 2003
5. Cold-formed steel design, 3<sup>rd</sup> Edition, Wei-Wen Yu, John Wiley & Sons, Inc, 2000
6. Structural Design of Stainless Steel, N.R. Baddoo & B.A. Burgan, The Steel Construction Institute, 2001
7. EN 10088-1, List of stainless steels, 2005
8. EN 10027-1, Designation systems for steels – Part 1 : Steel name, 2005
9. Full-range Stress-strain Curves for Stainless Steel Alloys, Research Report No R811, Kim JR Rasmussen, The University of Sydney - Department of Civil Engineering, 2001
10. Journal : Full-range stress–strain curves for stainless steel alloys, Kim JR Rasmussen, Elsevier, 2001
11. Journal : Finite element modelling of structural stainless steel cross-sections, Mahmud Ashraf - Leroy Gardner - David A. Nethercot, Elsevier, 2006
12. Journal : Structural design of stainless steel members - comparison between Eurocode 3, Part 1.4 and test results, B.A. Burgan - N.R. Baddoo - K.A. Gilseman, Elsevier, 2000
13. Journal : Interaction of Bending and axial compression of stainless steel members, R. Greiner & M Kettler, Elsevier, 2008
14. Report to the ECSC : Structural design of stainless steel welded I- beams,I-columns and beam-columns – Final Technical Report, Heiko Stangenberg & Richard A Weber, RWTH Institute of steel construction, 2000
15. Journal : Stainless steel beam-columns interaction curves with and without lateral torsional buckling, Nuno Lopes - Paulo Vila Real - Luís Simões da Silva, 7<sup>th</sup> EUROMECH Solid Mechanics Conference, 2009
16. Report to the ECSC : Test report on welded I and CHS Beams, columns and beam-columns, VTT Building Technology, 1997
17. Design of stainless steel RHS beams, columns and beam-columns, VTT Research notes no.1619, Asko Talja & Pekka Salmi, VTT Building Technology, 1995

18. Journal : Numerical Verification of stainless steel overall buckling curves, Petr Hradil & Asko Talja, VTT Building Technology, <http://www.steel-stainless.org/experts12/>.
19. Journal : Strength enhancements in cold-formed structural sections - Part I: Material testing, S. Afshan - B. Rossi - L. Gardner, Elsevier, 2012
20. ENV 1993-1-1 Design of steel structures Part 1.1 General rules and rules for buildings, European Commission for Standardization (CEN), 1992
21. Journal : Discrete and continuous treatment of local buckling in stainless steel elements; L. Gardner & M. Theofanous, Elsevier, 2008
22. Journal : New interaction formulae for beam-columns in Eurocode 3 : The Fench-Belgian approach; Nicholas Boissonnade, Jean-Pierre Jaspart, Jean-Pierre Muzeau, Marc Villette, Elsevier, 2003
23. Journal : Interaction formulae for members subjected to bending and axial compression in Eurocode 3 – The Method 2 Approach, R. Greiner, J. Lindner, Elsevier, 2005
24. Eurocode 3 : Design of steel structure, Part 1-1 : General rules and rules for buildings, European Committee for Standardization (CEN), 2005
25. Eurocode 3 : Design of steel structure, Part 1-4 : General rules – supplementary rules for stainless steels, European Committee for Standardization (CEN), 2006
26. Eurocode 9 : Design of Aluminium structures, Part 1-1 : General structural rules, European Committee for Standardization (CEN), 2007
27. Journal : On the calculation of deflections in structural stainless steel beams: an experimental and numerical investigation, Mirambell, E. and Real, E, Elsevier, 2000.
28. Thesis : A new approach to structural stainless steel design, L. Gardner, University of London, 2002
29. Eurocode 3 : Design of steel structure, Part 1-5 : Plated structural elements, European Committee for Standardization (CEN), 2006



**APPENDIX 1 : EN 1993-1-1 METHOD 1 : Interaction factor  $k_{ij}$**

**Annex A [informative] – Method 1: Interaction factors  $k_{ij}$  for interaction formula in 6.3.3(4)**

**Table A.1: Interaction factors  $k_{ij}$  (6.3.3(4))**

Interaction factors	Design assumptions	
	elastic cross-sectional properties class 3, class 4	plastic cross-sectional properties class 1, class 2
$k_{yy}$	$C_{my} C_{mLT} \frac{\mu_y}{1 - \frac{N_{Ed}}{N_{cr,y}}}$	$C_{my} C_{mLT} \frac{\mu_y}{1 - \frac{N_{Ed}}{N_{cr,y}}} \frac{1}{C_{yy}}$
$k_{yz}$	$C_{mz} \frac{\mu_y}{1 - \frac{N_{Ed}}{N_{cr,z}}}$	$C_{mz} \frac{\mu_y}{1 - \frac{N_{Ed}}{N_{cr,z}}} \frac{1}{C_{yz}} 0,6 \sqrt{\frac{W_z}{W_y}}$
$k_{zy}$	$C_{my} C_{mLT} \frac{\mu_z}{1 - \frac{N_{Ed}}{N_{cr,y}}}$	$C_{my} C_{mLT} \frac{\mu_z}{1 - \frac{N_{Ed}}{N_{cr,y}}} \frac{1}{C_{zy}} 0,6 \sqrt{\frac{W_y}{W_z}}$
$k_{zz}$	$C_{mz} \frac{\mu_z}{1 - \frac{N_{Ed}}{N_{cr,z}}}$	$C_{mz} \frac{\mu_z}{1 - \frac{N_{Ed}}{N_{cr,z}}} \frac{1}{C_{zz}}$
<b>Auxiliary terms:</b>		
$\mu_y = \frac{1 - \frac{N_{Ed}}{N_{cr,y}}}{1 - \chi_y \frac{N_{Ed}}{N_{cr,y}}}$ $\mu_z = \frac{1 - \frac{N_{Ed}}{N_{cr,z}}}{1 - \chi_z \frac{N_{Ed}}{N_{cr,z}}}$ $w_y = \frac{W_{pl,y}}{W_{el,y}} \leq 1,5$ $w_z = \frac{W_{pl,z}}{W_{el,z}} \leq 1,5$ $n_{pl} = \frac{N_{Ed}}{N_{Rk} / \gamma_{M0} \langle AC2 \rangle}$ $C_{my} \text{ see Table A.2}$ $a_{LT} = 1 - \frac{I_T}{I_y} \geq 0$	$C_{yy} = 1 + (w_y - 1) \left[ \left( 2 - \frac{1,6}{w_y} C_{my}^2 \bar{\lambda}_{max} - \frac{1,6}{w_y} C_{my}^2 \bar{\lambda}_{max}^2 \right) n_{pl} - b_{LT} \right] \geq \frac{W_{el,y}}{W_{pl,y}}$ <p>with <math>b_{LT} = 0,5 a_{LT} \frac{\bar{\lambda}_0^{-2}}{\chi_{LT}} \frac{M_{y,Ed}}{M_{pl,y,Rd}} \frac{M_{z,Ed}}{M_{pl,z,Rd}}</math></p> $C_{yz} = 1 + (w_z - 1) \left[ \left( 2 - 14 \frac{C_{mz}^2 \bar{\lambda}_{max}^2}{w_z^5} \right) n_{pl} - c_{LT} \right] \geq 0,6 \sqrt{\frac{W_z}{W_y}} \frac{W_{el,z}}{W_{pl,z}}$ <p>with <math>c_{LT} = 10 a_{LT} \frac{\bar{\lambda}_0^{-2}}{5 + \bar{\lambda}_z^4} \frac{M_{y,Ed}}{C_{my} \chi_{LT} M_{pl,y,Rd}}</math></p> $C_{zy} = 1 + (w_y - 1) \left[ \left( 2 - 14 \frac{C_{my}^2 \bar{\lambda}_{max}^2}{w_y^5} \right) n_{pl} - d_{LT} \right] \geq 0,6 \sqrt{\frac{W_y}{W_z}} \frac{W_{el,y}}{W_{pl,y}}$ <p>with <math>d_{LT} = 2 a_{LT} \frac{\bar{\lambda}_0}{0,1 + \bar{\lambda}_z^4} \frac{M_{y,Ed}}{C_{my} \chi_{LT} M_{pl,y,Rd}} \frac{M_{z,Ed}}{C_{mz} M_{pl,z,Rd}}</math></p> $C_{zz} = 1 + (w_z - 1) \left[ 2 - \frac{1,6}{w_z} C_{mz}^2 \bar{\lambda}_{max} - \frac{1,6}{w_z} C_{mz}^2 \bar{\lambda}_{max}^2 - e_{LT} \right] n_{pl} \geq \frac{W_{el,z}}{W_{pl,z}} \langle AC2 \rangle$ <p>with <math>e_{LT} = 1,7 a_{LT} \frac{\bar{\lambda}_0}{0,1 + \bar{\lambda}_z^4} \frac{M_{y,Ed}}{C_{my} \chi_{LT} M_{pl,y,Rd}}</math></p>	

**Table A.1 (continued)**

$$\bar{\lambda}_{\max} = \max \begin{cases} \bar{\lambda}_y \\ \bar{\lambda}_z \end{cases}$$

$\bar{\lambda}_0$  = non-dimensional slenderness for lateral-torsional buckling due to uniform bending moment, i.e.  $\psi_y = 1,0$  in Table A.2

$\bar{\lambda}_{LT}$  = non-dimensional slenderness for lateral-torsional buckling

$$\text{If } \bar{\lambda}_0 \leq 0,2\sqrt{C_1} \sqrt{\left(1 - \frac{N_{Ed}}{N_{cr,z}}\right) \left(1 - \frac{N_{Ed}}{N_{cr,TF}}\right)} :$$

$$C_{my} = C_{my,0}$$

$$C_{mz} = C_{mz,0}$$

$$C_{mLT} = 1,0$$

$$\text{If } \bar{\lambda}_0 > 0,2\sqrt{C_1} \sqrt{\left(1 - \frac{N_{Ed}}{N_{cr,z}}\right) \left(1 - \frac{N_{Ed}}{N_{cr,TF}}\right)} :$$

$$C_{my} = C_{my,0} + (1 - C_{my,0}) \frac{\sqrt{\varepsilon_y} a_{LT}}{1 + \sqrt{\varepsilon_y} a_{LT}}$$

$$C_{mz} = C_{mz,0}$$

$$C_{mLT} = C_{my}^2 \frac{a_{LT}}{\sqrt{\left(1 - \frac{N_{Ed}}{N_{cr,z}}\right) \left(1 - \frac{N_{Ed}}{N_{cr,T}}\right)}} \geq 1$$

$\langle AC2 \rangle C_{mi,0}$  see Table A.2  $\langle AC2 \rangle$

$$\varepsilon_y = \frac{M_{y,Ed}}{N_{Ed}} \frac{A}{W_{el,y}} \quad \text{for class 1, 2 and 3 cross-sections}$$

$$\varepsilon_y = \frac{M_{y,Ed}}{N_{Ed}} \frac{A_{eff}}{W_{eff,y}} \quad \text{for class 4 cross-sections}$$

$\langle AC2 \rangle C_1$  is a factor depending on the loading and end conditions and may be taken as  $C_1 = k_c^{-2}$  where  $k_c$  is to be taken from Table 6.6.  $\langle AC2 \rangle$

$N_{cr,y}$  = elastic flexural buckling force about the y-y axis

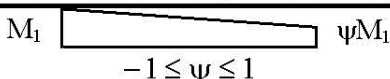

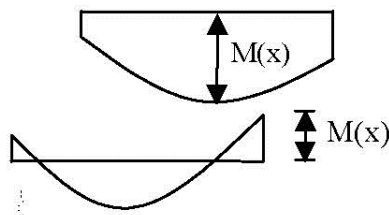
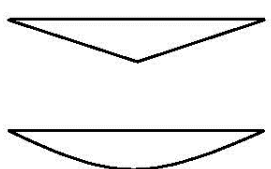
$N_{cr,z}$  = elastic flexural buckling force about the z-z axis

$N_{cr,T}$  = elastic torsional buckling force

$I_T$  = St. Venant torsional constant

$I_y$  = second moment of area about y-y axis

**Table A.2: Equivalent uniform moment factors  $C_{mi,0}$**

Moment diagram	$C_{mi,0}$
 <p><math>M_1</math>  <math>\psi M_1</math>  <math>-1 \leq \psi \leq 1</math></p>	$C_{mi,0} = 0,79 + 0,21\psi_i + 0,36(\psi_i - 0,33) \frac{N_{Ed}}{N_{cr,i}}$
 <p><math>M(x)</math>  <math>M(x)</math></p>	$C_{mi,0} = 1 + \left( \frac{\pi^2 EI_i  \delta_x }{L^2  M_{i,Ed}(x) } - 1 \right) \frac{N_{Ed}}{N_{cr,i}}$ <p><math>M_{i,Ed}(x)</math> is the maximum moment <math>M_{y,Ed}</math> or <math>M_{z,Ed}</math> <math>\langle AC_2 \rangle</math> according to the first order analyses <math>\langle AC_2 \rangle</math>  <math> \delta_x </math> is the maximum member <math>\langle AC_2 \rangle</math> deflection <math>\langle AC_2 \rangle</math> along the member</p>
	$C_{mi,0} = 1 - 0,18 \frac{N_{Ed}}{N_{cr,i}}$ $C_{mi,0} = 1 + 0,03 \frac{N_{Ed}}{N_{cr,i}}$

**APPENDIX 2 : EN 1993-1-1 METHOD 2 : Interaction factor  $k_{ij}$**

**Annex B [informative] – Method 2: Interaction factors  $k_{ij}$  for interaction formula in 6.3.3(4)**


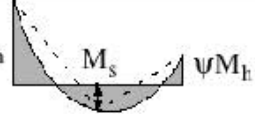

**Table B.1: Interaction factors  $k_{ij}$  for members not susceptible to torsional deformations**

Interaction factors	Type of sections	Design assumptions	
		elastic cross-sectional properties class 3, class 4	plastic cross-sectional properties class 1, class 2
$k_{yy}$	I-sections RHS-sections	$C_{my} \left( 1 + 0,6 \bar{\lambda}_y \frac{N_{Ed}}{\chi_y N_{Rk} / \gamma_{M1}} \right)$ $\leq C_{my} \left( 1 + 0,6 \frac{N_{Ed}}{\chi_y N_{Rk} / \gamma_{M1}} \right)$	$C_{my} \left( 1 + (\bar{\lambda}_y - 0,2) \frac{N_{Ed}}{\chi_y N_{Rk} / \gamma_{M1}} \right)$ $\leq C_{my} \left( 1 + 0,8 \frac{N_{Ed}}{\chi_y N_{Rk} / \gamma_{M1}} \right)$
$k_{yz}$	I-sections RHS-sections	$k_{zz}$	$0,6 k_{zz}$
$k_{zy}$	I-sections RHS-sections	$0,8 k_{yy}$	$0,6 k_{yy}$
$k_{zz}$	I-sections	$C_{mz} \left( 1 + 0,6 \bar{\lambda}_z \frac{N_{Ed}}{\chi_z N_{Rk} / \gamma_{M1}} \right)$ $\leq C_{mz} \left( 1 + 0,6 \frac{N_{Ed}}{\chi_z N_{Rk} / \gamma_{M1}} \right)$	$C_{mz} \left( 1 + (2\bar{\lambda}_z - 0,6) \frac{N_{Ed}}{\chi_z N_{Rk} / \gamma_{M1}} \right)$ $\leq C_{mz} \left( 1 + 1,4 \frac{N_{Ed}}{\chi_z N_{Rk} / \gamma_{M1}} \right)$
	RHS-sections		$C_{mz} \left( 1 + (\bar{\lambda}_z - 0,2) \frac{N_{Ed}}{\chi_z N_{Rk} / \gamma_{M1}} \right)$ $\leq C_{mz} \left( 1 + 0,8 \frac{N_{Ed}}{\chi_z N_{Rk} / \gamma_{M1}} \right)$
For I- and H-sections and rectangular hollow sections under axial compression and uniaxial bending $M_{y,Ed}$ the coefficient $k_{zy}$ may be $k_{zy} = 0$ .			

**Table B.2: Interaction factors  $k_{ij}$  for members susceptible to torsional deformations**

Interaction factors	Design assumptions	
	elastic cross-sectional properties class 3, class 4	plastic cross-sectional properties class 1, class 2
$k_{yy}$	$k_{yy}$ from Table B.1	$k_{yy}$ from Table B.1
$k_{yz}$	$k_{yz}$ from Table B.1	$k_{yz}$ from Table B.1
$k_{zy}$	$\left[ 1 - \frac{0,05\bar{\lambda}_z}{(C_{mLT} - 0,25)} \frac{N_{Ed}}{\chi_z N_{Rk} / \gamma_{M1}} \right]$ $\geq \left[ 1 - \frac{0,05}{(C_{mLT} - 0,25)} \frac{N_{Ed}}{\chi_z N_{Rk} / \gamma_{M1}} \right]$	$\left[ 1 - \frac{0,1\bar{\lambda}_z}{(C_{mLT} - 0,25)} \frac{N_{Ed}}{\chi_z N_{Rk} / \gamma_{M1}} \right]$ $\geq \left[ 1 - \frac{0,1}{(C_{mLT} - 0,25)} \frac{N_{Ed}}{\chi_z N_{Rk} / \gamma_{M1}} \right]$ <p>for <math>\bar{\lambda}_z &lt; 0,4</math>:</p> $k_{zy} = 0,6 + \bar{\lambda}_z \leq 1 - \frac{0,1\bar{\lambda}_z}{(C_{mLT} - 0,25)} \frac{N_{Ed}}{\chi_z N_{Rk} / \gamma_{M1}}$
$k_{zz}$	$k_{zz}$ from Table B.1	$k_{zz}$ from Table B.1

**Table B.3: Equivalent uniform moment factors  $C_m$  in Tables B.1 and B.2**

Moment diagram	range		$C_{my}$ and $C_{mz}$ and $C_{mLT}$	
			uniform loading	concentrated load
	$-1 \leq \psi \leq 1$		$0,6 + 0,4\psi \geq 0,4$	
 <p><math>\alpha_s = M_s / M_h</math></p>	$0 \leq \alpha_s \leq 1$	$-1 \leq \psi \leq 1$	$0,2 + 0,8\alpha_s \geq 0,4$	$0,2 + 0,8\alpha_s \geq 0,4$
	$-1 \leq \alpha_s < 0$	$0 \leq \psi \leq 1$	$0,1 - 0,8\alpha_s \geq 0,4$	$-0,8\alpha_s \geq 0,4$
		$-1 \leq \psi < 0$	$0,1(1-\psi) - 0,8\alpha_s \geq 0,4$	$0,2(-\psi) - 0,8\alpha_s \geq 0,4$
 <p><math>\alpha_h = M_h / M_s</math></p>	$0 \leq \alpha_h \leq 1$	$-1 \leq \psi \leq 1$	$0,95 + 0,05\alpha_h$	$0,90 + 0,10\alpha_h$
	$-1 \leq \alpha_h < 0$	$0 \leq \psi \leq 1$	$0,95 + 0,05\alpha_h$	$0,90 + 0,10\alpha_h$
		$-1 \leq \psi < 0$	$0,95 + 0,05\alpha_h(1+2\psi)$	$\boxed{AC2} 0,90 + 0,10\alpha_h(1+2\psi) \boxed{AC2}$

For members with sway buckling mode the equivalent uniform moment factor should be taken  $C_{my} = 0,9$  or  $\boxed{AC2} C_{mz} \boxed{AC2} = 0,9$  respectively.

$C_{my}$ ,  $C_{mz}$  and  $C_{mLT}$  should be obtained according to the bending moment diagram between the relevant braced points as follows:

moment factor	bending axis	points braced in direction
$C_{my}$	y-y	z-z
$C_{mz}$	z-z	y-y
$C_{mLT}$	y-y	y-y